VERSATILE, AUTOMATED SAMPLE PREPARATION AND DETECTION OF CONTAMINANTS AND BIOLOGICAL MATERIALS

By

MELANIE MARGARETE HOEHL

BA (Hons.), MA (Cantab), University of Cambridge (2012)

Submitted to the Harvard-MIT Division of Health Sciences and Technology
in Partial Fulfillment of the Requirements for the Degree of
DOCTOR OF PHILOSOPHY
at the
MASSACHUSETTS INSTITUTE OF TECHNOLOGY
September 2013
© 2013 Melanie Hoehl. All rights reserved.

The author hereby grants to MIT permission to reproduce and to distribute publicly paper and electronic copies of this thesis document in whole or in part in any medium now known or hereafter created.

Signature of Author: _____
Harvard-MIT Division of Health Sciences and Technology
July 22nd, 2013

Certified by: _____
Prof. Alexander H. Slocum
Pappalardo Professor of Mechanical Engineering
Thesis Supervisor

Accepted by: _____
Emery Brown, MD, PhD
Director, Harvard-MIT Program in Health Sciences and Technology
Professor of Computational Neuroscience and Health Sciences and Technology

VERSATILE, AUTOMATED SAMPLE PREPARATION AND DETECTION OF CONTAMINANTS
AND BIOLOGICAL MATERIALS

by
Melanie M. Hoehl

Submitted to the Harvard-MIT Division of Health Sciences and Technology
in September 2013 in partial fulfillment of the requirements for the degree of
Doctor of Philosophy at the Massachusetts Institute of Technology

ABSTRACT

Contamination of food, water, medicine and ingestible household products is a public health hazard that episodically causes outbreaks worldwide. Existing laboratory methods are often expensive, require a laboratory environment and/or trained staff to perform manual steps. The aim of this PhD thesis was to create and test methods and instruments for affordable diagnostic tests for contaminants and pathogens.

To achieve this goal, the LabReader was introduced, which employs a LED-based detection scheme for four simultaneous fluorescence- and UV-measurements. Assays were developed to detect (di-)ethylene glycol in consumables ≥ 0.1wt% and alcohols ≥ 1ppb. Pathogens in water, foods and blood were detected at $\geq 10^4$ CFU/ml using nonspecific intercalating dyes. To gain sensitivity and specificity for cell-based analysis, biochemical amplification methods had to be incorporated. To be deployable outside a laboratory, sample preparation needed to be automated.

Automation was achieved by combining the LabReader with the already developed LabTube, a disposable platform for automated DNA extraction inside a standard centrifuge. Performing DNA amplification/readout in an external optical reader, made the LabSystem broadly deployable and flexible. DNA extraction of food bacteria (*E.coli* and *Alicyclobacillus*) was optimized inside the LabTube for 10^2-10^9 inserted DNA copies. The extracted DNA was amplified using the qualitative isothermal LAMP method and semi-quantitative, real-time PCR inside the LabReader. The combined extraction and amplification detection limit of the LAMP-LabSystem and the quantitation limit of the PCR-LabSystem were as low as 10^2 copies. Performing extraction and amplification *inside* the centrifuge/LabTube was also outlined, which may be preferable when contamination risks are high. After theoretically evaluating heating methods, a battery-driven heated LabTube was designed, in which 10^2-10^8 DNA copies of VTEC *E.coli* were extracted, LAMP-amplified and visually readout within 1.5 hrs.

The major contribution of this thesis is the full system integration of versatile, automated sample preparation and detection systems. They offer great flexibility as they may be used with each other or in combination with other analytic methods, depending on the application. At the same time, they are frugal and deployable at low-to-medium throughput - even outside a traditional laboratory. Whilst the focus was put on food safety, the systems were also used for medical, environmental or consumer product quality applications, hence demonstrating their broad applicability.

Thesis Supervisor: Alexander H. Slocum
Title: Papallardo Professor of Mechanical Engineering

ACKNOWLEDGMENTS

CONTENTS

ABBREVIATIONS

∂	Density
ADH	Alcohol Dehydrogenase
A.acidoterrestris	Alicyclobacillus Acidoterrestris
BAC	Blood Alcohol Content
c	Heat Capacity
C_t	Threshold Cycle
c_α	Alcohol Mass Fraction
c_ε	EG Mass Fraction
c_∂	DEG Mass Fraction
c_μ	Microbial Mass Fraction
CFU	Colony-Forming Units
DEG	Diethylene Glycol
DEP	Dielectrophoresis
DNA	Deoxyribonucleic Acid
E.coli	Escherichia Coli
EG	Ethylene Glycol
ELISA	Enzyme Linked Immunosorption Assay
f	Frequency
FAD	Flavin Adenine Dinucleotide
FCM	Flow Cytometry
FRET	Förster Resonance Energy Transfer
γ	Power-Law Exponent for UV LEDs
γ'	Normalized Power-Law Exponent for UV LEDs
H	Enthalpy
HRP	Horseradish Peroxidase
ICH	International Conference on Harmonization
iqPCR	Immune-Quantitative PCR
LAMP	Isothermal Loop-Mediated DNA Amplification
LoD	Limit of Detection
LoQ	Limit of Quantification
M	Molar Mass
m	Mass
n	Number of Repeats
NAD	Nicotinamide Adenine Dinucleotide
NASBA	Nucleic Acid Sequence Based Amplification
P	Power
PCR	Polymerase Chain Reaction
PPB	Parts Per Billion
PPM	Parts Per Million
Q	Energy [J]
q	Energy (Heat) Flow [J/s]
q-PCR	Quantitative, Real-Time PCR
RCA	Rolling Circle Amplification

RFU	Relative Fluorescence Units
RIA	Radioimmunoassay
RNA	Ribonucleic Acid
RPA	Recombinase Polymerase Amplification
rRNA	Ribosomal RNA
RT-PCR	Reverse-Transcriptase PCR
rt-cycler	Real-time Cycler
SD	Standard Deviation
S. enterica	Salmonella Enterica
Sn	Sensitivity
Sp	Specificity
SPR	Surface Plasmon Resonance
T_{vap}	Boiling Temperature
UV	Ultraviolet
v	Power-law Exponent for Green LEDs
v'	Normalized Power-Law Exponent for Green LEDs
V	Volume
V_{ua}	Voltage of the UV-Absorption Detector
V_{uf}	Voltage of the UV-Fluorescence Detector
V_{gf}	Voltage of the Green-to-Red Fluorescence Detector
V_{gf}	Voltage of the Green-to-Red Absorption Detector
V. cholerae	Vibrio Cholerae
Vis	Visual
w	Tolerance Value
W	Work
WHO	World Health Organisation
Wv	Warning Value

LIST OF FIGURES

LIST OF TABLES

XI

CHAPTER 1: INTRODUCTION

Episodically, hundreds to thousands of people die from ingestion of toxins, as well as from pathogenic bacteria. Outbreaks could be prevented if biological and chemical contaminants were identified in time. Similarly, non-pathogenic product spoilers cause billions of Dollars in losses to the food industry each year. Traditional methods (such as immunoassays or polymerase chain reaction, PCR) require specialized scientific equipment, a continuous refrigeration chain for reagents, and/or specially trained staff to perform numerous manual steps [1, 2, 3, 4, 5, 6], all of which are expensive and generally preclude their use outside a specialized laboratory [7]. Moreover, small manufacturers or sales locations cannot afford buying expensive automation equipment or employing specialized staff [7]. In order to ensure safety and quality (for medical, food, consumer products and environmental applications), rapid detection methods are desirable that can be used at the location of an outbreak, at the production site or sales location. The aim of this thesis was to develop automated sample preparation and detection systems, which offer great flexibility, whilst being frugal, robust and versatile deployable outside a specialized laboratory. The aim was further to integrate different assay types into the system to demonstrate its broad applicability.

Initially, the LabReader, a handheld, low-cost optical fluorometer/UV-vis meter, is introduced and assays for a variety of applications are implemented. Next a fully integrated and automated DNA extraction and amplification system is outlined. The combined system consists of automated sample preparation using the already developed, disposable tube LabTube[8], which extracts DNA inside a standard laboratory centrifuge. The DNA amplification assay and readout can occur *outside* of the centrifuge using a modified, handheld LabReader. It can also occur *inside* a centrifuge using a fully closed system. Contamination in food, water, medicine and ingestible household products is detected using the introduced methods. Food safety applications are emphasized specifically in this thesis.

The introductory chapter is divided into four sub-sections. The first sub-section discusses the motivation behind the development of frugal, automated and versatile detection methods. The second sub-section provides a summary of major epidemics caused by the toxins and bacteria which were covered in this thesis. A summary of the various detection strategies that present the state of the art is outlined in the third section, followed by an overview of relevant analytic markets.

1.1   CHEMICAL AND CELLULAR CONTAMINANTS

Common contaminants for global mass poisoning outbreaks include the toxic ethylene glycol (EG) and diethylene glycol (DEG) [9, 10] in medicines, household products, and foods [11, 12]. In addition to chemical poisoning, contamination of food and water by microbes, such as *E.coli* and salmonella (*S.enterica*) in food[13, 14, 15, 16, 17] or cholera (*V. cholerae*) in water[18, 19], regularly causes death and sickness worldwide[20]. Unlike pathogens, product spoiling bacteria do not cause sickness, but cause great monetary losses to industry. One prevalent product spoiler is *Alicyclobacillus,* which is found in fruit juices [21, 22]. In this section, poisons (diethylene glycol, ethylene glycol), pathogens (*E.coli, S. enterica, V. cholerae, P. falciparum)* and product spoilers (*Alicyclobacillus*), are outlined, for which detection methods were developed in this thesis.

1.1.1   ETHYLENE GLYCOL AND DIETHYLENE GLYCOL

The contamination of foods, water, medicines and ingestible household products with ethylene glycol (EG) and diethylene glycol (DEG) has resulted in many deaths up to the present day. Lower-cost EG and DEG have repeatedly been substituted for the more-expensive non-toxic glycerol and propylene glycol, which are ingredients in medicines, household products, and foods [11, 12]. EG and DEG contamination is a longstanding problem that led to the 1938 Food, Drug and Cosmetic Act, establishing the modern drug-approval process within the United States Food and Drug Administration (FDA) [23]. Episodes of DEG poisoning have killed hundreds, particularly in developing countries in the past 15 years [23, 24, 25, 26, 27, 28, 29, 30, 31, 32][33, 34, 35, 36, 13, 37]. EG and DEG ingestion can cause central nervous system depression, renal failure and cardio-pulmonary compromise, which may ultimately lead to death[26]. Table 1 and Table 2 below summarize major incidents of lethal EG and DEG contamination. The results indicate that most outbreaks occur at EG and DEG concentrations above 2wt%, which is higher than the FDA limit of 0.1wt% and 1wt% for EG and DEG, respectively[26]. Usually EG and DEG are detected with gas chromatography or mass spectrometry[26], which are expensive laboratory methods not easily deployable in the field or in developing countries.

Substance	Location	Date	Wt % EG	Fatalities	Reference
Antifreeze	Worldwide		~50	>2400 per year	[27, 38]
Paracetamol syrup	Nigeria	1990	90	196	[39]
Wine	Netherlands	1990	1.5	0	[24]
Drinking water	Indiana	1990	2	6	[24]
Drinking water	North Dakota	1987	7	29 ill	[29]
Dialysis machine	Illinois	1985	3	4	[29]
Drinking water	New York	1985	-	1	[29]

TABLE 1: Ethylene glycol contamination.

Substance	Location	Date	Wt% DEG	Fatalities	Reference
Acetaminophen	Nigeria	2008	17-21	84	[30]
Toothpaste	China, USA	2007	1.5-4	100s ill	[12]
Antihistamine	Panama	2006	7.6-8.1	51	[25]
Cough syrup	India	1998	17.5	36	[37]
Paracetamol syrup	Haiti	1995	14.5-19.6	109	[31]
Propolis syrup	Argentina	1992	65	15	[40, 41]
Paracetamol syrup	Bangladesh	1990-92	40-48	236	[32]
Paracetamol syrup	Nigeria	1990		47	[33]
Glycerin (medical)	India	1986	18.6	21	[34]
Wine	Austria, Germany	1986	0.3	-	[11]
Topical cream	Spain	1985	0.6-0.7	5	[42]
Drinking water	Sahara	1979	2	4	[43]
Sedative elixirs	South Africa	1969	4.5	6	[35]
Sulfur drug	USA	1937	50	105	[23, 36]

TABLE 2: Diethylene glycol contamination.

1.1.2 ALCOHOL

Blood alcohol content (BAC) is most commonly used as a metric of alcohol intoxication by ethanol for legal or medical purposes. A BAC of ≥0.08% is considered "legally intoxicated" for driving in most American states and ≤0.05% is considered not impaired. Alcohol levels in blood are usually detected via breath analysis or blood analysis[44]. Portable methods that are more sensitive than breath analysis may be beneficial, which is why alcohol in blood serum was detected using the methods developed in this thesis.

Alcohols can also be an indicator for fuel contamination in groundwater. If there is groundwater contamination with fuel[45], alcohols are the most water-dissolvable components, whilst most of the rest will remain in the soil[46, 47, 48]. Moreover, alcohols can get into groundwater through inappropriate industrial waste disposal, as was recently the case in Punjab, India, where four

distilleries discharged their untreated effluents directly into the soil[49]. Alcohol can also get into water during remediation of water to strip it from organic compounds, such as fuel[50]. The acceptable levels of alcohols in water include: methanol 4ppm, propanol 100 ppb, tertiary butyl-alcohol 100ppb, phenol 2ppm, butanol 700ppb[51].

Even though methods like gas chromatography or mass spectrometry can be used to detect these alcohols in water, they are not practical in the field or in developing countries due to their high cost and operation complexity. Here, lower cost, automated and more broadly deployable methods are desirable, which is why alcohol detection was evaluated in this thesis.

1.1.3 PATHOGENS

1.1.3.1 FOOD PATHOGENS

Contamination of food primarily arises during the manufacturing process. Under certain conditions, the presence of at least one bacterium in a food package can lead to the complete spoilage of the product over time. It is therefore crucial to eliminate the presence of low amounts of bacteria early in the manufacturing process to avoid massive outbreaks. The common way of clearing foods, such as milk or juice, from bacteria is by sterilization and pasteurization [52]. Bacteria are commonly detected by cell-plating and pre-enrichment cultures with subsequent immunoassays or DNA analysis. However, these methods are time-intensive and require specialized labs and personnel. The main pathogens causing most foodborne disease are *Campylobacter, Shigella, S. enterica, and E.coli* [52, 17]. An overview of common food bacteria is listed in Table 3 [17].

E.COLI

Due to its projected market growth for analytic testing in low-to-medium throughput applications (see 1.3.1), *E.coli* testing is of high relevance and was evaluated in this thesis.

In 1982, the U.S. Centers for Disease Control and Prevention (CDC) investigated two outbreaks of severe bloody diarrhea, associated with the same fast food restaurant chain. As part of the investigations, the CDC identified a new strain of *E.coli* that had not previously been recognized as a pathogen [53, 54]. In the years since the discovery of this pathogen, *E.coli* O157:H7 (VTEC) has become increasingly prominent, causing an estimated 20,000 illnesses and 250 deaths each year in the United States alone [55]. *E.coli* can be passed from person to person, but serious (especially VTEC) *E.coli* infection is more often linked to contaminated food,

including: raw milk; fruit juice that isn't pasteurized (e.g. apple cider); drinking water (e.g. unchlorinated water poisoned with *E.coli* after a pipe burst [56, 57, 58, 59]); vegetables grown in cow manure or washed in contaminated water; and undercooked ground beef.

E.coli outbreaks in the USA in recent years are summarized in Table 4[16]. When infecting humans, *E.coli* have been linked with the severe complication hemolytic uremic syndrome [20]. The infectious dose of (VTEC) *E.coli* has been calculated to be as low as 10-100 cells [60].

There is an increasing market for testing *E.coli* (any strain) at the point of care with low-medium throughputs (several hundreds to thousands of tests per year) [61]. The required detection limits of *E.coli* (any strain) in foods range from 10^2-10^5 CFU/g and are summarized in Table 5.

Disease or agent	Estimated total cases	Reported cases by surveillance type			Foodborne transmission (%)	Hospitalization rate	Case-fatality rate
		active	passive	outbreak			
Bacillus cereus	27,360		720	72	100	0.006	0
Botulism, foodborne	58		29		100	0.8	0.0769
Brucella spp.	1,554		111		50	0.55	0.05
Campylobacter spp	2,453,926	64,577	37,496	146	80	0.102	0.001
Clostridium perfringens	248,520		6,540	654	100	0.003	0.0005
Escherichia coli O157:H7	73,480	3,674	2,725	500	85	0.295	0.0083
E.coli, non-O157 STEC	36,740	1,837			85	0.295	0.0083
E.coli, enterotoxigenic	79,420		2,090	209	70	0.005	0.0001
E.coli, other diarrheogenic	79,420		2,090		30	0.005	0.0001
Listeria monocytogenes	2,518	1,259	373		99	0.922	0.2
Salmonella typhi	824		412		80	0.75	0.004
Salmonella, nontyphoidal	1,412,498	37,171	37,842	3,640	95	0.221	0.0078
Shigella spp.	448,240	22,412	17,324	1,476	20	0.139	0.0016
Staphylococcus (food)	185,060		4,870	487	100	0.18	0.0002
Streptococcus, foodborne	50,920		1,340	134	100	0.133	0
Vibrio cholerae, toxigenic	54		27		90	0.34	0.006
V. vulnificus	94		47		50	0.91	0.39
Vibrio, other	7,880	393	112		65	0.126	0.025
Yersinia enterocolitica	96,368	2,536			90	0.242	0.0005
Subtotal	5,204,934						

TABLE 3: Disease caused by foodborne pathogens in the United States per year averaged between 1983 and 1992 (adapted with permission from [17]).

Date	Substance	# states	# sick	# hospitalized
2013	Frozen foods	15	27	8
2012	Organic spinach	33	5	13
2012	Unspecified	9	18	4, 1 dead
2012	Clover sprouts	11	29	7
2011	Romaine lettuce	9	58	33
2011	Travels to Germany (here 852 sick)	5	6	1 death
2011	Lebanon Bologna	3	14	3
2011	Hazelnuts	3	8	4
2010	Apple cider	1	7	3
2010	Shredded lettuce	5	33	12
2009	Beef from National Steak & Poultry	16	21	17
2009	Beef from Fairbank Farms	8	26	19
2009	Beef from JBS Swift Beef	9	17	12
2009	Cookie dough	30	72	34
2008	Kroger/Nebraska Ltd	7	49	27
2008	Totino's/Jeno's Pizza	4	71	53
2007	Topp's Ground Beef Patties	8	40	21
2006	Taco Bell		52	N/A
2006	Fresh spinach		102	N/A

TABLE 4: *E.coli* outbreaks in the USA from 2006-2010 [16].

Food Matrix	Country	w (CFU/g)	Wv (CFU/g)
Raw milk	EU	10	10^2
Raw milk for production	EU	-	$<10^5$
Butter	EU	10	10^2
Cheese	EU	10^2	10^4
Whipped cream	EU	10	10^2
Juice[62]	Gulf Region	10	10^2

TABLE 5: Safety limits for *E.coli* in foods (w= tolerance value, which is the maximum recommended value; Wv= warning value above which the product is deemed unsafe and cannot enter the market) [63].

SALMONELLA ENTERICA

40,000 cases of salmonellosis are reported in the United States each year[64]. The actual number of infections may be thirty or more times larger, as many cases go unreported[64]. Children have the highest risk to suffer from salmonellosis. The rate of diagnosed infections in children less than five years old is higher than the total infection rate. Furthermore, young children, the elderly, and the immuno-compromised have the highest risk of suffering from

severe infections [64]. It is expected that in the US 400 persons die each year from salmonellosis [64]. A large fraction of reported *salmonella* infections are caused by eggs or egg-related products: up to 77% of reported outbreaks with identified food vehicles were reported to have been caused by grade-A shell eggs or foods that contained such eggs [65, 66]. Most cases of *salmonella* infections are isolated, local cases that affect individuals or few people [64]. However, mass outbreaks of *salmonella* infections also can occur, often in food served by chain restaurants, or those distributed throughout large regions via supermarkets (see Table 6). FDA safety regulations demand extensive *salmonella* testing to prevent further mass outbreaks [64]. The safety limits are as low as 0 CFU/10g, such as for salmonella in eggs [64]. Due to extensive FDA testing requirements, s*almonella* testing (especially for eggs) in an industrial setting is suitable for high-throughput applications, rather than low-frequency batch processes (see 1.3.1). However, small-scale testing in the field or in consumer households was still considered to be of interest, which is why *salmonella* were still chosen as a sample application in this thesis.

Year	Contaminated product	# states	# sick	# hospitalized
2013	Chicken	11	128	23
2013	Ground beef	6	22	7
2012	Poultry (3 incidents)	27, 23,11	266	68, 3 dead
2012	Ground beef	9	46	12
2012	Mangoes	15	127	33
2011	Sprouts	5	25	9
2011	Papaya	12	106	25
2011	Cantaloupes	10	20	N/A
2011	Teaching laboratory *E.coli*	38	109	13, 1 dead
2010	Raw alfalfa sprouts	N/A	44	7
2010	Marie Callender's Cheesy Chicken	18	44	16
2010	Frozen rodents (for reptile feed)	17	34	1
2010	Eggs in Iowa	multiple	1600	N/A
2010	Italian-style meats	44	272	52
2010	Restaurant chain A	multiple	47	15
2009	Raw alfalfa sprouts	14	235	15
2009	Pistachios			
2009	Water frogs	31	85	16
2008	Cantaloupes	16	52	16
2008	Malt-O-Meal rice/wheat cereals	15	32	23
2008	Peanut butter	15	28	
2007	Banquet pot pies	35	272	65
2007	Peanut butter	44	425	71
2007	Veggie booty	20	65	N/A
2006	Tomatoes	21	111	22

TABLE 6: *Salmonella* outbreaks in the USA from 2006-2010 [64].

1.1.3.2   ENVIRONMENTAL PATHOGENS (VIBRO CHOLERAE)

Cholera is an infection caused by the bacterium *Vibrio cholerae*, whose main symptoms include diarrhea and vomiting [67]. Transmission is primarily via fecal contamination of food and water due to poor sanitation. It remains both epidemic and endemic in many areas of the world [67]. Cholera affects 3-5 million people and causes 100,000–130,000 deaths a year as of 2010, mostly in the developing world [68]. The World Health Organisation (WHO) estimates that the officially reported cases represent around 5-10% of actual cases worldwide [69]. Recent cholera outbreaks include the 2010 cholera outbreak in Haiti following the large earthquake, which caused 1,034 fatalities and 167,000 hospitalizations [70]. In August 2010, 12 of the 36 states in Nigeria were affected with cholera; 6,400 cases have been reported with 352 reported deaths, which the health ministry related to heavy seasonal rainfall and poor sanitation [71]. In 2012 a cumulative total of 18,508 cases including 271 deaths (with a case fatality ratio of 1.5%) were reported in Sierra Leone [72].

Lack of treatment of human feces and lack of treatment of drinking water greatly facilitate the spread of cholera; also, seafood shipped long distances can spread the disease [73]. Typically, about 10^8 bacteria must be ingested to cause cholera in a normal healthy adult [67]. This minimum dose, however, is less in the elderly, immuno-compromised and children (<4 years), which have the highest rates of infection [67]. The safety limit for cholera in water is <1 CFU/100ml [74]. As most cholera cases occur in developing countries, affordable, rapid and field-deployable detection methods are desirable.

Region	Cases	Deaths
Africa	174,000,000	596,000
America	1,100,000	1,100
Eastern Mediterranean	10,400,000	15,000
Europe	-	-
South-East Asia	32,000,000	43,000
Western Pacific	1,700,000	4000
Total	**219,000,000**	**660,000**

TABLE 7: Estimated malaria cases in 2008 by region[75].

1.1.3.3 BLOOD PATHOGENS (MALARIA)

Malaria is a mosquito-borne infectious disease of humans caused by eukaryotic protists of the genus Plasmodium (*P.falciparum*). It is widespread in tropical and subtropical regions, including Sub-Saharan Africa, Asia and the Americas [76]. The disease results from the multiplication of malaria parasites within red blood cells, causing symptoms that typically include fever and headache, in severe cases progressing to coma and death [76]. Each year, there are more than 243 million cases of malaria, killing nearly a million people [75]. The majority of deaths occurs in Sub-Saharan Africa, and primarily affects young children [77]. The number of cases and deaths due to malaria in 2012 are summarized in Table 7 [75]. During infection between 0.1-1% of cells in the blood consists of the organism *P.falciparum* [78]. Malaria is usually confirmed by the microscopic examination of blood films or by antigen-based diagnostic tests[79]. Because field-deployable, frugal testing methods are desirable, malaria was used as a sample application in this thesis.

1.1.3.4 PRODUCT SPOILERS (ALICYCLOBACILLUS)

Some bacteria like *Alicyclobacillus* are non-pathogenic, but they are of great interest to the juice industry [80]. Because their presence spoils products, they can cause great economic damage and are therefore important bacteria to test for during quality control [80]. *Alicyclobacillus* is a gram-positive, thermo acidophilic, non-pathogenic, spore forming and aerobic microorganism [80]. It has been detected in several spoiled commercial pasteurized fruit juices, such as orange and apple juices [80]. Additionally, products such as ice tea and canned tomatoes may also be contaminated by *Alicyclobacillus* [65]. It has been shown that they can withstand standard commercial pasteurization procedures [81]. This is because *Alicyclobacillus* can survive in different temperature conditions from 20-60°C and in adverse acidic conditions (pH 2-6). This allows the bacteria to grow in acidic fruit juices (which most other bacteria cannot), thereby causing off-flavor hence spoiling the product. Under high temperature conditions, these bacteria will produce heat-resistant spores, which eventually grow into bacteria at the right conditions. Practically, every fruit that is picked is potentially contaminated, because harvesting typically occurs in a non sterile environment. *Alicyclobacilli* live in soil and reach the surface of fruits by dust, water or when the fruit falls on the ground. The contamination can spread inside one factory during a few critical processing steps, which have to be checked repetitively [82]. One of these steps is the reuse of water used for washing the fruits [83]. Fruit concentrate itself is not at risk of spoilage [84], therefore the product will develop its off-flavor when reaching the customer. The process of spoiling does not produce color changes or gas; hence it is not possible to

identify a spoiled package of juice without opening it. Due to all these circumstances, internal requirements demand a zero tolerance of *Alicyclobacilli* (0 CFU/10g) [85]. The associated economic loss due to spoilage is the reason for why it is very crucial to be able to detect *Alicyclobacillus* early on and in small amounts during the manufacturing process [86]. Sales of fruit juice and fruit juice products have reached a volume of about 64 billion liters [86], which resembles annual sales of about bn$ 80. To ensure zero tolerance, routine measurements are necessary. The demand for testing has been increasing over the years and several PCR and culture-based kits have entered the testing market [85]. Most of these methods require expensive testing equipment or take a long time. Therefore, affordable and rapid detection methods are desirable.

Commonly, the species *Alicyclobacillus acidoterrestris* (*A.acidoterrestris*) is used as a reference organism to design pasteurization and testing methods[87]. It was also used in this thesis.

1.1.4 SUMMARY

Table 8 summarizes the contaminants covered in this thesis, their occurrence and safety limits. These contaminants and bacteria have repeatedly caused mass outbreaks and disease across the world or compromise product quality hence causing monetary losses to the industry. Covered applications include food, environmental and product quality and safety and medical diagnostics. In this thesis, versatile, frugal and automated devices will be developed to detect these contaminants and bacteria outside a stable laboratory environment, in order to prevent further outbreaks.

Contaminant	Occurrence	Safety limit
Ethylene glycol (EG)	Antifreeze, medicines, water	0.1wt%
Diethylene glycol (DEG)	Medicines, toothpaste	1wt%
Ethanol	Blood	0.08wt%
Alcohols	Groundwater, drinking water	100ppb – 4ppm
E.coli	Water, meat, dairy products	$10^2 – 10^4$ CFU/ml (in production)
Salmonella	Eggs, foods	0 CFU/25g (eggs)
V. cholerae	Water, feces	<1 CFU/100ml (water)
Malaria	Mosquitoes, human blood	0.1 – 1 % of red blood cells
Alicyclobacillus	Fruit juices, canned products	0 CFU/10g

TABLE 8: Overview of contaminants and detection limits.

1.2 STATE OF THE ART OF ANALYTIC TESTING METHODS

This section outlines the various tactics and strategies used in the detection of contaminants and pathogens, both traditional and new ones. The focus is put on methods that are relevant to this work or that were even used as references in this thesis.

1.2.1 TRADITIONAL STRATEGIES FOR POISON DETECTION

1.2.1.1 GAS CHROMATOGRAPHY

Gas chromatography is a chemical method to separate constituent components of a substance. Particles of the substance are blown through a chamber by an inert noble gas [88]. On the chamber wall, various chemical agents are present. Constituent molecules are slowed down differently based on their individual chemical affinities to the wall agents [88]. Subsequently, different molecules pass through the chamber at different speeds and reach the top of the chamber at different times [88]. A detector at the top identifies individually the different components of the sample [88].

Gas chromatography is commonly used to identify toxins and contaminants; it is not traditionally used for the detection of cells or cellular components. Out of the contaminants covered in this thesis, gas chromatography is used to detect alcohols (e.g. in blood), as well as EG and DEG in household products and medicines. For DEG in toothpaste and household products, detection limits of 2.5 mg/l are achieved [89]. Gas chromatography requires specialized, expensive equipment, trained staff and laboratory facilities.

1.2.1.2 MASS SPECTROMETRY

The constituent molecules of a substance can be identified using mass spectrometry, a procedure that takes advantage of the varying charge-to-mass ratio of different molecules [90]. The particles from the test sample are accelerated by an electric field and are then deflected by a magnetic field. Sensors are placed at different points to measure the number of the molecules at each deflection angle [90]. The concentration of different molecules can be identified based on the angle of deflection, which depends on the specific charge-to-mass ratio [90].

Mass spectrometry is often used for identification of toxins (such as alcohols, EG and DEG in household products and medicines). It is commonly used in combination with gas

chromatography, electro spray ionization or liquid chromatography. For example, DEG in toothpaste can be detected at 1ppm using neutral desorption reactive extractive electro spray ionization tandem mass spectrometry [91]. Even though it is not routinely used for it, mass spectrometry has been used in the detection of pathogens as well [92]. Even though it is highly specific and sensitive, expensive equipment and trained staff are required for mass spectrometry analysis, which does not make it deployable broadly, like in developing countries, at the production site or at the point of care.

1.2.1.3   OPTICAL SPECTROSCOPY

Optical spectroscopy identifies constituent molecules of substances on the basis of their optical properties. The main two methods commonly used are absorption and fluorescence optical spectrometry [93, 94].

In absorption spectrometry, different wavelengths of light are passed through a substance. The intensity of the light is then measured after its passage through the substance. Molecules absorb specific wavelengths of light differently. By measuring absorption, different constituent molecules can be identified [93].

In fluorescent spectroscopy, the fluorescent properties of molecules are used to identify the constituent molecules of a substance. Light of different wavelengths is passed through the substance. A detector is normally placed at 90 degrees from the direction of the light source to avoid interference from the latter [94]. The detector measures the intensity of different wavelengths emitted by the sample as a result of the incident wavelengths [94]. Hence, fluorescent spectra for different incident wavelengths are produced. These spectra can be used to identify the different molecules present in the sample [94]. In addition, a change in fluorescence signal over time at a certain wavelength can be monitored during a reaction and different fluorescent levels at a fixed wavelength can be compared between samples [94].

Alcohols and glycols (such as EG and DEG) can, for example, be detected by combining enzymes, such as alcohol dehydrogenases, with the coenzyme NAD. In the reaction, NAD gets reduced to NADH, which absorbs light at 340nm [95]. These assays can also be coupled to fluorescent dyes (e.g. Amplex Red in the Glucose Oxidase detection kit, Invitrogen A22189 or [95]), which are commercially available (see Chapter 2.2). Example detection limits include 0.01wt% of alcohol in blood and 10^4 CFU/ml for many cells[96].

Optical spectroscopy methods are used for all contaminants covered in this thesis. Even though conventional optical spectrometry analysis is sensitive and specific, expensive equipment (e.g. fluorescence plate readers cost around k\$ 33 [97]) and manual labor time are required. Hence, there is a need for lower cost, versatile deployable (i.e. stable, portable and easy-to-use) optical spectroscopy devices (see 1.2.3).

1.2.2 TRADITIONAL STRATEGIES SPECIFIC FOR CELLULAR DETECTION

1.2.2.1   CELL CULTURING, PLATING AND COUNTING:

The gold standard for bacterial detection (and quantification) is cell plating (and colony counting). Here, bacteria samples are grown in certain nutrient media such as Agar and Lowenstein-Jensen media, which differentially allow bacteria with certain characteristics to grow whilst others are not able to survive [92, 98]. Usually, a few micro liters of the test sample are spread over the nutrient media in an agar plate [99]. The appearance of spots after culturing on the media in an incubator (usually at 20-37°C) is used to identify the presence of pathogens in the sample [92, 98]. To determine the concentration of bacteria, the number of spots is counted manually or with a colony counting machine [100]. Each spot is a bacteria colony and usually originated from one colony forming unit (CFU) in the sample [99]. As little as one CFU can be detected by this method. The culture time, which depends on the pathogen and the media chosen, can take up to several days, or even weeks [92, 98]. Cell plating is one of the cheapest cell-detection methods and nearly all bacterial strains can be identified by it [92, 98]. Because the method is slow and labor-intensive, more rapid methods are desirable, especially when a time-critical result is needed.

1.2.2.2   FLOW CYTOMETRY (FCM)

In flow cytometry (FCM), the cells are directed through a chamber. Light via lasers is emitted onto the sample molecules and the subsequent fluorescence and scattering is measured to detect the presence of cells [101]. The use of cell-type specific fluorescent antibodies makes it possible to distinguish and sort different cell types and other particles. The method is rapid and has a very high resolution (single cells can be detected), which is why it is commonly used to detect specific cells [102]. It has been deployed in the field but it is generally not easily portable or robust. Flow cytometry usually requires training for operation, as well as a laboratory environment [103].

1.2.2.3 IMMUNOASSAYS

Immunoassays are commonly used to detect cells, such as malaria or food bacteria, and cellular components. An immunoassay detects the presence or levels of a component of the cell of interest (e.g. antigen, protein, or a different macromolecule) in a solution through the use of a target-specific antibody or immunoglobulin. Immunoassays may be run in multiple steps with reagents being added and washed away at different stages. Immunoassays can be visualized through different types of labels (e.g. chemically linked to the antibody or antigen or using enzymes) [104].

Immunoassays that are visualized using enzymes are called "enzyme-linked immunosorbent assays (ELISA)". Enzymes coupled to the antibody or antigen (e.g. horseradish peroxidase, alkaline phosphatase or glucose oxidase) cause fluorescent changes in certain reagents (e.g. fluorescent dyes) or they can chemiluminesce themselves upon reaction [104, 92]. In addition, radioactive isotopes can be coupled to immunoassay reagents, in a reaction called radioimmunoassay (RIA). However, due to its dangers it is no longer commonly used [105, 106, 104]. Another approach is the real-time immune-quantitative PCR (iqPCR), which couples the immunoassay to PCR. Here, the label used in these assays is a DNA probe [107, 108, 104]. In addition, fluorogenic [109] or electroluminescent [104] tags can be used. The usual detection limit for cells is 10^3–10^5 CFU/ml. For many of the applications covered in this thesis (Table 8), the LoD cannot be achieved, hence making pre-enrichment steps necessary.

Immunoassays are used to specifically detect cells/cellular components of interest. However, they require extensive handling steps, refrigeration of reagents and often pre-enrichment steps. Therefore, robust and automated alternatives are desirable.

1.2.2.4 NUCLEIC ACID EXTRACTION AND DETECTION (PCR, RT-PCR)

NUCLEIC ACID AMPLIFICATION (PCR, RT-PCR)

An alternative strategy used in bacteria detection involves the extraction, purification, amplification and then detection of DNA or RNA of interest via amplification. The commonly used traditional method for DNA amplification is Polymerase Chain Reaction (PCR). To amplify DNA, temperature cycling between high temperatures (to dissociate DNA double strands) and low temperatures (to duplicate DNA strands with a polymerase enzyme) is employed. Reverse Transcriptase–Polymerase Chain Reaction (RT-PCR) is used for RNA amplification [103].

These methods are highly specific and sensitive, usually being able to detect less than 10 inserted copies of DNA or RNA.

PCR can be performed quantitatively (qPCR) in real-time using fluorescent reporter dyes that are readout in a real-time cycler. Examples are intercalator dyes or target-specific "Förster resonance energy transfer" (FRET) probes, such as TaqMan, LoopTaq, Light Cycler probes, molecular beacons, intercalator dyes and scorpion/Lux primers. Using target-specific FRET-probes it is possible to multiplex and hence to differentiate between different targets. Additionally, PCR can be performed qualitatively, which is commonly cheaper. Here, PCR is run in a thermocycler and a specific product is detected through bands of a specific size using electrophoresis instead of fluorescence readout[110]. Overall, PCR and RT-PCR are highly specific and sensitive, which is why they are commonly used in analytic applications. However, it requires a sterile and DNA-free environment, expensive equipment and it is labor intensive.

NUCLEIC ACID EXTRACTION

In order to perform a PCR or RT-PCR reaction, nucleic acids (e.g. DNA and RNA) need to be extracted from the cells prior to the test. DNA extraction in specific (which is covered in this thesis) consists of cell-disruption, lysis, removal of protein and contaminants and finally DNA purification[111]. Common methods for DNA extraction are outlined below.

- Magnetic beads: Paramagnetic beads with DNA binding capacity can be used for DNA extraction. Samples are lysed, after which they are brought in contact with beads and DNA binds to it. The resin is subsequently washed [111]. The magnetic beads are separated from the sample on a magnetic stand and DNA is eluted of it, typically at 65°C [111, 112, 113]. This method can be used in conjunction with PCR and can also be used to extract proteins.
- Ion exchange column: Solid-phase anion-exchange chromatography is based on the interaction between positively charged substrate and negatively charged nucleic acids [111]. Under low-salt conditions, the DNA/RNA binds to the substrate and contaminants get washed away. Using high salt conditions, DNA/RNA is eluted at high quality [111]. Many of these columns are based on silica-matrices. For PCR analysis, ion exchange columns are the most frequently used method and they were hence used for DNA extraction in this PhD thesis. [111, 112, 113]
- (A quick method for isolation of genomic DNA is to incubate cell lysates at high temperatures, or to perform enzymatic digestion. The lysates can then be used directly in downstream applications, though these are limited due to the presence of enzyme-inhibiting

15

contaminants, hence making it not deployable for PCR. [111] Therefore, this method is only used in this thesis when DNA is stained with intercalating dyes, rather than when a PCR reaction is performed. Similarly, in salting out and in organic solvent methods, proteins and other contaminants are precipitated from the cell lysate at high salt concentrations or using organic solvents [111]. These methods often contain high levels of contaminants [111], rendering it unsuitable for PCR and hence for use in this thesis [112].)

Overall, nucleic acid extraction strategies require a sterile and DNA-free environment and are labor intensive, as they require manual pipetting steps. In big analytic laboratories DNA extraction and amplification is currently automated with robots, such as the Roche COABS[114] or the Abbott M2000SP/RT [115], which can process up to 72 and 96 samples simultaneously. Generally, these high-throughput DNA/RNA extraction and amplification robots are expensive. For example, the combined COBAS system for DNA/RNA extraction and amplification costs between k$ 120-220 [116], which is why they are commonly only employed in big diagnostic laboratories. DNA extraction robots for small-to-medium throughputs (<25 parallel samples), which are relevant to the applications in this thesis, are also commercially available. They have been used successfully to minimize manual nucleic acid extraction processes in smaller laboratories. Nevertheless, as summarized in Table 9, these extraction devices require specialized equipment, costing tens to hundreds of thousands of dollars, which is why they are not yet broadly employed. Further, the extraction is commonly not easily scalable, meaning that the system can only run with a set number of parallel samples [117] [118] [119]. Often manual pipetting steps are still necessary (e.g. addition of elution buffer[120] or RNAse [117]), extraction reagents are often stored in large containers (rather than individually for each reaction [121]) and extraction kit variety is limited to the manufacturer [118] [119] [121]. The devices are usually not coupled to a specific DNA amplification device and the lack of an interface increases contamination risks and makes a special, DNA-free laboratory environment necessary [117] [118] [119]. Hence, lower-cost automated DNA extraction methods are needed that can be used with standard laboratory equipment. The system should be coupled to a DNA amplification and readout device with a contamination-free interface. Further it should be broadly applicable to different extraction and kit types. These attributes would make this system more broadly deployable, for example at the production site, sales location or in the field.

	QIACube	Magna Pure	Maxwell 16	NucliSENS® easyMAG	Nordiag Arrow	M24SP	EZ 1 Advanced
Manufacturer	Qiagen [122]	Roche Diagnostics [120]	Promega [117]	bioMérieux [121]	Autogen [118]	Abbott [115]	Qiagen [123]
Working principle	Pipetting and centrifuging; silica column. [122]	Pipetting; magnetic beads. [120]	Pipetting; magnetic beads.[117]	Pipetting; magnetic beads. [121]	Pipetting; magnetic beads. [118]	Pipetting; magnetic beads. [115]	Pipetting; magnetic beads [119]
Max. parallelization	12 [122]	8 [120]	16 [117]	24 [121]	12 [118]	24 [115]	6, 14 [119]
Turnaround time	~8 min [122]	~30 min [120]	~35-55 min [117]	~60 min [121]	~30 min [118]	~60 min [115]	~20 min [119]
Instrument costs ($)	~23,000 [122]	~30,000 [124]	~20,000[117]	~80-95,000 [124] [125]	~30,000 [118]	~90,000 [125]	30,000 (6 samples) [124]
	[122]	[120]	[117]	[121]	[118]	[115]	[119]

TABLE 9: Small-to-medium throughput (<25 parallel samples), automated DNA extraction methods.

1.2.3 NEW STRATEGIES FOR FIELD-USE

The traditional laboratory methods to detect contaminants require specialized scientific equipment, a continuous refrigeration chain for reagents and/or specially trained staff. They are often time-intensive, especially when a sample first has to be sent to a specialized laboratory for analysis. Field-deployable systems need to be automated, robust and portable. This section outlines novel detection methods and devices that have been used for field-deployable, low-cost and automated analytic applications.

1.2.3.1 NEW NUCLEIC ACID DETECTION STRATEGIES

There are several novel strategies for DNA and RNA amplification that do not require thermal cycling, but instead run at constant, isothermal conditions. This feature can lower detection and readout costs and is therefore particularly relevant for low-resource and field-use applications. Loop-mediated isothermal amplification (LAMP) is a new technique to amplify DNA (and RNA with reverse transcriptase) without the need for an expensive precision thermal cycler for heat regulation during PCR. Amplification of DNA by a scale of 10^9 can be achieved in less than 1 hour [126]. LAMP amplification requires temperatures between 60 and 70°C. The results can be readout using fluorescent, UV or visible dyes. LAMP is one of the most used isothermal DNA amplification methods, as it is particularly temperature robust. Furthermore, there are more primers available than for other methods. Alternative isothermal DNA amplification methods include the rolling circle amplification, RCA, as well as the recombinase polymerase amplification method, RPA. One example for isothermal RNA amplification method is NASBA (nucleic acid sequence based amplification) [126]. These methods are highly specific, usually being able to detect less than 10 inserted copies of DNA or RNA [126]. The isothermal nature of these reactions, as well as their sensitivity and specificity allow them to be field-deployable. Even though many isothermal DNA amplification methods still lack the ability to multiplex and to quantify results[126], they represent viable alternatives to PCR in point-of-care or field-use applications. The methods have been incorporated into portable isothermal DNA amplification devices, which are outlined in section 1.2.3.2.

1.2.3.2 PORTABLE OPTICAL READERS

This section summarizes portable, economic fluorometers and DNA amplification devices for field use at low-medium throughput (<25 parallel samples), which are already commercially available. They can perform fluorescent readout (Table 10) or DNA amplification (Table 11) using isothermal and PCR methods. As shown in Table 10 and Table 11, the commercially

available portable readers cost thousands to tens of thousands of dollars, due to the use of expensive detection methods, such as LCD cameras [127], optical setups employing beam splitting and lenses [119]. They have limited wavelengths, often cannot perform realtime readout [127] and can often be coupled to specially designed testing methods (e.g. isothermal amplification[128], PCR [129], LATE-PCR [128]) and custom kits only [130] [127]. Further, they still require manual sample preparation. Hence more versatile applicable, lower cost and automated (with a sample preparation strategy and interface) methods are desirable.

	Plate reader	ESE Log
Manufacturer	Various, e.g. Perkin Elmer, Tecan, Molecular Devices	Qiagen [128]
Price ($)	~33,000 [97]	2,800 [119]
Number of samples	96 [97]	8 [128]
Multiplex ability (# of wavelengths)	340-800 in 1nm increments [97]	2 [128]
Sample volume	μl-ml [97]	10-200 μl [119]
Temperature control	Yes [97]	No [128]
Flexibility	Flexible [97]	150 [128]
	[131]	[128]

TABLE 10: Comparison of portable fluorometers (<25 parallel samples). The grey column indicates a standard, reference laboratory device.

	Real-time cycler	**Hunter**	**Spartan DX**	**Bioseeq Plus**	**ESEQuant**
Manufacturer	Various [122]	Instantlabs	Spartan	Smith Detection	Qiagen
Price ($)	~20,000-69,000 [132]	14,000 [129]	12,495 [133]	37,900 [130]	4,500 [119]
Number of samples	96 [134]	6 [129]	12 [127]	6 [130]	8 [128]
Multiplex (# of lambda)	5-6+ [134]	2 [129]	2 [127]	2 [130]	2 [128]
Sample volume (µl)	>10µl [134]	20µl [129]	10- 25µl [127]	Swaps, or up to 5-10ml	50-200µl [119]
Temperature control	Yes [134]	Yes [129]	Yes [127]	Yes [130]	Yes [128]
Time-to-result (hrs)	1-3 [134]	1-2 [129]	1-2 [127]	1-2 [130]	0.5-2 [119]
Flexibility	Flexible [134]	Custom kit [129]	Flexible [127]	Custom kit [130]	Flexible [128]
DNA amplification	PCR, RT-PCR, isothermal; melt curve [134]	PCR [129]	PCR, RT-PCR, isothermal; melt curve [127]	LATE-PCR [130]	Only isothermal (no PCR) [128]
	[134]	[129]	[127]	[135]	[128]

TABLE 11: Comparison of different DNA amplification devices (<25 parallel samples). The grey column indicates a reference laboratory device.

1.2.3.3 BIOSENSORS FOR FIELD-USE

MICROFLUIDICS

Microfluidic (lab-on-chip) devices to perform the full analytic workflow (sample preparation/amplification and detection) for field use have been the focus of numerous research publications for the past decade. They have the advantage of being small, a few hundred micrometers in length. Lab-on-chip devices consist of micro-scale fluid channels and sensor chambers. They require only a small amount (micro liters) of reagent and test sample and have a high surface area-to-volume ratio, allowing for an easier localizing of the target substance to

the sensing surface [136]. They also provide automated and fully integrated assays that require fewer manual steps than traditional methods. Microfluidic sensors have been used to analyze a wide variety of biological substances and contaminants [6]. They have been used to automate sample preparation, because manual preparation commonly employs various manual labor steps. The systems have been used to prepare components of blood and DNA upstream a PCR, as well as for the purification of small molecules upstream of an immunoassay [6]. They have been integrated with most common laboratory bioassays, including PCR, immunoassays, flow-cytometry and electric impedance measurements [6, 136]. For cells, detection limits between 10^1 and 10^7 CFU/ml have been reported [136, 6]. The perspective to automate and miniaturize assays by using microfluidics has led to a large research boom in microfluidics over the last two decades [8]. However, only a limited number of devices are commercially available (e.g. Agilent Bioanalyzer, Fluidigm or Cepheid GeneXpert). Drawbacks of microfluidic devices include that generally commercial maturity is lacking, they require expensive hardware for fluidic control and optical readout and they are often still inflexible, being usable for a single application or processing step only [6].

NANOTECHNOLOGIES

Nano-structures (which have submicron dimensions) have been incorporated into biosensors (e.g. microfluidics) in various publications to broaden the application range and to reduce costs [136]. They commonly involve nanosensors, nanoparticles (magnetic or metal ones), as well as quantum dots. They have been used as probes, which are immunologically attached to pathogens to facilitate detection through fluorescence, dielectrophoresis, magnetoresitivity, and electrochemical methods [136]. Because most nanotechnology involves imaging as readout, the main challenge is to keep costs of the system low in order to make it field-deployable. Further, the applications are often still inflexible [6].

SURFACE PLASMON RESONANCE

Surface Plasmon resonance (SPR) is increasingly used in biosensors, such as microfluidic devices, to reduce costs of the optical readout [6]. SPR uses the reflective and refractive properties of thin films placed on surfaces of a dielectric material. Monochromatic p-polarized light is applied onto the surfaces and the reflected intensity of the light is measured for different incident angles. For a specific incident angle the reflected intensity dips [98]. This is the resonance angle and depends on the surface material, specifically the refractive index [137]. SPR can be used with any type of binding assay. For example, the antibody specific to a cell

can be cultured on a protein layer which is grown on top of a metallic film attached to glass, thereby allowing for a detection of cells. The sample solution is placed on top of this setup. The reflection intensity for different incident angles is measured continuously and the change in resonant angle is related to the concentration of pathogens in the test solution [138]. SPR has already been incorporated into (microfluidic) biosensors [6]. It is expected that they can contribute towards lowering the costs for optical readout, making microfluidic devices more field deployable [6]. However, the method is still inflexible, implying that the user cannot easily alter assay types or methods, but instead has to use the provided application.

1.2.4 SUMMARY

The introduced traditional and novel detection methods are summarized in Table 12. Traditional laboratory methods, such as gas chromatography and mass spectrometry, are precise methods to detect a variety of contaminants, such as alcohols, EG and DEG. Optical spectroscopy can be used to detect both contaminants and cells with high sensitivity and specificity. Traditional methods for cell-based analysis include cell culturing, flow cytometry, immunoassays and nucleic acid detection methods, such as PCR. To run PCR, extraction of nucleic acids is necessary, which is either performed manually or using expensive pipetting robots. Automated extraction robots for low-to-medium throughput (<25 parallel samples) are commercially available. They are often still expensive, require specialized kits and have no interface with a readout unit. Overall, the introduced traditional laboratory methods are accurate, sensitive and specific. However, they are time and labor intensive, often require expensive equipment and a specialized laboratory. Portable optical readers and biosensors have therefore been developed for field-use. Portable optical readers are generally still expensive, often applicable to limited applications and still require manual sample preparation. Biosensors include, for example, microfluidic devices, which can be coupled with nanotechnology and SPR-based methods, and whose goal is to pursue the entire analytic workflow. Even though first products are available, biosensors still lack commercial maturity, often require expensive hardware and are inflexible, suitable for a single application or step in the workflow only. The disadvantages of current strategies motivate the development of broadly deployable detection methods that are flexible, frugal and perform fully automated sample preparation and detection.

Detection Strategy	Detection limit	Time	Pros	Cons
Gas chromatography	e.g. 2.5mg/l of EG /DEG (84)(85)	Min-hrs	High accuracy and specificity.	Expensive lab equipment; not portable; special training required.
Mass spectrometry	e.g. 500μg/g or 2ppm of EG/DEG (84, 85)	Min-hrs	High accuracy and specificity.	Expensive lab equipment; not portable; special training required.
Optical spectroscopy	e.g. 0.01wt% alcohol in blood ; 10^4 CFU/ml for many cells	Min	High accuracy and specificity.	Expensive lab equipment; not portable; special training required.
Cell plating & colony counting[98]	1-10 CFU	hrs-14 days	Accurate.	Long-time; manual effort high; laboratory needed.
Flow cytometry (FCM)	Single cells	Min	High resolution.	Expensive lab equipment. special training required.
Immunoassays, e.g. ELISA[98]	$1.2 \times 10^3 - 10^6$ CFU/ml	Min	Specific.	Pre-enrichment; laboratory needed.
PCR (with DNA/RNA extraction) [103]	<10 to ca. 10^3 (depending on the matrix)	1 to 4hr	Specific; sensitive; multiplexing possible.	Heat regulation needed; expensive equipment (especially when automated); specialized training and manual steps with high contamination risk needed (when not automated).
Low-to-medium throughput, automated DNA/RNA extraction	<10 to ca. 10^3 (depending on the matrix)	1-2 hr	Low contamination risks; automated.	Expensive equipment, limited kits and applications, often not easily scalable.
Isothermal amplification (LAMP, NASBA, etc.)	<10 to ca. 10^3 (depending on the matrix)	0.5-1hr	Low-cost; sensitive; robust; ease-of-use.	Not quantitative; no multiplexing.
Biosensors (e.g. microfluidic chips or nanostrategies) [136]	>10^1 CFU/ml	Min-hrs	Small; easy to use; disposable.	(Still) expensive; inflexible.
Portable DNA amplification devices	<10 to ca. 10^3 (depending on the matrix)	>30min-hr	Portable; generally cheaper than real-time cyclers.	(Still) expensive, limited wavelengths and flexibility; no sample preparation.

TABLE 12: Comparison of different analytic testing methods.

1.3 RELEVANT ANALYTIC MARKETS

In this thesis, versatile, automated and robust detection methods were developed. As a first sample application the focus was put on food safety. This section outlines the food safety, as well as other relevant markets to the systems introduced in this thesis.

1.3.1 FOOD SAFETY MARKET

The food safety testing market size is bn\$ 2-4 ([61] and extrapolated from [139, 140]), with about half of the tests being for pathogens [139, 140, 61] as shown in Figure 1. In 2008 the share of rapid tests was 40%, whilst in 2013 it is estimated to be 49.3% of the food testing market [61, 141, 142, 143]. Rapid testing methods include nucleic acid based assays (e.g. DNA hybridization, PCR, DNA micro assay), immunological methods (e.g. ELISA), flow cytometry and biosensors [144]. Immunoassays and PCR (15-20%) make up the largest segment of the rapid testing methods. The rapid testing method market is witnessing double digit growth at twice the growth rate of the global food testing market [61]. Currently, the market players are focusing on the development of new products and applications, which account for the highest share of the total competitive developments in the global food safety testing market [61].

1.3.1.1 FOOD PATHOGEN TESTING

In pathogen testing segment, *salmonella* testing accounts for the major share, namely 40% of the overall contaminants testing in 2010 [61]. Because it is usually tested at high throughputs in specialized laboratories, *salmonella* testing was not incorporated into the (low-to-medium throughput) devices introduced in this thesis. In terms of growth in rapid testing, *E.coli* testing is witnessing the fastest growth with a CAGR of 11% from 2010 to 2015 [61]. *E.coli* tests for low-to-medium throughputs (up to 10,000 tests per year) could be used in batch processes, by small manufacturers, at sales locations or by food services.

1.3.1.2 GLOBAL DISTRIBUTION OF FOOD TESTING

According to one report, Europe accounts for the major market for global food safety testing, because stringent regulations are forcing food processors to test for hazardous material and microorganisms in food products. Increasing food poisoning outbreaks will ensure more regulatory guidelines pertaining to food testing in future. Europe accounted for 38% of the global food safety testing market in 2010. North America was the second largest market for food testing, contributing around 30% [61].
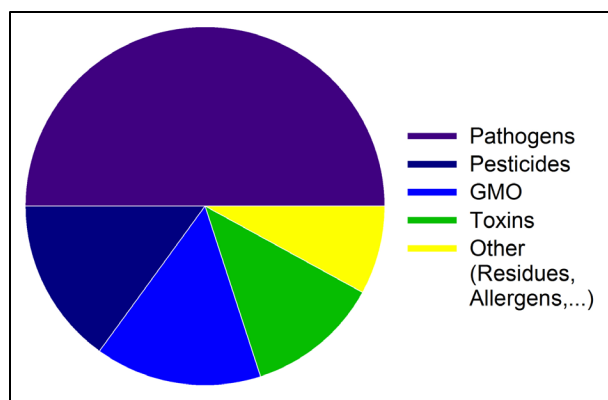
FIGURE 1: Global food safety market distribution by contaminants, 2010. GMO stands for genetically modified organisms. Adapted from [61].

1.3.2 OTHER MARKETS

The global point-of-care market (bn$ 13.8 in 2011 [145]), which is part of the global in-vitro-diagnostics market (bn$ 44[146]), is larger than the food diagnostic testing market of around bn$ 2-4 ([61] and extrapolated from [139, 140]). The latter is part of the global food safety product market with a size of bn$ 16.8 in 2016 [147]. Even though the market for medical in-vitro diagnostics is significantly larger than that for food safety, the latter is expected to be more easily accessible. Food safety diagnostics do not qualify as medical devices or consumer products and are not subject to the same regulatory approvals of clinical IVD markets. This means that companies can save costs by going through less stringent FDA protocols as regulatory guidelines relating to medical applications [146].

In terms of entry barriers and size, the environmental water analysis market is expected to be similar to that of food safety. The global water testing market was bn$ 2.9 in 2009 with an annual growth rate of 5% and with an EU share of the global market of 38% [148, 149]. The EPA recommendation for coliform bacteria in drinking water is 0 CFU/100ml [150] and 1-4 CFU/ml for recreational waters [151]. Generally, this means that safety limits for water are generally more stringent than for food safety applications, which is why the latter is focused as a first application in this thesis.

In addition to the regulated medical, food and environmental diagnostics markets, the academic research market is of great interest for versatile, affordable and automated sample preparation and detection methods. This is because fewer regulations lower the entry barriers into this

market. It was estimated that the global academic DNA analysis market for both extraction and amplification in academia is bn$ 0.69[1]. According to this number and the global DNA extraction (without amplification) market for all industries being bn$ 1.5 with an annual growth rate of 10-15% [152], the share for academic laboratories in DNA extraction is ~25%. Assuming the same share for protein extraction, its market for academic labs is bn$ 0.30 for protein extraction and bn$ 0.55 for both protein extraction and readout [152, 153]. DNA and protein extractions in the academic testing market are hence applications that frugal, automated and versatile methods could also be used for.

1.3.3 SUMMARY

In this thesis, rapid testing methods for food safety applications are emphasized. The global food safety market for rapid testing methods has a size of bn$ 2-4, with half of the tests being for pathogens. There is an increasing need for rapid detection methods, for which *E.coli* is witnessing the fastest growth. Even though the medical diagnostics market is larger (bn$ 13.8) than the food safety market, it has more stringent regulations and hence higher entry barriers. Academic analytics (DNA, RNA and proteins), followed by environmental testing (such as water safety) were also identified as promising markets.

---

[1] 7,800 biological/agricultural PhD students graduate each year in the US[210], which account for 25% of the global PhD student population[209]. Assuming on average 8 PhD students per lab and an average PhD duration of 4 years, the worldwide number of academic labs is 62,400. Assuming that 1,000 DNA extractions ($6 each) are run per year in each lab and that half of the extracts are processed consecutively with PCR or an immunoassay ($5 each including system depreciation), the global academic DNA analysis market for academia is expected to be bn$ 0.69.

CHAPTER 2: LOW-COST OPTICAL DETECTION (LABREADER)

Commercial laboratory methods described in Chapter 1 are useful for identifying the presence of contaminants. One of these methods is fluorescence and absorption spectroscopy. The commonly used laboratory method, a fluorescent plate reader, characterizes the absorption, emission and/or fluorescent spectra over a broad range of specific wavelengths, which are selected flexibly. However, plate readers generally require a laboratory environment. The mechanical components enabling wavelength-selection (such as movable diffraction gratings and lens assemblies) demand mechanical and thermal stability. The halogen lamps that generate UV-wavelengths and the readout require significant electrical power [154]. As a result, these precision instruments are generally unsuitable for use outside the laboratory. However, there are many situations where the ability to measure absorption and fluorescence outside of the laboratory is important: for example, detecting contaminants in food, medicine and agricultural products in the field or at the production site, or evaluating microbial contamination of drinking water. As mentioned in Chapter 1, there are a number of portable devices that are starting to bridge the gap between laboratory and field analysis, but these are still typically orders of magnitude too expensive and not flexible and robust enough for widespread field use where they are needed, for example, to test for food pathogens. Therefore, a low cost, portable multi-channel, multi-sample UV/vis absorption and fluorescence reader (referred to as LabReader) is introduced. The LabReader is robust and has the sensitivity of commercial instruments costing significantly more [154, 96]. In the future, it could be adjusted for wireless operation with batteries and interfacing with mobile devices. In this thesis, new and existing assay methods were integrated into the LabReader to detect pathogens and contaminants for medical, food, environmental and consumer product detection [96].

2.1   DESIGN (MECHANICAL AND ELECTRICAL)

This section describes in detail the mechanical design and the electronics of the LabReader (Figure 2). For detection, a device made from a rapid manufactured plastic housing was used that encases simple LEDs and detectors surrounding the sample. Detection robustness is achieved by concurrently using UV absorption and fluorescence. The LabReader employs a round geometry allowing for simultaneous four-channel measurement of a baseline and an unknown contaminated sample inside a glass test tube. The LabReader uses a particularly narrow range of wavelengths relevant to the chemistry of interest. For the design, the author collaborated with Jim MacArthur (electrical design), Alexander Slocum (mechanical design) and Peter Lu (optical layout and data readout) (see Chapter "Contributions"). The section is adapted from publications cited in references [154, 96].

2.1.1   ELECTRICAL DESIGN

The general geometry for absorption detection is shown in the device schematic in Figure 2 and Figure 3 (section adapted from [154]). To measure absorption, the liquid sample is illuminated with an LED (L1). Using a photodiode, the intensity change after the light has passed through the sample is measured. For simplicity and robustness, a form of photodiode integrated with an op-amp in a single package (D1) was chosen, which outputs a voltage proportional to the incident light striking the photodiode (Texas Advanced Optoelectronic Solutions TSL257). This semiconductor light-to-voltage detector costs ~$1. The low cost of this detector component allows for including a second detector (D4) next to the LED in addition to using the detector for primary absorption measurement. This detector is coupled to an active feedback loop with an op-amp (A1) to stabilize the LED's intensity at a constant level even as temperature changes, due to the external environment or as the LED is powered on.
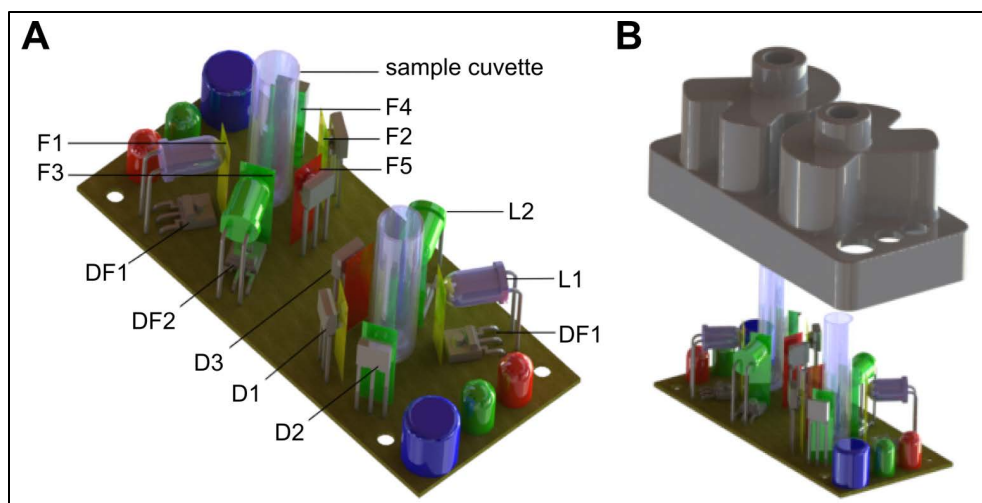
FIGURE 2: Schematic overview and rendering of the multichannel LabReader. (A) Interior device electronics. UV-light emitted by an LED (L1) passes through an excitation filter (F1), the sample, and another filter (F2) before absorption is detected (D1). Detector DF1 provides a feedback signal to an op-amp that maintains constant light output from L1, whose baseline level is set by a microcontroller. Light from a similarly stabilized green LED (L2) is filtered (F3) before passing through the sample. Green light is filtered and detected for green absorption (F4, D2) and red fluorescence (F5, D3). Voltage outputs from the detectors (D1, D2, and D3) are digitized and sent from a microcontroller to an external computer. LED 1 ("yes") and LED 2 ("no") are simple light-readouts telling the end-user whether the sample is contaminated or not (LED1 and LED2 are design suggestions and have not been integrated into the used prototype). (B) To assemble a device, two mirror image enclosure units are placed over the circuit board containing the LEDs and detectors. The optical setup and electronics are precisely aligned in the enclosure.[2]
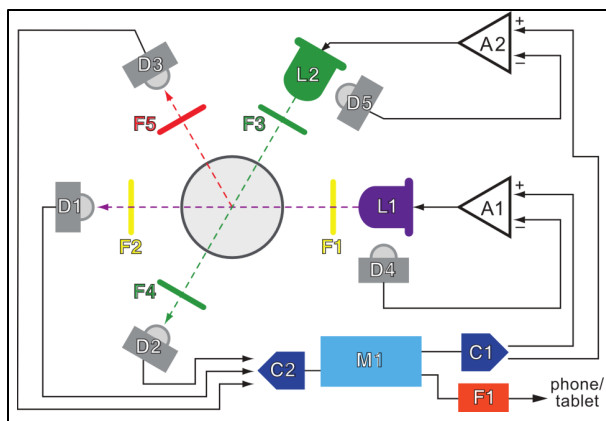
FIGURE 3: LabReader optical schematic. UV light emitted by an LED (L1) passes through an excitation filter (F1), the sample, and another filter (F2) before its absorption is detected (D1). Optical feedback using an additional sensor (D4) and op-amp (A1) maintains a constant light output from L1, whose level is set by the micro-controller (M1) via a voltage generated by a D/A converter (C1). Light from a similarly stabilized green LED (L2, D5, and A2) is filtered (F3) before passing through the sample; green light is filtered and detected for green absorption (F4, D2) and red fluorescence (F5, D3). Voltage outputs from the detectors (D1, D2, D3) are digitized by an A/D converter (C2) and sent to the microcontroller (M1), which formats and transmits the data via USB (F1) to a computer, smart mobile-phone or tablet.[3]

The circuit is a single-amplifier proportional servo with a bandwidth of 1 KHz, which effectively removes thermal drift and reduces errors from mechanical vibration. The high-level voltage output of the sensor makes for a simplified servo circuit. Each LED's driver adjusts the LED current until the sensor voltage equals the voltage set by the microcontroller (M1) via a D/A converter (C1). This active illumination stabilization, a feature found in advanced laser systems, is crucial to reproducible light intensity measurements. The analog voltage from the detector is converted via an A/D converter (C2) to a digital value that is sent to a microcontroller (M1), then as ASCII over wired or wireless USB (U1) to a Linux-based (Ubuntu) host, where the data processing and analysis (C++), storage and communication are performed [154]. The output data is a simple list of 16-bit integer, corresponding to the digitized voltage levels from each

---

light-to-voltage detector. A variety of host computing platforms were used, including an ordinary Intel-based laptop, and an ARM-based mobile phone/tablet platform (NVIDIA Tegra family), with equivalent functionality. A circuit diagram with specific components is shown in Figure 4A; a photograph of the circuit boards and the LabReader itself is shown in Figure 4B.

2.1.2 MECHANICAL DESIGN

The LED, sample, detector and filters are held in place deterministically by an opaque plastic enclosure. The experimental unit was made by stereolithography (SLA). In mass production it could be injection molded, making it simpler to manufacture and cheaper than $1. High-precision location of the LED, sample, and detectors was achieved by using the components' leads themselves as flexure spring features, which force the components against reference features, all within the same monolithic part. The bottom of the enclosure is depicted in Figure 5, showing a clear view of the cavities to hold the components; a close-up of one of the light-to-voltage detector cavities is shown on the right hand side of the figure. A key to successful optical detection was the incorporation of plastic filters without any light leakage. To achieve this, creating a thin slit (<1mm) would not be practical. Instead, larger near-overlapping mold cores were designed. When the mold is opened, an effective thin gap is created, as shown in Figure 5C. For the sample to be illuminated from multiple sources, a round glass test tube (Durham 6×50 culture tube) was selected as the chemical reaction chamber. Clearance around the test tube walls accommodates tolerances, while the use of a test tube with length-to-diameter ratio greater than ten keeps the tilt of the test tube to a level that does not affect the readings. This mechanically-robust design has no moving parts and ensures positional repeatability: samples removed, reinserted, or measured in different test tubes, yielded results varying by only 5% (n=10).
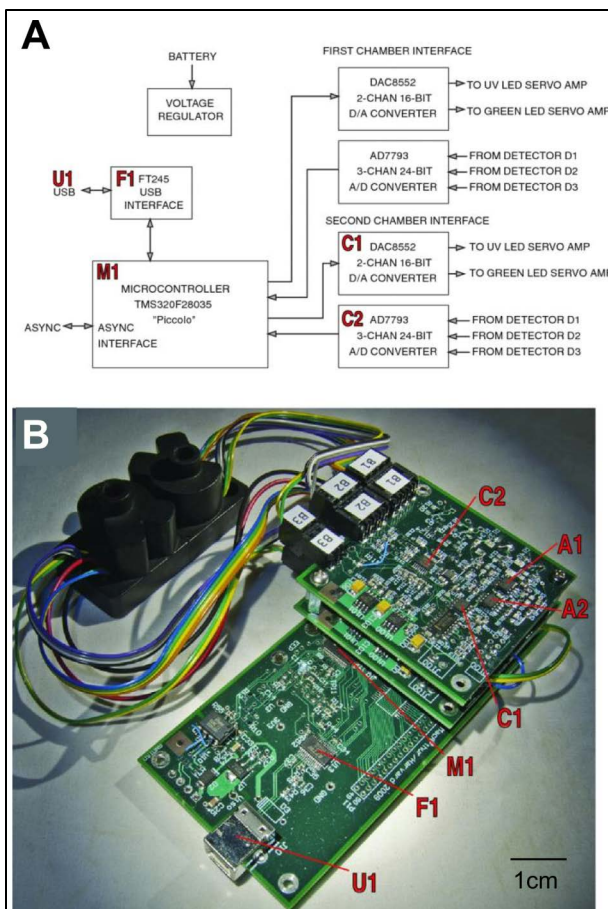
FIGURE 4: LabReader circuit diagram and electronics. A) Circuit diagram showing specific electrical components of the detector, with microcontroller (M1), D/A converter (C1), A/D converter (C2) and USB Interface (F1) components labeled as in Figure 3. (B) Photograph of the detector (black, upper left) and circuit boards, with major components labeled with red letter corresponding to labels in (A) and in Figure 3.[154][3]
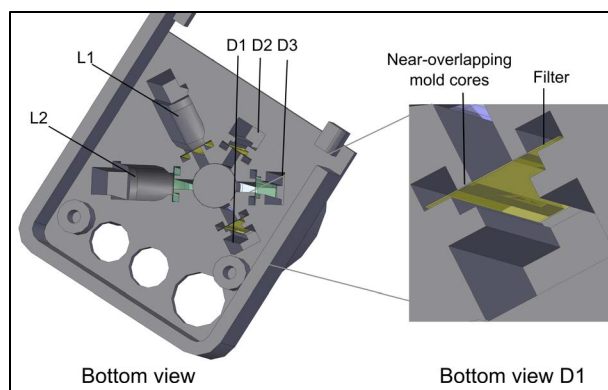
FIGURE 5: Mechanical LabReader design. View of the bottom of the plastic enclosure, showing openings for two LEDs (L1 and L2 in Figure 1) and 3 light-to-voltage detectors (D1, D2 and D3). A close-up of the opening for a light-to-voltage detector, D1, showing the slit created by near-overlapping mold cores for thin filter plastic.

2.2   CHEMICAL ASSAYS

There are many situations, where the ability to measure absorption and fluorescence outside of the laboratory can be critically important: for example, detecting contaminants in food, medicine, drinking water and agricultural products in the field, at the point-of-care or at the production site (Chapter 1). In many countries, contamination testing is simply not performed, on account of the cost of analytical laboratory equipment and a scarcity of trained users. In many of these cases, the specific wavelengths of interest to be probed are *a priori* known, and the user would simply like to measure the absorption or emission, and/or the subsequent time evolution of these quantities, at known wavelengths. Hence, using the LabReader with fixed wavelengths opens up the possibility of precise measurements outside the laboratory. In this section, chemical methods are introduced for the rapid quantification of a wide range of chemical and microbial contaminations using the portable device described above. Detection methods are described for: EG, DEG, alcohol, and the presence of the following bacteria: *S. enterica, V. cholerae, E.coli* and yeast used in a malaria model (section adapted from [96]).

2.2.1 CHEMICAL MATERIALS AND METHODS

2.2.1.1 COMPARISON WITH PLATE READER

For comparing the sensitivity of the plate reader with the LabReader a Glucose Oxidase Assay Kit from Invitrogen was used (Amplex Red Glucose⁄ Glucose Oxidase Assay Kit - Cat. No. A22189). In this assay, glucose oxidase reacts with d-glucose to form d-gluconolactone and H_2O_2. In the presence of horseradish peroxidase (HRP), the H_2O_2 then reacts with the Amplex Red reagent in a 1:1 stoichiometry to generate the red fluorescent oxidation product, resorufin. The reagents were prepared according to the kit protocol. To start a reaction for measurement in the LabReader, 175mg of glucose samples were added to 175mg of the reaction mixture in a round 6×50mm glass tube (Durham Culture Tubes 6×50). A positive control (200µM) was always run in parallel, in the second sample chamber. The absorption and fluorescence values were monitored in the detectors for 5 minutes (i.e. initial kinetics). The reaction gradient was calculated over the first 5 minutes and normalized by the positive control. To start a reaction in the fluorescent plate reader (Molecular Devices, SPECTRAmax™ GEMINI XS) 50 µl of glucose samples/controls were added to 50µl of reaction mixture in a 96 well-plate. The reactions were monitored for 30 minutes in 15s intervals with excitation/emission wavelengths set to 530nm and 590nm. Negative controls were run in parallel. The reaction gradient was calculated by the normalized fluorescence change (with respect to the negative control) in the first five minutes.

2.2.1.2 ETHYLENE GLYCOL

Samples, S, containing ethylene glycol (obtained from Sigma Aldrich SAJ first grade) were mixed with household products and medicines at different mass percentages. To prepare the enzyme stock solutions, an alcohol-dehydrogenase-NAD reagent (A) was made by adding 15ml of Tris-HCl buffer, pH 8.8, 0.1M (Bio-Rad) to 50 mg NAD (Sigma Aldrich N8535). In mixture B, 0.1 ml of Tris-HCl buffer, pH 8.8, 0.1M (Bio-Rad) was added to 100mg yeast alcohol dehydrogenase (USB/Affymetrix #10895). To start a sample reaction, 120µl of the sample, S, were placed in a round 6.50mm glass tube (Durham Culture Tubes 6.50). Next an enzyme mixture, C, containing 480µl of solution B and 40µl of solution A was prepared. All volumes were confirmed by weighing with a scale (Mettler Toledo). To start the reaction in our device, 240µl of C were added to each tube containing sample, S. A 5.4wt % EG sample in buffer were always run in parallel as a control.

2.2.1.3   DIETHYLENE GLYCOL AND ALCOHOLS

Samples, S, of diethylene glycol and alcohols at different mass percentages were prepared in Tris-HCl buffer, pH 7.8, 0.1M (Bio-Rad). Stock solutions A and B (see above) were prepared. In addition stock solutions of 0.05wt% Amplex Ultrared in DMSO (solution D), 0.044wt% Horseradish Peroxidase Type 1 (Sigma Aldrich P8125) in Tris-HCl buffer, pH 7.8, 0.1M (solution E), 12wt% Peroxidase from *Enterococcus faecalis* (Megazyme, E.C. 1.11.1.1) in phosphate buffer, pH 6.0, 0.1M (solution F) and 0.2 mg/ml Flavin Adenin Dinucleotide (Sigma Aldrich) in deionized water (solution G) were prepared. The final enzyme mixture H contained 480µl of solution B, 40µl of solution A and 20µl each of the solutions D, E, F and G. The reaction was started and read out as described for EG above. For the DEG samples, a reference sample of 5.4wt% DEG and for alcohols a sample of $5.4 \cdot 10^{-3}$wt% was always run in the second chamber as a control.

ENZYME AND PH-OPTIMIZATION

To screen different alcohol dehydrogenases for their specificity in reacting with DEG the fluorescence product was measured in a plate reader (Molecular Devices) for 5.4wt% EG samples in cough syrup and in glycerol, respectively. Pure buffer with one enzyme (USB) was used as a control. The "relative interference" of each enzyme was measured by dividing the initial fluorescence and UV reaction gradient of each sample by the pure control. The pH of the assay solution was optimized by varying the buffer pH from 6 to 9 and choosing the pH that gives the highest signal-to-noise ratio. The use of NADH oxidase instead of NADH peroxidase made the assay unstable, as NADH oxidase solution decays within minutes at room temperature.

2.2.1.4   E.COLI, SALMONELLA AND CHOLERA BACTERIA IN FOODS AND WATER

Cultures of *E.coli* (strain: DH5alpha), *S. enterica* (strain: LT2 Delta PhoP/Q S typhi) and *V. cholerae* (strain: VC O395NT) were grown. Bacteria were stained with 2.5µM SYTO 85 (Invitrogen Cat. No. S11366) in deionized water for 3-30 minutes at 250rpm and 30°C in the dark; the resulting solutions of stained bacteria are referred to as samples I. The concentration of bacteria in each solution I was measured using the absorption value at 600nm (Nanodrop 2000). In addition, samples of water (J), milk (K) and egg whites (L) were stained with 2.5µM SYTO 85. Water (J) and milk (K) samples were stained directly as described above. Egg whites (L) were first diluted at a volume ratio 1:1 with deionized water, then vortexed and filtered with a

100µm filter (BD). The filtrate was centrifuged at 4300rpm for five minutes and the pellet was reconstituted with water at the same volume of the original egg white sample (L). Mixtures (M) of stained bacteria (I) were prepared with the respective stained products (J, K, L) at different mass fractions. Mass fractions were determined using a scale (Mettler Toledo). To optically measure M using the detectors, 360µl of a stained sample mixture M were placed in a round 6.50 mm glass tube (Durham Culture Tubes 6.50). All volumes were confirmed by weighing the samples (Mettler Toledo). A negative, buffer-only control was run in parallel and measured in the detectors. For SYTOX Orange staining cells were lysed and stained with 0.1µM SYTOX Orange (Invitrogen Cat. No. S-34861) in TE-buffer for 5 minutes. Further protocols as part of the bacterial staining optimization may be found in [96].

2.2.1.5   YEAST IN RED BLOOD CELLS (MALARIA MODEL)

Baker's yeast (2.86 Mio yeast cells/ml in distilled water) was stained with 5µM SYTO 85 (Invitrogen Cat. No. S11366) in deionized water for 5-60min in the dark. After centrifugation, the bacteria were reconstituted with an equi-volume amount of water in 0.5g/ml sucrose (yielding solution N). The concentration of bacteria of the resulting solution, N, was measured using the absorption value at 600nm (Nanodrop 2000). The same procedure was used to stain 2.86 Mio cells/ml bovine red blood cells (Lampire Biologicals #7240807) in sucrose-water, yielding stained solution O. After cell staining, mixtures P containing the components N and O at different mass fractions were prepared utilizing a scale (Mettler Toledo). For the measurement in the LabReader, 360µl of a stained sample mixture P (prepared above) was placed in a round 6.50mm glass tube (Durham Culture Tubes 6.50). The volumes were confirmed by weighing the samples (Mettler Toledo). A negative, buffer-only control was run in parallel. For SYTOX Orange staining, cells were lysed and stained with 0.1µM SYTOX Orange (Invitrogen Cat. No. S-34861) in TE-buffer for 5 minutes.

2.2.1.6   DETECTION AND QUANTIFICATION LIMITS

Detection and quantification limits were determined according to ICH standards. The detection limit, LoD, was determined according to the International Conference on Harmonization (ICH) standards, which defines the LoD as 3 standard deviation of the negative control, implying that the probability of false positive is small (1%) and that of a false negative is 50% for a sample that has a concentration at the LoD[155][156]. The limit of quantification, LoQ, was calculated as 10 standard deviation of the negative control[155][156].

2.2.2 RESULTS

2.2.2.1 COMPARISON WITH A PLATE READER

The LabReader fluorescence (at emission/excitation wavelengths of 530/560 nm) has a sensitivity comparable to a commercial plate reader, as was tested by comparing them with the fluorescence emission of a standard glucose assay. The results in Figure 6 represent averages of initial reaction gradients in the first five minutes for at least three independent runs. Both the LabReader and plate reader have LoDs of ~7μM (LoD calculation defined in Chapter 2.2.1.6).

2.2.2.2 ETHYLENE GLYCOL

Many reactions involving EG are known; however, those involving enzymes are particularly promising because they offer great specificity and sensitivity. To detect EG, a known, naturally occurring enzymatic reaction is used, where alcohol dehydrogenase (ADH) converts a hydroxyl group to an aldehyde and simultaneously converts the coenzyme nicotinamide adenine dinucleotide into its reduced form (NAD^+ into NADH) (Figure 7A)[24][91]. Hence, the absorption of NADH at 350-370nm should reflect the concentration of EG. The EG sample was illuminated with the UV LED and the intensity change was measured using a semiconductor light-to-voltage detector, after the UV light had passed through the liquid EG sample.
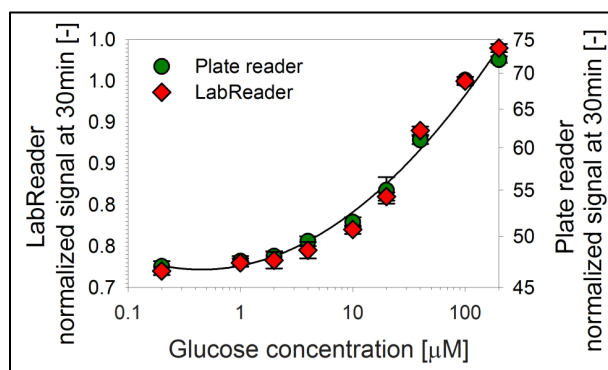
FIGURE 6: Comparison of the LabReader fluorescence intensity with a plate reader. A fluorescent glucose assay with three independent runs each is used (Invitrogen; emission/excitation = 530/560 nm). The data represent the reaction gradient of the first 5min normalized by a reference glucose sample (adapted from[96]).
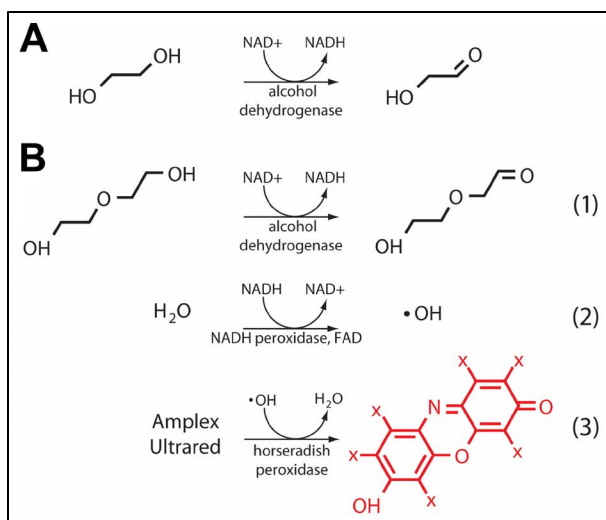
FIGURE 7: Chemical reactions. (A) ADH converts EG to an aldehyde in the presence of NAD+, which is converted to NADH; the increase in NADH concentration is measured with the UV absorption detector. (B) The DEG reaction begins with the same first step (A), but instead of detecting NADH directly, NADH peroxidase converts NADH back to NAD+ with an FAD coenzyme. This reaction generates hydrogen peroxide, which forms radicals that convert a resazurin-based dye into its fluorescent form. The increase in fluorophore concentration is detected with the fluorescence detector.[96][2]

To determine c_ε, the concentration of EG, a solution of ADH was added to the sample, the sample was inserted into the sample chamber, and the voltage, V_{ua} (t, c_ε), measured by the UV absorption detector, was recorded once per second for five minutes. For pure EG (c_ε=100%), the V_{ua}(t, c_ε) data show linear relationship on a log-log plot, demonstrating a power-law behavior, as indicated by the purple line in Figure 8A. Because the test tube has a circular cross section and the LED has a distribution of illumination angles, a single path-length was not well defined. Therefore, a simple Beer's Law calculation could not be relied upon for the absolute absorbance. Instead, the LabReader was calibrated with samples of known c_ε in water, from the FDA safety limit of c_ε=0.1% to the pure case, c_ε=100% [1]. In all cases lines on the log-log plot were observed as shown with colored lines in Figure 8A. As shown with the blue circles in Figure 8B, the power-law exponent magnitudes, $\gamma(c_\varepsilon)$, monotonically increases with c_ε. An optical feedback loop ensured that the LED intensity remained constant irrespective of environmental changes. Thus, there were no adjustable parameters in the determination of the power law exponent, $\gamma(c_\varepsilon)$. These data demonstrate the ability to measure c_ε in drinking water with a detection limit below 0.1% EG at all concentrations deemed unsafe by the FDA.

Quantifying c_ε in water, however, does not itself demonstrate the effectiveness of the detection methods in real-world products and medicines.

These have a number of other ingredients that could interfere with the reaction. In particular, most products involved in historical EG poisoning incidents normally have a large fraction of glycerol, propylene glycol or polyethylene glycol [157, 26]. These three-carbon glycols have hydroxyl groups that ADH could in principle act upon, altering the measured reaction rate and obscuring the true c_ε. There are a number of ADH variants commercially available. While in general they give similar results for c_ε in water, subtle differences in structure could have a greater impact in their relative sensitivity to EG in the presence of other glycols. This sensitivity was expected to be even more relevant for DEG, as it is less reactive than EG due to its longer carbon chain. It was hypothesized that it was possible to screen the relative interference from glycols in different ADHs. This would allow the selection of the ADH with the least interference from glycols compared with DEG. To investigate the effects of these differences, five different ADH variants were screened for interference by mixing DEG with glycerol, and separately with a mixture of cough syrup containing polyethylene glycol (see 2.2.1.3). The results of the DEG assay were then compared to the same concentration of DEG in water (see Table 13). The particular ADH variant (USB/Affymetrix) that exhibited the least interference was selected for the assay, and it was used in all measurements (including the calibration of EG in water).

With the optimized ADH reaction, EG was detected in real-world scenarios, namely household products containing glycols (see Figure 8B). Samples with different c_ε were measured in a variety of unmodified ingestible household products, where contamination has led to historical poisonings that resulted in fatalities: toothpaste, cough syrup, acetaminophen/paracetamol syrup and antihistamine (allergy) syrup[26]. Several name brands and generics of each type were chosen, to assure a broad sampling, and the measurements were repeated analogue to the procedures used for water.
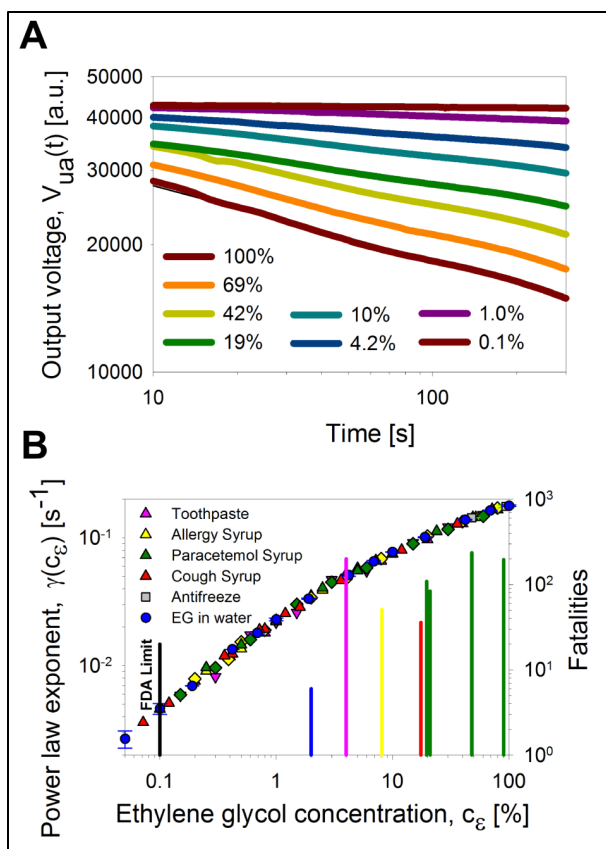
FIGURE 8: Detection of ethylene glycol contamination using UV absorption. (A) Time evolution of output voltage $V_{ua}(t)$ from the UV detectors shown on a log-log plot with symbols for different EG concentrations, c_ε, in water. The data fall onto a straight line for each sample, demonstrating power-law scaling. (B) The power law exponent, $\gamma(c_\varepsilon)$ of each line varies monotonically with c_ε, shown with blue circles for pure EG. The $\gamma(c_\varepsilon)$ values for a variety of different household products (colored triangles) and antifreeze (squares) all fall onto the same master curve. The FDA safety limit is indicated with a grey vertical line. EG concentrations of historical epidemics are indicated with bars whose color indicates the type of contaminated product; the number of deaths in each incident is represented by the height of the bar, indicated on the right-hand vertical axis. Each data point is the result of one measurement. [96][2]

Enzyme manufacturer	Product #	Relative interference: glycerol	Relative interference: cough syrup
Sigma	A7011	10.82±0.41	6.11±0.28
USB	10895	7.24±0.35	2.58±0.09
Worthington	LS001069	12.92±0.76	5.64±0.12
AppliChem 1	A7827	15.69±0.91	6.46±0.24
AppliChem 2	A7892	11.43±0.99	6.85±0.52

TABLE 13: Relative activity of alcohol dehydrogenases in the DEG assay. The "relative interference" of each enzyme was measured by dividing the initial fluorescence and UV reaction gradient of each sample by the pure control. The data are the results from at least 3 independent runs [96].

Using the optimized ADH assay it was found that the power law exponent, $\gamma(c_\varepsilon)$, increases monotonically with c_ε, as in the pure case shown in Figure 8A. It was also observed that the numerical values of $\gamma(c_\varepsilon)$ remain consistent irrespective of the product tested, as shown with colored symbols in Figure 8B (each data point is the result of one measurement). It was observed that all data from all products collapse onto a single master curve (with a standard error of 2.58 %), which is indicated with a black line in the figure. Optimizing the ADH enzyme variants had indeed removed any interference from other glycols normally present in the products and universal scaling was achieved. This enzyme method can quantify c_ε at all unsafe levels above the FDA limit of 0.1wt%, in all real products involved in historical contamination incidents. The results furthermore suggest that the method could work well even for products where EG contamination has not yet been observed.

2.2.2.3   DIETHYLENE GLYCOL

Like EG, DEG poisoning has also caused mass outbreaks worldwide (see Chapter 1.1.1). ADH measurements for different DEG concentrations, c_δ, in water were taken, expecting it to be less reactive because of the longer carbon chain of DEG compared to EG. Experimentally, it was observed that DEG has significantly lower ADH activity. Hence, it was not possible to distinguish low concentrations of DEG with this simple UV absorption assay alone. Therefore, it was decided to amplify the DEG reaction products by adding enzymatic steps involving fluorescence-based dyes. Fluorescent dyes principally should have a higher signal-to-noise ratio than absorption. Beginning with the ADH reaction, the NADH product reacts with NADH peroxidase and the coenzyme flavin adenine dinucleotide (FAD), which generates free radicals that, in the presence of horseradish peroxidase (HRP), convert an essentially non-fluorescent resazurin-based dye into a resorufin-based fluorophore[95], as shown in Figure 7B. However,

the pH for maximum activity differs significantly for the different components in the reaction chain: ADH is most active at pH~8-10; NADH peroxidase, pH=5; HRP, pH=6-6.5; NAD and FAD, pH=7. It was therefore not obvious that these particular steps could be coupled at a single fixed pH, and still result in detectable fluorophore generation. This possibility was investigated by running the complete reaction chain under a variety of pH conditions. The data depicted in Figure 9 represent results from a single measurement. The greatest amount of activity was found at pH=7.8, which was used for all subsequent measurements. NADH peroxidase is used, rather than NADH oxidase, as the latter solution is unstable and decays within minutes at room temperature. Under the optimized assay conditions, a pure DEG sample, c_δ =100%, produced a visible red color change in a few minutes while a c_δ=0 did not. This result demonstrated, at least qualitatively, the success of the reaction chain in the presence of DEG. In order to more precisely quantify the progress of this reaction, a green LED spaced 60° from the UV LED was positioned for excitation, and two additional light detectors, using differently-colored theater gel plastic to filter the green absorption and red fluorescence, were placed at 180° and 60°, respectively, relative to the green LED (see Chapter 2.1). Due to the round geometry absorption and fluorescence could be measured with two excitation wavelengths—which is not possible with a common square cuvette geometry traditionally found in laboratory fluorometers and spectrophotometers. To measure c_δ in water, the enzymes and dye were mixed into the sample, and voltage data was immediately collected over time from the green and red fluorescence detector, $V_{gf}(t,c_\delta)$. As the reaction proceeded, the increase in fluorescence was manifested as an increase in $V_{gf}(t,c_\delta)$. These data fall onto a straight line when plotted on a semi-log plot, demonstrating the exponential functional form $V_{gf}(t, c_\delta) \sim e^{v(c_\delta)t}$ as shown in Figure 10A. It was observed that the power law exponent of this line, $v(c_\delta)$, increases monotonically with diethylene glycol concentration, c_δ. However, the reaction involves the coupling of three enzymes and a dye, all of which may have slight variations in activity due to environmental factors. These could significantly influence $v(c_\delta)$. To account for these variations, the second, identical sample chamber of the sensor was utilized to simultaneously run a 100% DEG sample as a standard reference. Using $v_\delta^1 \equiv v(c_\delta=100)$, as a normalization constant, the normalized $v'(c_\delta) = v(c_\delta)/v^1_\delta$ was used to account partially for the effects of variation in total enzyme activity. Furthermore, the LabReader also automatically collected UV absorption voltages, $V_{ua}(t,c_\delta)$, in addition to collecting green fluorescence voltages, $V_{gf}(t,c_\delta)$. This UV data should be sensitive only to the activity of the ADH. Therefore, the quantity $\gamma'(c_\delta) \equiv \gamma(c_\delta)/ v^1_\delta$ was calculated, which provides a correction for the variations in absolute ADH activity.
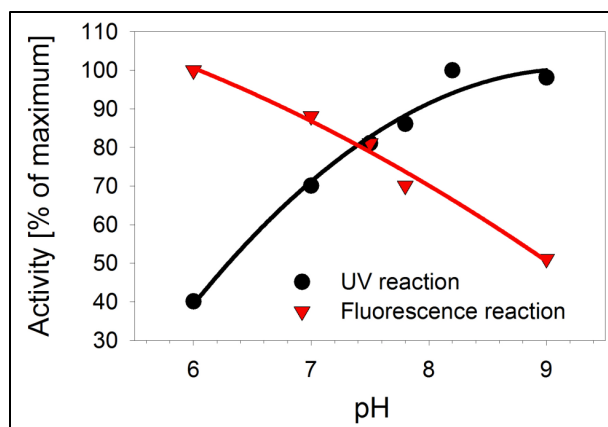
FIGURE 9: PH optimization of the DEG assay. By varying the buffer pH from 6 to 9 (n=1) the highest overall signal-to-noise levels are observed between pH 7.5-8. Here, both fluorescence and absorption reactions are at a high percentage of their maximum measured activity.[96][2]

Combining the fitted data from the UV- and green-illuminated channels, it was observed that $v'(c_\delta)\gamma'(c_\delta)$ rises monotonically with c_δ for DEG in water at all $c_\delta > 1\%$, the safety limit, as shown in Figure 10B. Each data point in Figure 10B is the result of at least three independent runs, for which percentage errors decrease with increasing c_δ. The percentage errors are on average 10%, and as low as 3.1% for $c_\delta = 25\%$. As in the EG case, the measurements for DEG in various household products were repeated: it was observed that the data for some products collapse onto a single curve, though with slightly more scatter than in the EG case, as shown in Figure 10B. The scatter at each data point decreases from 33% to 1.5% as c_δ increases from 0.1 to 100%. These data demonstrate the ability to detect DEG, just as for EG, in several ingestible household products and medicines. The ability to detect these contaminants in remote areas would be greatly enhanced if the chemistry was stable without refrigeration. Indeed, the enzymes and dyes used are packaged in dry, lyophilized form, and can be shipped overnight without temperature control. However, how long the activities of these components remain consistent is not well characterized. To test the longer-term stability of the assays, large samples were created with $c_\delta = 10\%$ and $c_\varepsilon = 10\%$, and over the course of several weeks, all samples, and lyophilized enzymes and dyes were left at room temperature, without any temperature control (see Figure 11). For each measurement, a new enzyme solution was made, and the EG and DEG assays were conducted. Strikingly, in all cases, the absolute variation in the measured glycol concentrations was less than ±1%, even as the enzymes were at room

43

temperature for more than three weeks, as shown in Figure 11. The data demonstrate that the approach to normalizing variations by a combination of LED output stabilization, calibration with reference samples at known concentrations, and combining data from multiple channels, allowed the elimination of any changes in enzyme activity within the measurement uncertainty. Consequently, the device and chemistry are accurate without requiring a continuous chain of refrigeration (which, for example, is required for immunoassays and other sensitive biochemistry) or other infrastructure, and therefore may be suitable for field deployment outside a specialized laboratory.
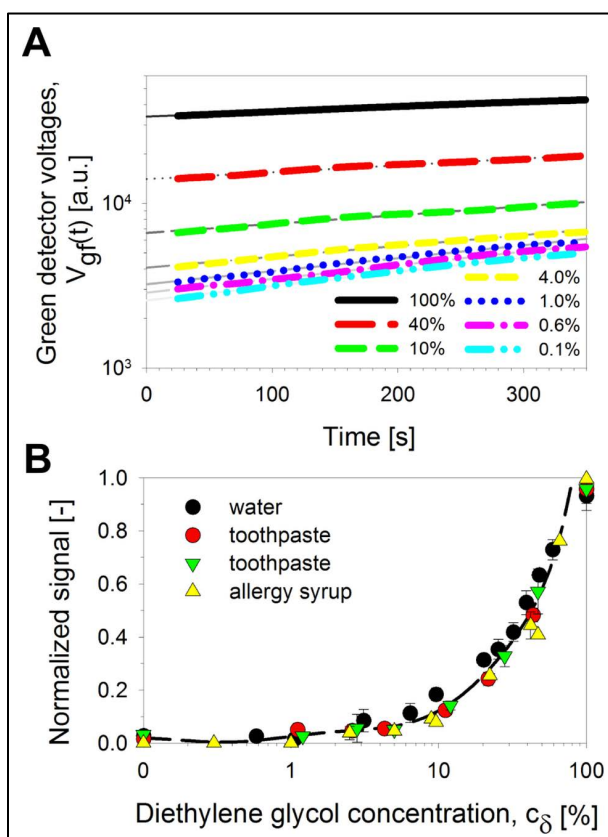
FIGURE 10: Detection of diethylene glycol. (A) Time evolution of output voltage $V_{gf}(t)$ from the green→red fluorescence detector, digitized as 16-bit integer, shown on a semi-log plot with symbols for different DEG concentrations in water. The data fall onto a straight line for each sample, indicating exponential behavior. (B) Combination of normalized UV absorption and green→red fluorescence data, $v'(c_\delta)\gamma'(c_\delta)$, shown with solid black circles for DEG in water (n=3). Data for other ingestible household products (n=3) fall on the same master curve.[96][2]

44
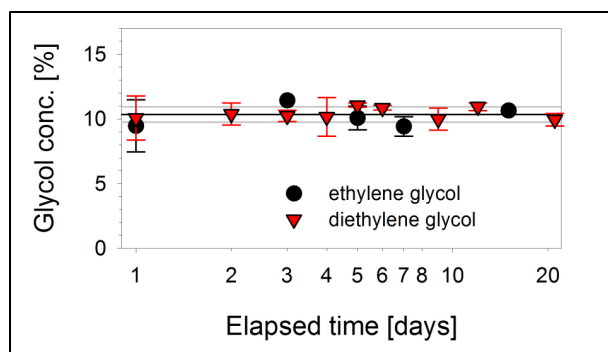
FIGURE 11: Assay stability measurement. The same c_δ=10% (DEG) and c_ε=10% (EG) samples are measured over time, with enzymes left to sit at room temperature. Average and standard deviation of measurements are marked with solid and dotted lines, respectively (n=3). In all cases, the measured glycol concentrations remained stable to within ±1% throughout the course of more than three weeks.[96][2]

2.2.2.4   ALCOHOLS

ADH can be used to detect glycols that have multiple hydroxyl groups; however, the enzyme originally evolved to convert simple alcohols, with a single hydroxyl group. ADH reacts far faster with alcohols, which suggests the assay might detect alcohols at far lower concentrations, c_α. To test this hypothesis, the assay was conducted on several alcohols mixed with buffer, including ethanol, 1-propanol, 2-propanol, 1-butanol, 1-pentanol, 1- hexanol, 1-heptanol and 1-octanol. As for the DEG measurement, the normalized power law exponents γ′ and v′ were calculated from the UV-and green-illuminated channels. Here a reference concentration of c_α=0.01=1% for each alcohol was used (instead of c_δ = 100%, in the case of DEG, because alcohols are expected to react faster with ADH). It was observed that the γ′(c_α)v′(c_α) data for all primary alcohols collapse onto a single master curve, for all c_α above the part-per-billion (ppb) level, as shown in Figure 12A. Each data point is the result of at least three independent runs. The average percentage error between different alcohols at a certain concentration is as low as 7.5% at c_α=0.001=0.1%. This detection limit is sufficient for the detection of most alcohols in groundwater, which are between ppm-ppb (see Chapter 1.1.2). Furthermore, for c_α=0.01=1%, the γ′(0.01)v′(0.01) data for primary alcohols decrease monotonically with the alcohol carbon number. The curve is nearly linear within a range of 3 (propanol) to 7 (hexanol) carbons as shown in Figure 12B (results from three independent measurements). These data demonstrate how the device and chemistry may provide an extremely sensitive probe for the presence of alcohols. When the
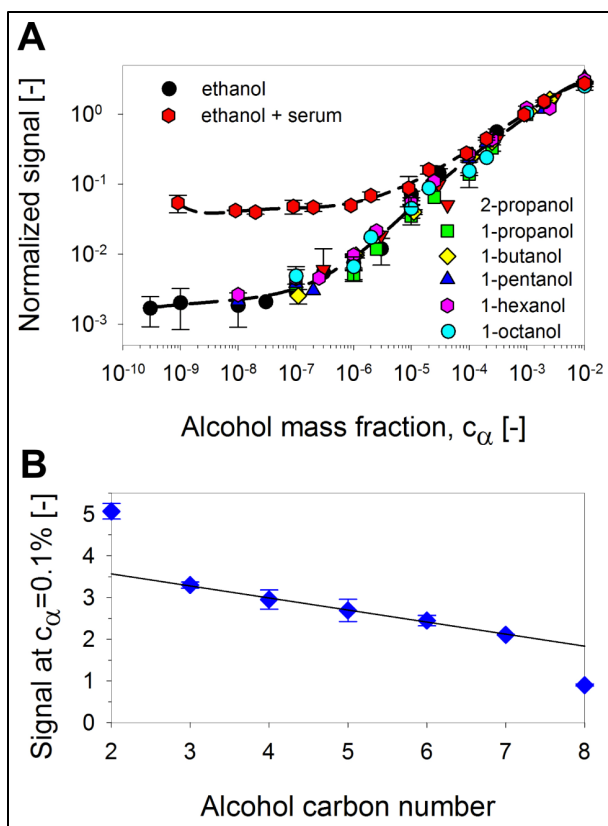
Figure 12: Detection and characterization of alcohols. (A) Combination of normalized UV absorption and green→red fluorescence power-law exponents, v′(c_α)γ′(c_α), for various alcohols in water, as a function of alcohol mass fraction, c_α. The data collapse onto a single master curve (black), for all concentrations greater than a few parts per billion. Data for ethanol in blood serum plateaus to a background of a few parts per million, well below the legal blood-alcohol limits in a variety of countries, which range from $c_\alpha = (2\text{-}8) \cdot 10^{-4}$. (n=3). (B) The product of the normalized fluorescence and UV power law exponent, v′(0.01) γ′(0.01), for primary alcohols decreases monotonically with increasing carbon number. For alcohols with 3 to 7 carbons, this decrease is linear, marked with a solid line (n=3).[96][2]

concentration is known, some primary alcohols can be identified. For example, this test could be used to detect alcohol in groundwater, which is a sign of gasoline spills or leaks (see Chapter 1.1.2). In addition, the measurement of ethanol in blood serum was measured, as a way to measure blood alcohol content, shown with hexagons in Figure 12A. These data overlap the other alcohols exactly for γ′($c_\alpha > 10^{-5}$). The c_α for ethanol in blood serum two order of magnitude

below the standard drunk-driving limits of $c_\alpha = (2\text{-}8)\cdot 10^{-4}$ can be accurately quantified. Hence, this method may provide another avenue for rapid, low-cost blood-alcohol measurement in the field, with greater accuracy than breath-based tests.

2.2.2.5   E.COLI, SALMONELLA AND CHOLERA

The ability to detect transmission and fluorescence from two excitation wavelengths simultaneously allows for the detection of a broad range of other chemical reactions or interactions that generate a change in optical activity. For example, DNA can be detected with low-cost intercalator dyes, known to be stable at room temperature for months. This suggested a new use for the system: the detection of microbial DNA in materials where no DNA should be found. These include recreational water and many foods, where contamination has lead to epidemics. To test the ability to detect such microbial contamination, different microbial concentrations, c_μ, of *V. cholerae, S. enterica* and *E.coli* bacteria were mixed in water, a DNA intercalator dye was added, free dye was removed, and the final, static green-red fluorescence intensity $V_{gf}^{\infty}(c_\mu) \equiv V_{gf}^{\infty}(t \to \infty, c_\mu)$ was measured. The total preparation and measurement time was only a few minutes. In both cases, it was observed that $V_{gf}^{\infty}(c_\mu)$ rises with bacterial concentrations $c_\mu > 10^5$ CFU/ml and has a LoD of 10^6 CFU/ml (Figure 13). The LoD calculations were outlined in Chapter 2.2.1.6 and three repeats were run per concentration. The minimum-detectable c_μ is comparable to total organism concentrations detected in several historical epidemics [158, 159]. Furthermore, the concentration of pathogens in pond water was tested (Bow, New Hampshire) and a baseline activity indistinguishable from background levels was measured in doubly distilled water. These data demonstrate the utility of this method to potentially prevent recreational water epidemics, where fast turnaround times are desirable. Another major area where DNA should not be present is foods that do not contain cellular tissue from animals or plants. Many of these, such as milk and eggs, have been involved in massive food poisoning outbreaks when contaminated by bacteria such as *E.coli* or *salmonella* [13, 17]. Unlike drinking water, however, these complex biological materials contain other components with the potential to interfere with the DNA intercalator dyes. To test the ability to quantify microbial contamination in these materials, the above procedure was repeated with *E.coli* in milk, and *salmonella* in egg white, combinations that have caused lethal food poisoning in the past. Once again, in both cases, the static green-red fluorescence intensity, $V_{gf}^{\infty}(c_\mu)$, rose with bacterial concentration, c_μ. However, the curves of $V_{gf}^{\infty}(c_\mu)$ for the four bacterial data sets did

47

not overlap on the same curve, possibly due to differences in auto fluorescence of the materials and foods. With a traditional fluorometer, little could be done without further sample modifications. However, the multichannel design of the detector provides a number of additional options, as the final, static green absorption $V_{ga}^{\infty}(c_{\mu})$ and UV→ red fluorescence $V_{uf}^{\infty}(c_{\mu})$ were collected automatically. Combinations of channel metrics were investigated, for which all four bacteria collapsed onto the same master curve. It was determined that universal data collapse for the normalized multichannel metric $V_{gf}^{\infty}(c_{\mu})\sqrt{(V_{uf}^{\infty}(c_{\mu}) \cdot V_{ga}^{\infty}(c_{\mu}))}$, as shown in Figure 13A. Again, using SYTO 85 it was found that $V_{gf}^{\infty}(c_{\mu})\sqrt{(V_{uf}^{\infty}(c_{\mu}) \cdot V_{ga}^{\infty}(c_{\mu}))}$ rises with bacterial concentration $c_{\mu}>$ 10^5 CFU/ml at a LoD of 10^6 CFU/ml. These data demonstrate how this device can be used in a general way to measure microbial concentration in substrates that should not contain DNA, irrespective of particular bacteria or substrate. This is particularly important in foods and medicines, where a wide range of bacteria are known to cause poisoning [17, 18]. It should be emphasized that the measurements were taken directly on samples and require only a few minutes of dye exposure. The results were unchanged while varying dye incubation times from 3 to 30 minutes. Even though the methods introduced here can detect bacteria at concentrations found in several historical epidemics [158, 159], lower detection limits may be desirable because the presence of as few as 10 cells of *salmonella* or *E.coli* O157:H7 could be an infectious dose [98]. The EPA recommendation for recreational waters is around 1 CFU/ml [103], even though higher detection limits may be acceptable, especially where fast turn-around times are needed. To increase detection sensitivity, the fluorescent dyes were optimized and lysed cells were used rather than whole cells, where the DNA is expected to be more accessible to the dyes. As shown in Figure 14, a LoD of $c_{\mu}= 10^4$ CFU/ml was achieved in both the LabReader and a plate reader, by lysing the cells and using the DNA dye SYTOX Orange rather than SYTO 85. SYTOX Orange was chosen, as it is compatible to the current optical setup of the device. Further optimization of dyes and lysis conditions could improve this detection limit even more. The detection limit of 10^4 CFU/ml is comparable to most electrical, electrochemical (e.g. impedance, DEP) and immunochemical biosensors, which usually have detection limits between 10^3 and 10^5 CFU/ml with an assay time of at least two hours under ideal conditions [160, 161, 162, 163, 164]. Other optical methods (e.g. SPR, IR, optical fibers etc.) may achieve even lower detection limits, but often require several hours [160] and/ or cost around 2 orders of magnitude more than the sensor described here [98, 165]. Traditional methods (such as cell culture, PCR or ELISAs) have lower detection limits between 10^1 and 10^6 CFU/ml. However, they require incubation of several hours (PCR 4-6 hrs) to days (culture methods up to 5-7 days),

as well as a stable laboratory environment often in combination with expensive equipment [98]. The introduced detection scheme may therefore be used as a simple, low-cost first screen and line of defense for pathogen contamination in a range of consumer products, recreational water, medicines and food products.

2.2.2.6   MALARIA (USING A YEAST MODEL)

In addition to prokaryotes, the same method could be applied to a eukaryotic biological system where the presence of DNA indicates the presence of pathogenic microbial invasion. Several blood-borne pathogens, for example malaria-causing plasmodium, invade red blood cells (RBCs), which have no DNA of their own. Moreover, RBCs can be separated from other DNA-bearing cells in blood using existing low-cost methods [166]. Using this methodology, it might be possible to detect this type of parasitic blood infection. To test this concept qualitatively, a rudimentary model for malarial invasion was used by dyeing suspensions of yeast with SYTO 85, because yeast is safe to handle and has a total genome size about half that of plasmodium. Yeast was dyed both in water, and mixed with red blood cells. After a brief incubation, fluorescence and absorption were measured, following the protocol analogue to the one used for bacteria. As in the bacteria, a different scaling of the individual data sets was attained when using fluorescence and absorption alone. In particular, the data for yeast in red blood cells did not overlap that for yeast in water. The different parameters therefore were combined until universal data collapse was achieved. It was observed that, when normalizing the green→red fluorescence intensity by the cube of the green absorption, $V_{gf}^{\infty}(c_{\mu})/V_{ga}^{\infty}(c_{\mu})^3$, the data from both sets fall onto the same curve—and at low concentrations asymptote to the baseline value measured for red blood cells alone, as shown in Figure 13B. Using SYTO 85, it was observed that the normalized signal, $V_{gf}^{\infty}(c_{\mu})/V_{ga}^{\infty}(c_{\mu})^3$, rises with cell concentration, c_{μ}, at a LoD of $c_{\mu} >$ $8 \cdot 10^5$ CFU/ml, which correspond to ~0.1% of blood cells. The detection limit could again be improved by using lysed cells and the DNA-dye SYTOX Orange instead of SYTO 85 (see results from a plate reader in Figure 14 B). These preliminary data demonstrate that the intercalator has no significant background interference from residual RNA or ribosomal nucleotides in the red blood cells. Therefore, this method has the potential to quantify rapidly the concentration of blood-borne DNA-bearing parasites, such as plasmodium (malaria), trypanosoma (sleeping sickness and chagas) and the eggs of trematodes (schistosomiasis), in RBC suspensions.
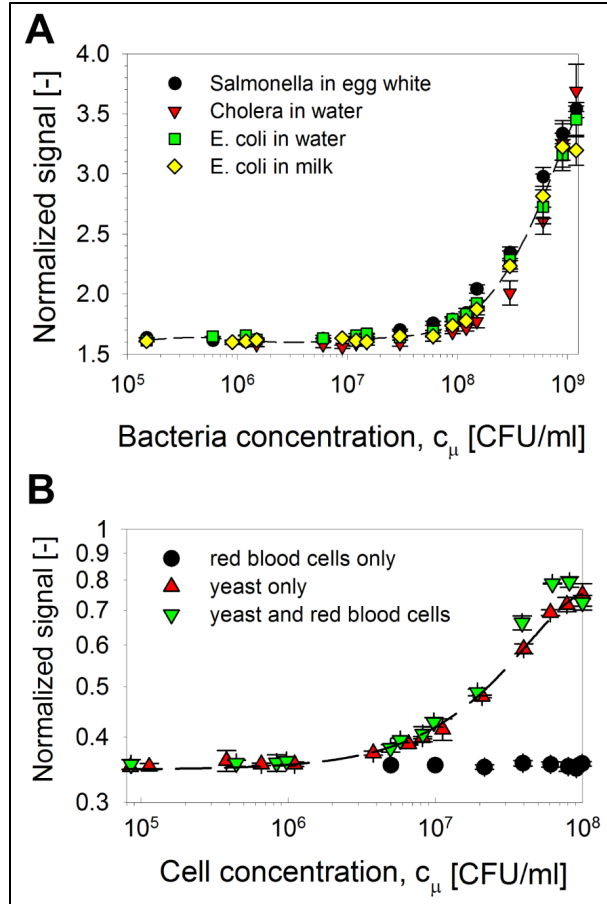
FIGURE 13: Detection of microbial contamination. (A) Combined, normalized multi-channel data $V_{gf}^{\infty}(c_{\mu})\sqrt{V_{uf}^{\infty}(c_{\mu})\cdot V_{ga}^{\infty}(c_{\mu})}$ from the DNA intercalator dye in the presence of prokaryotic pathogens at different bacterial concentrations, c_{μ}. 3 measurements were run per concentration. In all cases, the data from *V. cholerae* in water, *E.coli* in water and in milk, and *salmonella* in egg white, all collapse onto the same master curve (dotted line). This demonstrates universal, species-independent behavior of the bacterial detection scheme. (B) Rudimentary model for the detection of eukaryotic blood parasites, such as malaria. Combined normalized multichannel data $V_{gf}^{\infty}(c_{\mu})/V_{ga}^{\infty}(c_{\mu})^{3}$ for dyed yeast both in water (grey triangles) and in red blood cells (inverted, grey triangles) scale onto the same master curve (dotted line), and at low concentration plateau to the background sample of red blood cells alone (circles) (n=3).[96][2]
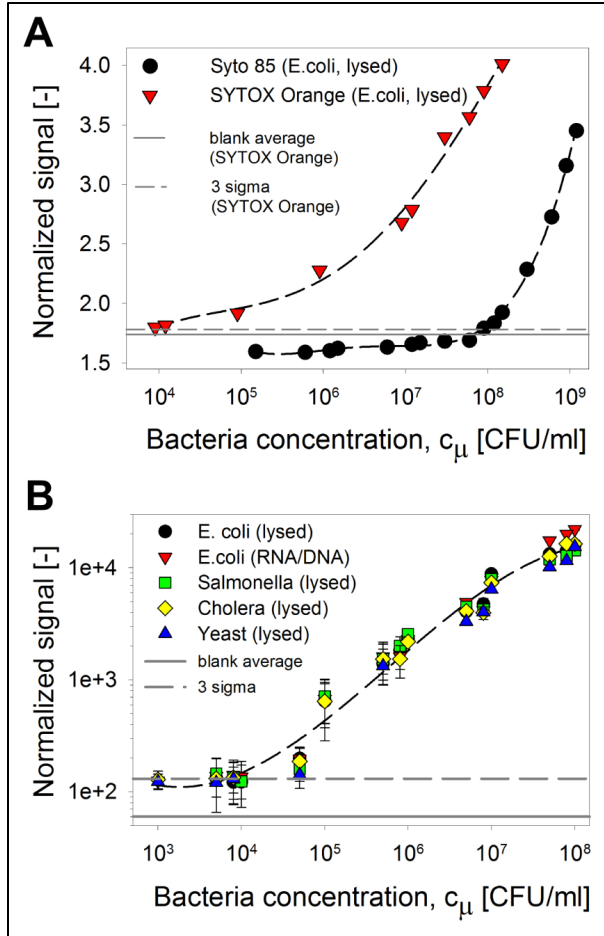
FIGURE 14: Dye optimization. (A) Comparison of SYTOX Orange and SYTO 85 detection limits. Shown are the combined normalized multi-channel data $V_{gf}^{\infty}(c_{\mu})\sqrt{V_{uf}^{\infty}(c_{\mu}) \cdot V_{ga}^{\infty}(c_{\mu})}$ from DNA intercalator dyes in the presence of *Ecoli* cells at different concentrations c_{μ}. Using SYTOX Orange with lysed *E.coli* cells improves the detection limit to $c_{\mu} = 10^4$ CFU/ml, compared with 10^6 CFU/ml in SYTO 85. (B) Validation of SYTOX Orange staining for different bacteria (*salmonella, cholera, E.coli*) and yeast. This graph shows SYTOX Orange stained lysed bacteria and lysed yeast cells at different concentrations measured in a plate reader (whose sensitivity is comparable to the LabReader, see Figure 6). The fluorescence values are normalized by the pathogen genome size and represent the averages of three independent runs.[96][2]

2.3   DISCUSSION AND SUMMARY

The LabReader was introduced, which employs a detection scheme involving fluorescence and/or UV absorption measurements made on samples in a small, round test tube. It consists of low-cost LEDs and light-to-voltage converters in conjunction with low-cost injection molded housings. This simple LabReader makes it practical to use multiple channels and samples for normalization by references and combination of data from up to four simultaneous measurements. The fluorescence channel within the detector has sensitivities comparable to commercial plate readers costing significantly more. Contaminants were detected directly in various substances, without separation, purification, concentration or incubation. New enzyme- and dye-based methods were introduced and they are summarized in Table 14. Enzyme reactions based on alcohol and aldehyde dehydrogenase coupled to a fluorescent reporter dye (Amplex Ultrared) were developed. They were used to detect (di-)ethylene glycol in consumables above 0.1wt% without interference and alcohols (either in groundwater or blood) above 1ppb. For fluorescence-based detection of bacteria, a nonspecific DNA intercalator dye was chosen due to its low cost and high stability. A range of pathogens in water, foods and blood was detected without background signal at a LoD of 10^4 CFU/ml. The chemistry was stable for weeks without refrigeration and the rapid detection time of the assays allows testing of perishable foods and ingestible products, which often are not tested due to lengthy testing methods. In addition, contaminant concentrations measured did not change with background substrate, which demonstrates that these detection methods are broadly effective in a wide variety of substances. Only a limited number of contaminants were examined, but this strategy should be applicable to any chemical reaction that leads to a change in optical activity in the presence of a contaminant. For example, commercial kits are available that use a fluorescence-generating reaction to detect melamine in milk products. The LabReader design is also robust and simple-to-use. In the future, it could be run on batteries and a smart mobile-phone/ tablet platform could be used to aggregate data for use in remote areas. A device consisting of LEDs or a number readout that gives the end-user a simple yes or no answer of whether the sample is contaminated could also be envisaged (as indicated in Figure 3). The sensitivity of the detectors could be further improved by adding a third LED or by optimizing LEDs, filter specifications and optical paths.

The advantages and limitations of the LabReader are summarized in Table 15. Compared with benchtop optical detectors outlined in Chapter 1.2.3.2, the LabReader has increased application flexibility by detecting four wavelengths simultaneously, reading out data in realtime and

because it has not moving parts it is robust. Because low-cost LEDs and filters are used without sophisticated optical strategies (e.g. lenses, beam splitting), the LabReader is expected to be lower in cost than the described commercial benchtop readers.

Even though enzyme-based detection for contaminants and toxins (ethylene glycol, diethylene glycol and alcohols) was specific and sensitive enough to comply with safety limits, the introduced bacteria detection assays were insensitive to the actual genome being detected and the sensitivity was limited to 10^4 CFU/ml. This limitation is caused by the nature of the assay, rather than the optics, as the same detection limits were observed in the plate reader control. In many situations, it is required to specifically detect bacteria/cells at low concentrations in order to ensure safety or to make a diagnosis (see Table 5 and TABLE 14). To gain both sensitivity and specificity of the cell-based assays, DNA amplification (isothermal or PCR) or immunoassays (e.g. antibodies, ELISAs) could be incorporated into the LabReader. In addition, the sample preparation of the optical detection system was not yet automated, which is crucial for deployment in the field. These attributes would make the LabReader even more broadly applicable in food, environmental and consumer product safety and for medical diagnostics.

Contaminant	Contaminated materials	Detection mechanism	Spectral range	Required LoD	Achieved LoD
Ethylene glycol	Consumer household products and medicines	Enzymatic	UV	0.1%	0.1%
Diethylene glycol	Consumer household products and medicines	Enzymatic	Fl. + UV	1%	1%
Alcohols	Groundwater, blood	Enzymatic	Fl..+ UV	ppb-%	ppb
Food pathogens (*E.coli, salmonella*)	Foods, e.g. milk, eggs, cider	DNA dye	Fl.	$0-10^4$ CFU/ml	10^4 CFU/ml
Environmental pathogens (V. *cholerae*)	(Recreational) Water	DNA dye	Fl.	<1 CFU/100ml	10^4 CFU/ml
Bloodborne pathogens (*P.falciparum*)	Blood	DNA dye	Fl.	0.1-1%	0.1% (yeast model)

TABLE 14: Overview of the developed/integrated assays for detecting poisons, contaminants and pathogens, their mechanism and detection limits.

Advantages	Limitations
Low cost (LED-based, theater filters)	Low chemical sensitivity and specificity for bacteria/cells
Robust (no moving parts)	No automated sample preparation
Flexible usage (coupled to cell-phone)	
Simple to use	
Four simultaneous wavelengths	
High sensitivity of optics	
High sensitivity and specificity using enzyme reactions	

TABLE 15: Advantages and limitations of the LabReader.

CHAPTER 3: FULL SYSTEM INTEGRATION

As outlined in Chapter 2, it was necessary to automate the sample preparation and to increase the sensitivity of the LabReader in order to make it deployable for work in the field, at the production site or at the point-of-care. This chapter outlines the combination of the LabReader with the automated DNA extraction platform, the LabTube, into a fully-integrated, automated DNA extraction, amplification and readout system. Chapter 3.1 describes the LabTube for automated DNA extraction. In Chapter 3.2 the LabTube, is made compatible with food safety applications, namely the extraction of DNA from VTEC *E.coli* in milk and water, as well as *Alicyclobacillus* from apple juice. In Chapter 3.3, two options are outlined in which the optical detection scheme and the LabTube can be combined. Furthermore, the preferred system layout for this thesis is identified.

3.1   AUTOMATED DNA EXTRACTION (LABTUBE)

The University of Freiburg has recently introduced the LabTube, which is a microfluidic platform for automation of biological assays. The LabTube can be used for different tests, such as DNA and protein extraction. It runs with standard lab-centrifuges. The LabTube consists of three stacked disposable microfluidic cylinders, as depicted in Figure 15. Pen mechanics, actuated by centrifugal forces, rotate cylinder II by varying centrifugal speed over times. This mechanism allows for regulation of fluidic paths through the stacked system and hence liquid routing [8].

Cylinder I contains pre-stored liquid reagents. Cylinder II contains lancing structures for sequential release of reagents from cylinder I. It can be used to perform unit operations such as mixing, separation, and extraction of target molecules. Cylinder III separates the waste liquids from the eluate. In the near future, analytic reactions, such as ELISA, could be incorporated into cylinder III [8]. Figure 16 demonstrates the LabTube components and the centrifuge processing protocol for automated, silica column-based DNA extraction. For DNA extraction, cylinder I is loaded with lysis buffer, binding buffer, washing buffer and elution buffer. Also, the sample is added in this cylinder. A silica column for DNA binding is integrated into cylinder II. After fully automated processing in the centrifuge, DNA eluates are taken out of cylinder III and are analyzed e.g. by real-time PCR. As a first demonstration, fully automated column-based DNA extraction from human blood was integrated into the LabTube by the University of Freiburg [8].

Major advantages of the LabTube platform are the possibilities of reagent pre-storage and release, automated processing of different assays with volumes ranging from 50µl to 4ml [8].

Because it runs on a standard laboratory centrifuge (with costs ranging from k$ 2-8[167]), it does not require expensive equipment like other commercial pipetting robots (described in Chapter 1.2.2.4). It is further easily scalable and minimizes contamination risks by using prestored reagents for each extraction. It is broadly deployable for different extraction and assay types (e.g. DNA, RNA, protein extraction and protein assays). The LabTube can be used flexibly at the production site, in the field or point-of-care with a laboratory centrifuge. It was therefore used as a sample preparation device in the research presented in this thesis.
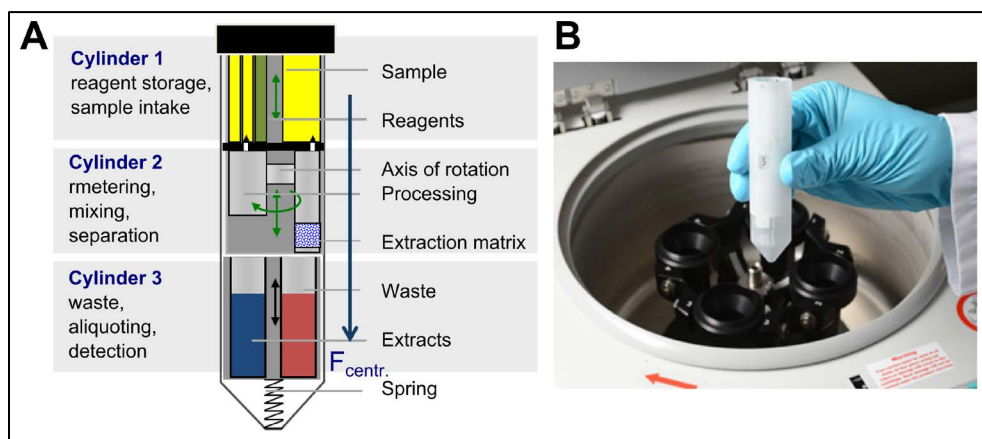
FIGURE 15: Concept (A) and first demonstrator (B) of the LabTube for the swinging bucket rotor of a standard lab centrifuge. (Adapted from[8]).
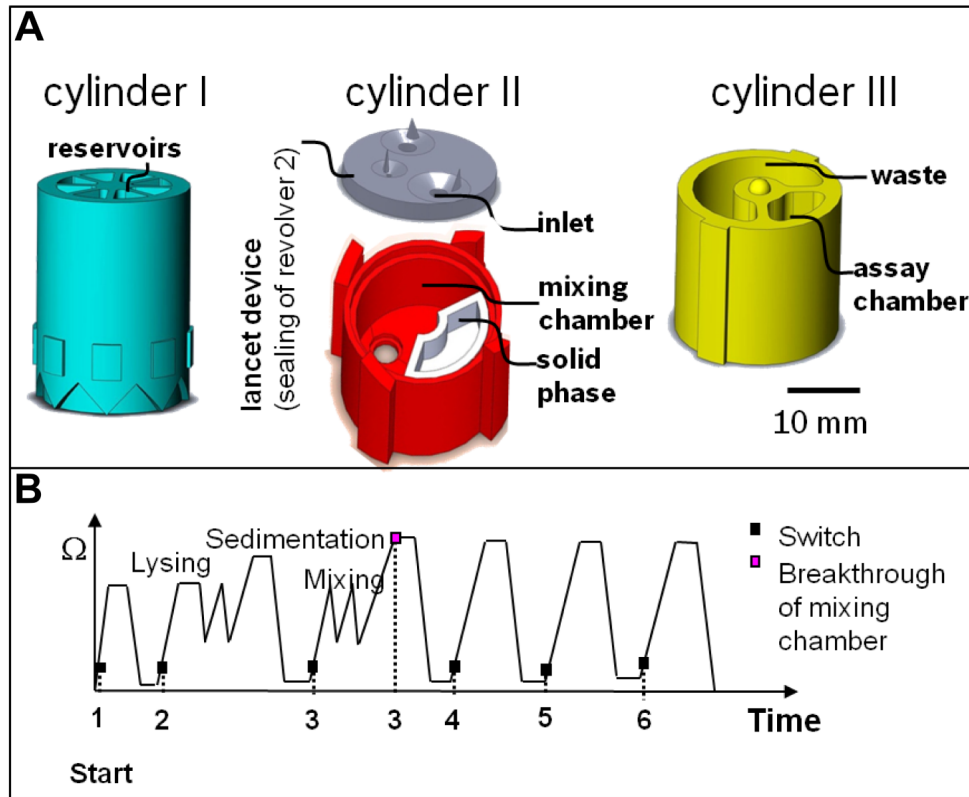
FIGURE 16: (A) Components of the LabTube for DNA extraction: Cylinder I contains the reagents for DNA extraction and its chambers are sealed on top and bottom with metal foil. The different chambers can be opened via the pen mechanism using thorn lids in cylinder II. Cylinder II contains mixing chambers, where the sample is lysed and mixed with the binding buffer. It also contains the silica column for DNA extraction. Waste and DNA eluate are collected in cylinder III. Cylinder III and the mixing chamber sit on springs with defined stiffness, required for the pen mechanism to work. (B) The centrifugation protocol is depicted. The pen mechanism and hence switching of the cylinder II is achieved by changing the centrifugation acceleration from high to low over time. Mixing is achieved with oscillating centrifugal forces in an intermediate range. (Image courtesy Robert Bosch GmbH)

3.2 DNA EXTRACTION OF FOOD BACTERIA (LABTUBE)

In this thesis, food safety is the first sample application for the combined, fully-integrated DNA extraction and amplification system (see Chapter 1.1.3). For pathogenic bacteria, the detection of *E.coli* in milk and water during production processes, and for product spoilers, *Alicyclobacillus* (*A.acidoterrestris*) in apple juice were selected.

Any analytic system needs to be able to detect *E.coli* (all strains) at concentrations between 10^2-10^4 CFU/ml and lower and *Alicyclobacilli* at 0 CFU/ml (see 1.1.4) in order to comply with safety standards. Routinely, pre-enrichment steps of several hours to days are performed in order to reach the relevant detection limit. Improving DNA extraction yields to shorten or eliminate pre-enrichment steps would be advantageous. Hence, the LabTube DNA extraction efficiency for food bacteria was optimized in this section.

3.2.1 MATERIALS AND METHODS

3.2.1.1 MANUAL DNA EXTRACTION PROTOCOLS

All manual DNA extractions were performed with standard column systems provided by the manufacturer. A Hermle Z326K centrifuge was used with a swing-bucket rotor and a maximum acceleration of 6,000g, to be comparable with the LabTube setup. All steps were performed at room temperature.

Cell lysis: Only experiments in Figure 21B required lysis, where an overnight culture of K12 *E.coli* was used. Here, samples were centrifuged at 10,000g for 5 min and the cell pellet was resuspended in 90μl ATL buffer and 10μl of proteinase K at 56°C for 30 minutes.

Manual extraction of bacterial DNA: 100μl of sample were mixed with 200μl AL buffer, which contained carrier RNA. The mixture was vortexed and then mixed again with 200μl ethanol (96-100%). The mixed samples were transferred to a Qiagen Mini Elute column and they were centrifuged at 6,000g for 1min. The flow-through was discarded and the column was washed twice with 450μl of AW1 and AW2 respectively (6,000g, 1min). Finally, the column was dry-spun for 7min at 6,000g. The DNA was eventually eluted at 6,000g for 2min using 20μl of AE buffer.

3.2.1.2 DNA EXTRACTION PROTOCOLS IN THE LABTUBE

LabTube extractions were performed in a programmable Hermle centrifuge (Z326-K). The program H-control was used to run the centrifugation protocol. Mixing was performed by

changing the centrifugal acceleration from 500 to 2,500g in 60 cycles. All flow-through and elution steps were performed at 6,000g for 1min. The dry-spinning of the sample was performed for 7min at 6,000g and elution for 2min at 6,000g. For each experiment, LabTubes were assembled under sterile conditions in a DNA-free room. A new disposable LabTube was used for each run. Cylinder I was filled with reagents and heat-bonded at the top and bottom with coated aluminum foil (Amcor) using a thermo-sealing machine (Ballerstädt). Figure 17 shows schematically how the cylinders were filled for different DNA extraction kits. The eluates were weighed out after the extraction with a scale (Mettler Toledo) to take into account variations in elution volumes.

3.2.1.3 DETAILS FOR DIFFERENT EXTRACTION EXPERIMENTS

The manual extractions shown in Figure 21B were performed using K12 *E.coli* (overnight culture). Concentrations were measured spectroscopically. All other extractions in the LabTube and their manual references were performed with cell lysates of VTEC *E.coli* (O157:H7) and of *A.acidoterrestris* (all purchased from Biotecon Diagnostics GmbH). For concentration series *E.coli* were diluted either in water or in milk (3.6 % fat) and *Alicyclobacilli* were diluted in apple juice.

In Figure 20, at least three concentrations (with n=3 each) between 10^6 and 10^8 inserted copies of VTEC *E.coli* lysate were extracted using the LabTube and manual reference. For DNA extractions shown in Figure 21, at least three independent manual extractions were performed. In Figure 21A, VTEC *E.coli* lysates with 10^4 inserted copies were used. In the experiments shown in Figure 21B the eluate was eluted 4 times overall. In Figure 22, at least three independent runs were performed at all concentrations using both manual and LabTube extractions.

3.2.1.4 DETECTION LIMITS AND QUANTIFICATION LIMITS

LoD and LoQs were calculated as described in Chapter 2.2.1.

3.2.1.5 COMPOSITION OF THE PCR REACTIONS

QPCR was always run to quantify the extracted DNA copy numbers in all performed extractions. A single 20µL PCR reaction was composed of a 2x concentrated ready-to-use PCR reaction mix (Qiagen QuantiFast PCR mix w/o ROX dye), forward and reverse primers (200nM in PCR mix), a specific TaqMan probe (200nM in PCR mix), ROX dye, PCR grade water and 2µL of DNA

eluate (Table 16). The PCR reaction was run in a 7500 Applied Biosystems real-time cycler with the temperature cycles shown in Table 17. Table 18 shows the primer and probe sequences for *Alicyclobacillus* and for *E.coli* PCR reactions. Note that the used primers are not specific to *VTEC E.coli* and *A.acidoterrestris*, but instead detect multiple *E.coli* and *Alicyclobacillus* strains, which is desirable in a real-world scenario given the mentioned LoDs in Chapter 1.1.3.1.

3.2.1.6 STATISTICAL PROBIT ANALYSIS OF THE PCR REACTIONS

Knowing the quantification limit of the used qPCR was crucial to accurately determine detection limit, LoD, and quantification limit, LoQ, values for DNA extraction. The quantification limit of the qPCR reaction was defined as the 95% confidence limit determined with a probit analysis: A dilution series from genomic DNA was prepared for *E.coli* and for *Alicyclobacillus acidoterrestris* according to Table 19 and Table 20. Subsequently, PCR replicate testing was conducted for each dilution and the proportion of positive PCRs compared to the number of replicates was calculated. Based on these results, the mean DNA concentration that can be amplified with 95% confidence was calculated to 20 DNA copies/eluate (i.e. #/20µl) for *E.coli* and to 22 DNA copies/eluate (i.e. #/20µl) for *A.acidoterrestris.* Standard real-time qPCR with three repeats was performed for DNA quantification, when the maximum possible DNA concentration in the eluate was expected to be above 20 or 22 DNA copies/elution and when all PCR reactions showed positive amplification results. When the maximum possible DNA concentration was expected to be below 20 or 22 DNA copies/elution or if single PCR reactions failed in being amplified, quantification was done by comparing the proportion of positive PCR reactions to the probit regression derived from the dilution series (Figure 18 and Figure 19).
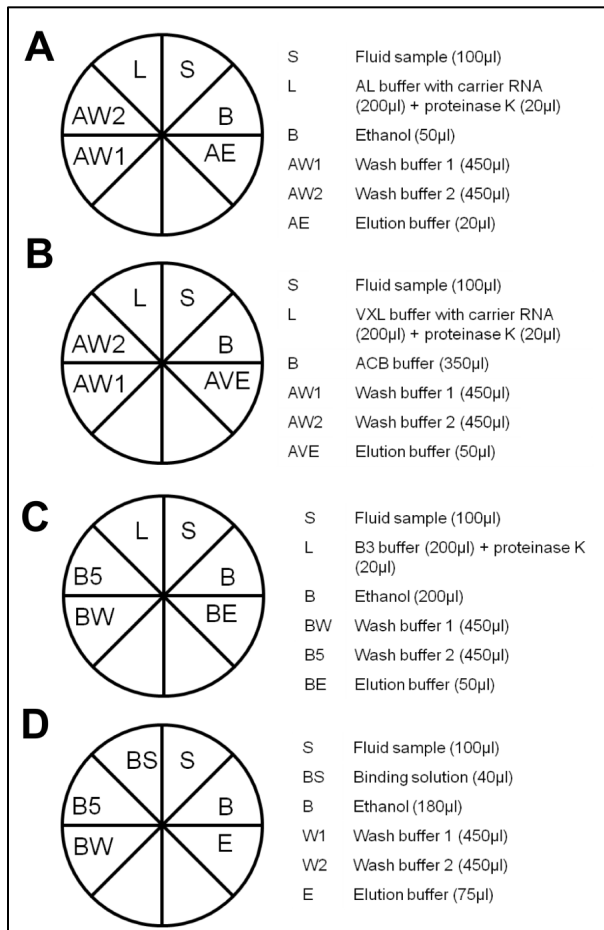
FIGURE 17: LabTube setup for different DNA extraction kits. (A) Cylinder I setup for QIAamp Micro DNA kit. (B) Cylinder I setup for QIAamp Cador Pathogen Mini kit. (C) Cylinder I setup for Macherey Nagel Tissue XS kit. (D) Cylinder I setup for Norgen Milk DNA extraction kit.

Reagent	Volumes for each reaction (µl)
QuantiFast master mix (w/o ROX dye)	10
Forward primer	0.4
Reverse primer	0.4
Probe	0.2
ROX dye	0.4
RNAse free water	6.6
Template DNA	2

TABLE 16: PCR mix composition.

Step	Time	Temperature
PCR initial heat activation	3 min	95°C
2-step cycling: Denaturation	3s	95°C
Combined annealing/extension	40s	60°C
# of cycles	40	

TABLE 17: Temperature protocol.

	E.coli	*Alicyclobacillus*
Forward Primer	GGCAATTGCGGCATGTTCTTCC	CGTAGTTCGGATTGCAGGC
Reverse Primer	TGTTGCATTTGCAGACGAGCCT	GTGTTGCCGACTCTCGTG
Probe	ATGCGAACGGCGGCAACGGCAACATGT	CGGAATTGCTAGTAATCGC

TABLE 18: Primer and probe sequences.

DNA copies (#/elution)	# Positives	# of experiments	Probability of positive PCR (%)
8E+5	2	2	100
8E+4	2	2	100
8E+3	7	7	100
8E+2	7	7	100
2E+2	7	7	100
8E+1	10	10	100
2E+1	9	10	90
1.2E+1	7	10	70
8E+0	5	10	50
2E+0	0	10	0
8E-1	0	15	0

TABLE 19: Number of PCR replicates, number of positive PCR reactions and the probability of a positive PCR reaction for different concentrations of inserted *E.coli* DNA.
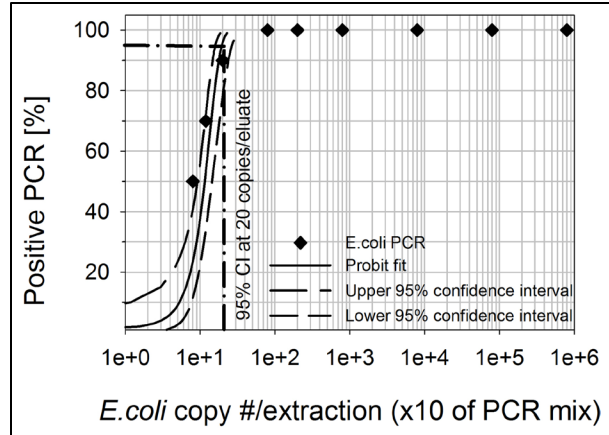
FIGURE 18: *E.coli* probit analysis. Probability for a positive PCR reaction as a function of inserted DNA concentration for *E.coli*. Rectangles depict the proportion of positive PCR reactions calculated from Table 19. The black line represents the probit regression fit with higher and lower 95% confidence limits (dashed lines). DNA concentrations of 20 copies/elution can be amplified with 95% confidence.

DNA copies (#/elution)	# Positives	# of experiments	Probability of positive PCR (%)
2E+7	3	3	100
2E+6	3	3	100
2E+5	3	3	100
2E+4	3	3	100
2E+3	5	5	100
2E+3	5	5	100
1E+3	5	5	100
2E+2	5	5	100
1E+2	5	5	100
2E+1	9	10	90
1.6E+1	8	10	80
1E+1	8	15	53
2E+0	3	15	33
0	2	15	15

TABLE 20: Number of PCR replicates, number of positive PCR reactions and the probability of a positive PCR reaction for different concentrations of inserted *Alicyclobacillus* DNA.
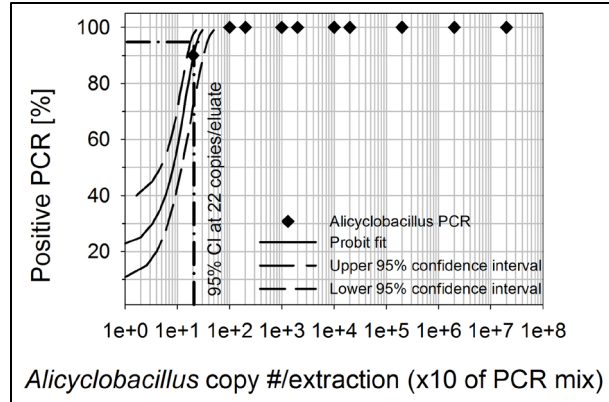
FIGURE 19: *Alicyclobacillus* probit analysis. Probability for a positive PCR reaction as a function of inserted DNA concentration for *Alicyclobacillus*. Rectangles depict proportion of positive PCR reactions calculated from Table 20. Black line represents probit regression fit with higher and lower 95% confidence limit (dashed lines). DNA concentrations of 22 copies/elution can be amplified with 95% confidence.

3.2.2 RESULTS

3.2.2.1   KIT OPTIMIZATION INSIDE THE LABTUBE

The goal was to optimize the extraction efficiency of the food bacteria, *Alicyclobacillus* and *E.coli*, inside the LabTube. Initially, commercially available column-based DNA extraction kits were screened. The goal was to find the one with the highest extraction yield for VTEC *E.coli* lysates. From all tested kits shown in Figure 20, the QIAamp Micro DNA kit achieved the highest extraction efficiency (157±37%, average of three concentrations between 10^6-10^8 inserted copies) inside the LabTube. The results are even better than the manual reference (100±29%). The other kits yielded efficiencies between 7-21%, which are significantly worse than the manual reference.

The errors of on average 26% are comparable with those of the manual reference. They are expected to be caused by variations in sample and buffer volumes, as well as in the fluidic paths. Errors in elution volumes were accounted for by weighing out and normalizing all eluates after the extraction. For the QIAamp Micro DNA kit, elution volumes in the LabTube (16±4µl) varied slightly more than in the manual control (18±2µl), which could be due to imprecisions in the fluidic paths associated with the batch variances of the rapid-prototyped components.

The QIAamp Micro DNA kit has a higher extraction efficiency compared with the manual reference than the other tested kits. This effect is likely caused by the lower volume of DNA lysate that is put on the column (370µl) in the QIAamp Micro DNA kit compared with other tested kits (>500µl). Large liquid volumes may cause residues that get trapped in corners of cylinder II or that get absorbed on the LabTube surfaces. Overall, there is no correlation between absolute DNA yield in the manual reference and LabTube performance. The LabTube likely yields higher extraction efficiencies than the manual reference for the QIAamp Micro DNA kit because of the higher mixing efficiency of the LabTube mixer compared with manual vortexing for mixing binding buffer with the sample (results University of Freiburg, IMTEK).

Due to the results shown in Figure 20, the QIAamp Micro DNA kit was used for all experiments in this thesis.

3.2.2.2   MANUAL PROTOCOL OPTIMIZATION

It was shown manually that the QIAamp Micro DNA kit has an extraction efficiency of 11±6% (see red bar in Figure 21A). In order to further increase the extraction yield, optimization of the kit protocol was performed. Parameters influencing the extraction efficiency were evaluated by extracting 10^4 inserted copies of VTEC *E.coli* DNA manually (with a sample volume of 100µl). The results in Figure 21A show that the extraction efficiency is increased by more than five times, from 11±7% to 56±21%, using 4 or more elutions of the eluate over the column (dark grey bars). However, multiple binding of the sample influences the extraction efficiency insignificantly (light grey bars). Using the optimized protocol with 4 elutions, ≥25 inserted copies of VTEC *E.coli* DNA were extracted manually in water, milk and juice. As indicated in Figure 21B, the extraction yield of inserted *E.coli* copy numbers is 61±27%. The error increases with decreasing copy numbers from 12 to 71%. Overall, the results imply that there is a potential to lower the extraction limit in the LabTube by incorporating multiple elution steps into the system.
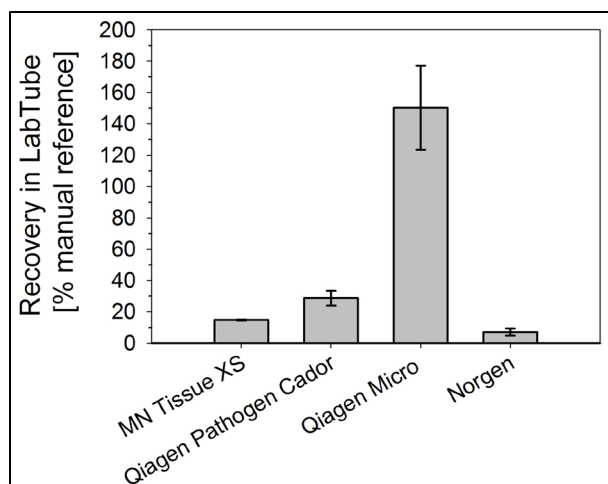
FIGURE 20: DNA extraction kit selection inside the LabTube. The recovery is normalized with the manual reference (100%). For each kit, at least three concentrations (with n=3 each) between 10^6 and 10^8 inserted DNA copies of VTEC *E.coli* lysate were extracted, measured and averages were taken.

3.2.2.3   EXTRACTION IN THE LABTUBE

Using the LabTube, bacterial DNA from VTEC *E.coli* lysate in milk and water, as well as from *A.acidoterrestris* lysate in apple juice were extracted. The extraction limit of VTEC *E.coli* is 10^2 inserted DNA copies in water and 10^3 inserted DNA copies in milk (Figure 22A and B). Figure 22C shows that *A.acidoterrestris* in apple juice can be extracted at a limit of $4.5 \cdot 10^1$ inserted DNA copies. 100μl of sample was inserted into the experiment. Assuming that the LabTube can hold 4ml of samples (i.e. 40x more), the theoretical extraction limits are 25, 250 and 113 DNA copies/ml for VTEC *E.coli* in water and milk and *A.acidoterrestris* in juice samples. As shown with the probit analysis in Chapter 3.2.1.6, the recovered DNA copy numbers from Figure 22 (>20 DNA copies) are within the detection range of the used PCR systems and could therefore be determined with >95% confidence. Below the extraction limits, no positive PCR reactions were observed. The average LabTube extraction yield is 163±44% compared with the manual reference, which confirms the results of Figure 20. The average error in the LabTube experiments is 27% and in the manual references 21%, which explains the extraction efficiency error of 44%. Slightly larger errors in the LabTube extractions may be due to imprecision in manufacturing and fluidic processing paths in the LabTube. Errors from eluate volumes were normalized out (see Chapter 3.2.2.1). The time-to-result of the LabTube extraction is <45min.
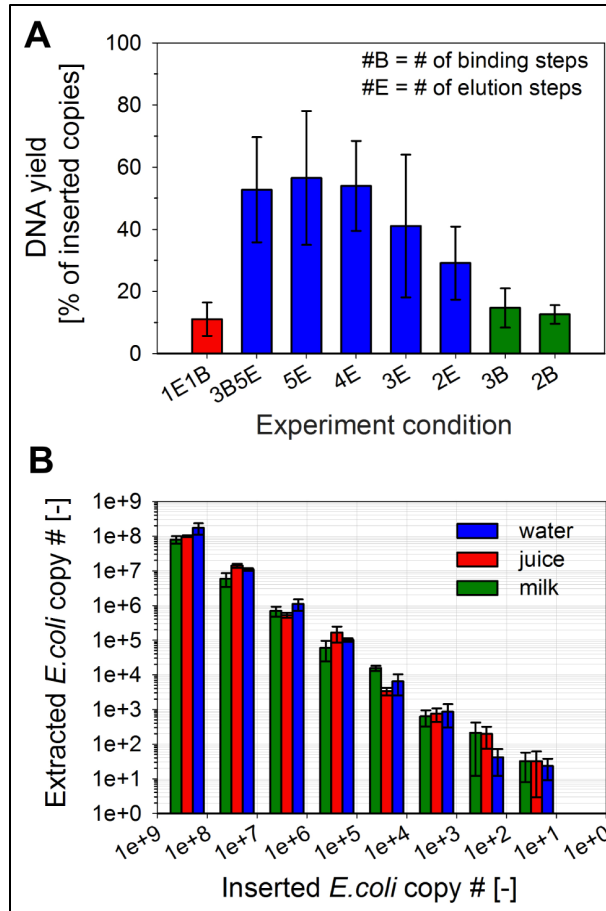
FIGURE 21: (A) Manual optimization of the QIAamp Micro DNA kit. B refers to the number of binding and E to elution steps. The red bar indicates the standard protocol (1B1E), which recovers 11±6% of inserted DNA. It was shown that multiple elutions of the eluate increase the extraction yield to 56±21%, whilst multiple binding steps of the sample have a negligible effect on the yield. (n=2 with 10^4 inserted *E.coli* DNA copies each.) (B) The figure shows manual extractions of *E.coli* in different media using 4 elutions of the eluate with a recovery of 61±27% (n≥3 per concentration).

It was evaluated whether the extraction limit can be improved by re-eluting the eluate. As indicated by the hatched columns in Figure 22, which is the result of 4 overall elutions, the improved detection limit for VTEC *E.coli* in milk is 10^2 and for *A.acidoterrestris* $4.5 \cdot 10^1$ inserted DNA copies. Note that even though there is a column for 10 inserted DNA copies of VTEC *E.coli* in milk its error bar is larger than its actual value and it was not reproducible for VTEC *E.coli* in water. According to ICH standards (see Chapter 2.2.1.6), it was therefore neglected as noise[155]. Overall the average error for 4 repeated elutions in the LabTube is 57%. This error is larger than the average observed LabTube error (27%). Errors, however, increase with decreasing copy numbers and they are comparable to that of one elution in water at a low concentration of 10^2 inserted copies (56%). It was hence concluded that eluting multiple times does not significantly affect the LabTube extraction error. The summarized extraction limits are shown in Table 21.
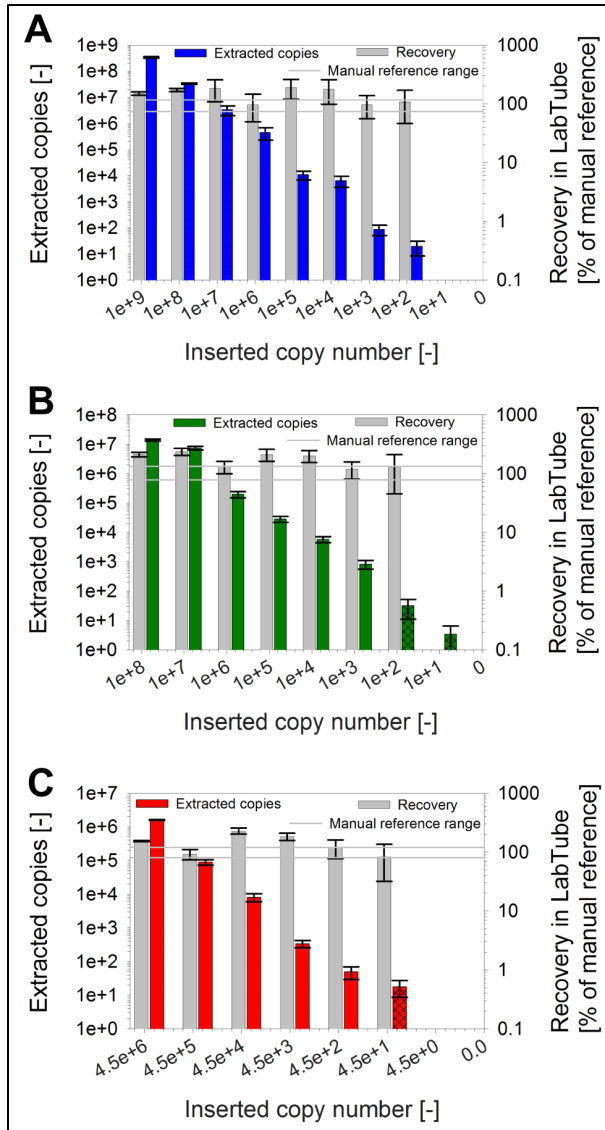
FIGURE 22: DNA extraction in the LabTube for (A) VTEC *E.coli* in water (B) VTEC *E.coli* in milk (C) *A.acidoterrestris* in apple juice. The solid bars represent DNA extracted with the standard protocol (1 elution) and the hatched bars with 4 repeated elutions of the eluate (n=3 at each concentration). Grey bars represent the yield in % of the manual reference (163±44%). The grey horizontal lines indicate the upper and lower average yields of the manual reference in %.

Bacterium	Medium	Extraction limit* (copies)	Yield compared with manual (%)	Improved extraction limit*† (copies)
E.coli (VTEC)	Water	10^2	147±49	10^2
E.coli (VTEC)	Milk	10^3	177±39	10^2
Alicyclobacillus	Apple juice	$4.5 \cdot 10^2$	165±57	$4.5 \cdot 10^1$

TABLE 21: Extraction limits inside the LabTube. Extraction with the Qiagen QIAamp Micro DNA kit (100µl inserted sample). * Extraction limit =3SD above the negative control (no extrapolation). †Extraction limit with 4 manual re-elutions.

3.3   DNA AMPLIFICATION INSIDE VS. OUTSIDE OF THE CENTRIFUGE

It was shown in Chapter 3.2 that as little as 10^2-10^3 DNA copy numbers of VTEC *E.coli* and *Alicyclobacillus* DNA in water, milk and apple juice can be extracted inside the LabTube. For specific detection, the extracted DNA of interest needs to be amplified. There are generally two options for amplifying DNA extracted from the LabTube. The first option is to amplify and readout the DNA *inside* the centrifuge. For example, the LabReader optical detection scheme could be incorporated into the centrifugation holders. Alternatively, DNA amplification can occur *outside* the centrifuge using separate detection unit, such as a handheld version of the LabReader. Both options have advantages and disadvantages that are outlined in Table 22.

Amplifying DNA *inside* the LabTube and the centrifuge offers the advantage of not having to transfer the sample from the LabTube into a separate readout device. This procedure eliminates an additional handling step and significantly reduces contamination risks. However, a custom-centrifuge would need to be developed, which is able to heat and readout the LabTube. Additionally, the centrifuge would be blocked during the amplification steps, lowering the overall throughput. Amplifying and reading out DNA *outside* of the centrifuge has the advantage that the centrifuge would not be blocked during the amplification step. There would be no need for a custom centrifuge and flexibility could be gained by being able to use a variety of downstream amplification/readout devices. However, the gained flexibility bears additional contamination risks due to the transfer of samples from the LabTube to the reader. Due to the advantages shown in Table 22, the focus of this thesis was put on a system, in which DNA amplification occurs *outside* of the centrifuge. Here, the LabTube was combined with a handheld version of the LabReader.

Inside	Outside
+ No additional handling step	+ No blocking of centrifuge
	+ No modified centrifuge needed
	+ More flexible optical reader
- Modified centrifuge	- One extra handling step
- Centrifuge blocked	

TABLE 22: DNA amplification and readout inside vs. outside of the centrifuge.

3.4 SUMMARY

In this thesis, the LabReader optical detection scheme (Chapter 2) is combined with the LabTube, a disposable platform to automatically extract DNA inside a standard laboratory centrifuge. This combined system will automate DNA extraction, amplification and readout at low-cost. Due to market and feasibility reasons, food safety was selected as a first application for the combined system. VTEC *E.coli* and *Alicyclobacilli (A.acidoterrestris)* were used as first example organisms.

Inside the LabTube, DNA from VTEC *E.coli* lysate in milk and water, as well as from *A.acidoterrestris* lysate in apple juice were extracted to as low as 10^2 copies using the standard protocol of the QIAamp Micro DNA kit (100µl sample). The kit yielded the best performance of all screened kits. As little as $4.5 \cdot 10^1$ copies were extracted by optimizing the extraction protocol using 4 re-elutions, whilst multiple binding steps did not increase the yield.

DNA amplification and readout can occur either *inside* or *outside* of the centrifuge. Due to increased flexibility and the use of a standard centrifuge that is occupied for shorter time periods, it was decided to focus on amplification/readout *outside* of the standard centrifuge. This approach is outlined in the next chapter.

CHAPTER 4: DNA AMPLIFICATION AND READOUT OUTSIDE OF THE CENTRIFUGE (LABSYSTEM)

4.1 LABSYSTEM WORKFLOW

In this section, the combination of the LabTube and the portable LabReader into the LabSystem is introduced. The combined system allows for fully automated sample preparation, amplification and readout *outside* of the centrifuge. A sample workflow is shown in Figure 23 .

4.2 CHANGES TO THE LABTUBE AND LABREADER

In order to minimize manual steps and hence contamination risks during the sample transfer from the LabTube into the LabReader, an interface is needed. Further, the required sample volumes need to be small enough to be commercially competitive. These requirements made adjustments to the previously described LabTube and LabReader designs necessary.

4.2.1 LABREADER ADJUSTMENTS

The LabReader introduced in Chapter 2 was originally designed to use 6.5mm glass tubes as sample reservoirs. With the glass test tubes, volumes of at least 240µl were required to get a reproducible signal. To reduce reagent costs and to be competitive with standard laboratory instruments, it was necessary to reduce the sample volume to 20-40µl. As a contamination-free interface between the LabTube and the LabReader, the use of a standard containment was preferred.

Initially, the sample volume of the LabReader was reduced. As shown in Figure 24, using a glass rod inside the PCR tube or filling up a PCR tube with paraffin for volume-reduction, yielded irreproducible results. Even though a glass capillary requires low volumes and yielded reproducible results, it is difficult to incorporate a glass capillary into the LabTube due to its thin diameter. The use of a PCR tube was shown to be feasible. Because the PCR tube initially required large volumes of ≥150µl, it was lifted up relative to the LEDs and detectors such as to readout the sample in the conical part of the PCR tube. The plastic housing of the LabReader was also altered to smoothly fit the PCR tube rather than the round glass tube. The observed signal-to-background ratio of the PCR tube is similar to that of a glass tube. Reproducible results were achieved with 20-40µl of sample. Overall, the glass capillary and PCR tube require
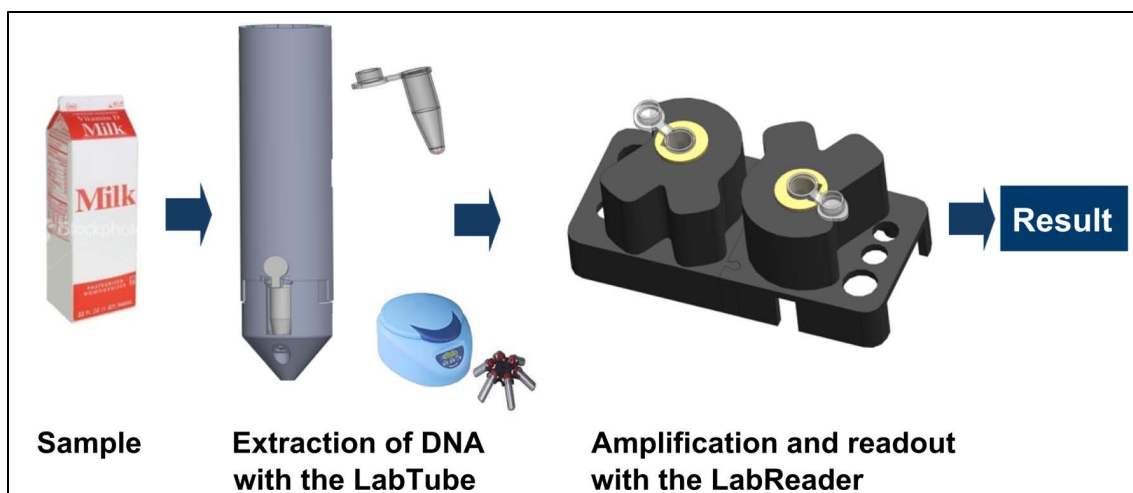
FIGURE 23: LabSystem workflow for the detection of pathogens in milk.

small sample volumes below 20-40µl and yield reproducible signals. The PCR tube was selected, because it is a standard containment.

As indicated in Figure 25, the PCR tube yields a higher relative fluorescence signal (RFU) than the glass tubes. The largest contribution to this increase in RFU is likely caused by the increased path length of the excitation light inside the sample chamber, hence exciting more fluorophores. This effect can be explained with the schematics shown in Figure 26.

	Original	PCR tube	Lifted PCR tube	Paraffin	Glass capillary	Glass rod
Standard lab container	No	Yes	No	Yes	No	No
Reproducibility	Yes	Yes	No	No	Yes	No
Volume (µl)	240	150	20 -40	N/A	30	N/A
Fluor.:Ref.	2.6	3.37	3.0	1.8	2.7	N/A

FIGURE 24: Sample volume reduction inside the LabReader.
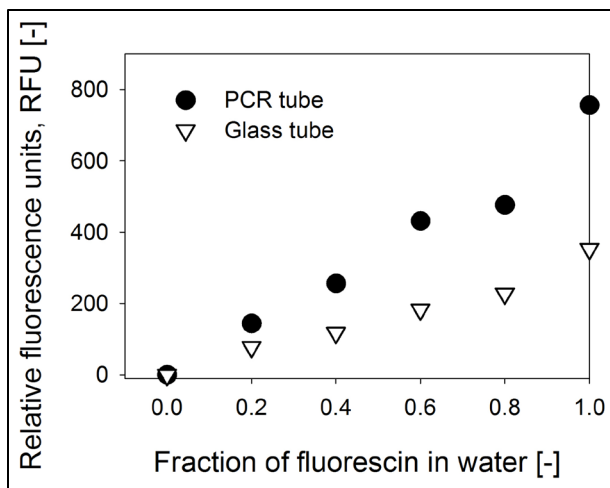
FIGURE 25: LabReader fluorescence with the glass and the PCR tube. Relative fluorescence units (RFU) of fluorescin and water mixtures at different ratios in both the glass tube and the PCR tube.
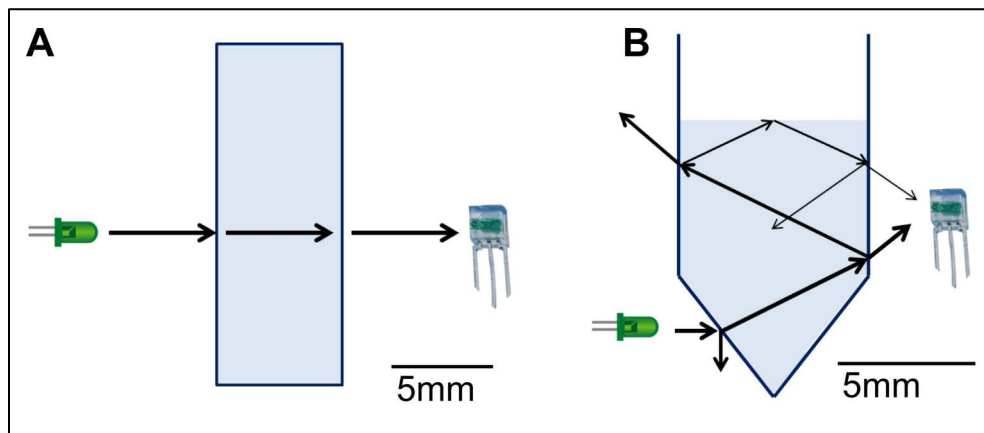
FIGURE 26: Optical paths in the LabTube. (A) Paths inside the glass tube. The incoming LED light gets transmitted straight through the glass column without being deflected. (B) Light path inside the PCR tube. Due to the angle in the PCR tube the incoming light gets deflected into the medium. As a result, light gets deflected in all direction and some of it is not captured by the detector. This causes the background signal to get reduced. Due to the longer path length more fluorescent particles get excited hence increasing the relative fluorescence. The thickness of the arrows qualitatively reflects the relative amount of light.

Light deflection by the glass/PE walls was neglected, because light passage through the walls (0.3-0.4mm) is significantly shorter than through the liquid sample (6.5mm). The figures show that light in a straight sample tube simply passes through without being reflected, whilst light in the PCR tube gets deflected into the medium due to the non-orthogonal walls. Due to this deflection, the excitation light travels a longer distance inside the PCR tube than inside the glass tube, hence exciting more fluorophores. In addition, more of the excitation light is lost from the PCR tube due to the deflection of light into various directions (see arrows), lowering the background signal.

4.2.2   LABTUBE ADJUSTMENTS

In order to minimize contamination risks during sample transfer into the LabReader, a removable PCR tube was incorporated into the LabTube as a DNA collection chamber. The design depicted in Figure 27 demonstrated full mechanical and fluidic functionality inside the centrifuge.
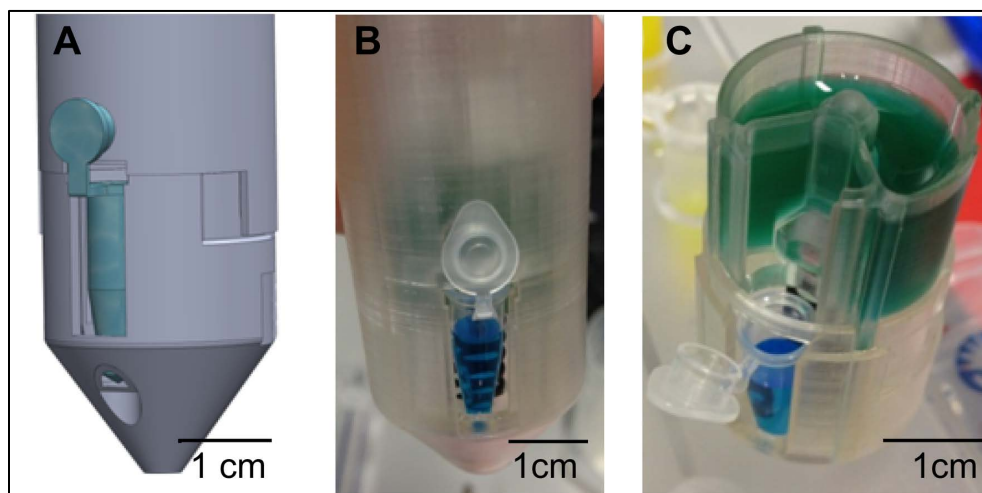
FIGURE 27: Removable PCR tube inside the LabTube. (A) 3D Solid Works model. (B) Fluidic and mechanical test inside the centrifuge. The eluate (blue) is collected in the PCR tube whilst the waste (green) is collected in the waste chamber (C).

4.3 QUALITATIVE DNA AMPLIFICATION

After reducing the sample volume and creating an interface between the LabTube and the LabReader, DNA amplification needed to be incorporated into the LabSystem. Different methods can be used to amplify DNA: These include quantitative DNA amplification via PCR and qualitative isothermal DNA amplification (e.g. isothermal loop-mediated DNA amplification, LAMP). The advantages and limitations of both approaches are summarized in Table 23. It was not possible to quantify amplification with the current setup, because the LabReader initially only employed two parallel detectors and because at least 4 references need to be run in order to get a quantitative result (a negative control, two data points for the standard series and a positive control [168][169]). An isothermal DNA amplification method (LAMP) was integrated into the LabReader, because in many cases the desired test result does not have to be quantitative, but instead the presence or absence above a certain threshold suffices (Chapter 1.1.3.1). Unlike PCR, LAMP does not require thermal cycling, allowing a simpler and cheaper, disposable heating system to be used. Out of several isothermal DNA amplification methods, the LAMP method is particularly temperature stable[170]. As shown in Table 24, the VTEC *E.coli* Mast Isoplex kit is temperature stable at 67±5°C (n=2; methods shown in Chapter 4.3.2). It was decided to incorporate isothermal LAMP amplification into the LabReader due to its temperature robustness and because it does not require temperature cycling steps.

	Real-time PCR	**LAMP**
Advantages	- Real-time monitoring of amplification - Quantitative - Multiplexing capability - Increased sensitivity due to fluorescent chemistry (target-specific probes) - High throughput analysis due to software driven operation	- Isothermal amplification without requiring a thermal cycler (e.g. 67±5°C) - Higher amplification efficiency and sensitivity - Naked eye visualization, turbidity or fluorescence readout - Short amplification time 30-60 min
Disadvantages	- Expensive detection equipments and consumables - Requirement for fluorescent probe - Restricted to referral laboratory with good financial support	- Complicated primer design (requirement for six primers) - Two long primers of HPLC grade purity - Restricted availability of reagents and equipment in some countries - Requires a laboratory

TABLE 23: Advantages and limitations of LAMP amplification and real-time PCR [171].

T (°C)	58	62	65	72	79
Pos.	±	+	+	+	+
Neg.	±	-	-	-	±

TABLE 24: Temperature stability of the VTEC *E.coli* Mast Diagnostica LAMP reaction, n=2.

4.3.1 TEMPERATURE CONTROL INSIDE THE LABREADER

In order to achieve uniform temperature profiles inside the LabReader, a thermal mass for temperature stabilization is needed. A metal (brass) piece with holes for heating elements and sensors can fulfill this task. Such a metal piece was fitted into the LabReader and it was heated with a Minco foil (10Ω, HK5565R10.0L12F) from the bottom. A NTC (EPCOS, NTC B57540G1103F) is used as a temperature sensor. The NTC is connected to a serial resistor of 1.2kΩ, whose voltage is picked off from the temperature regulation module (Carel, IR33DIN). Using this setup, the target temperature can be reached within 6 minutes and it is held stable to ±1.5°K for at least 30 min, as depicted in Figure 28.
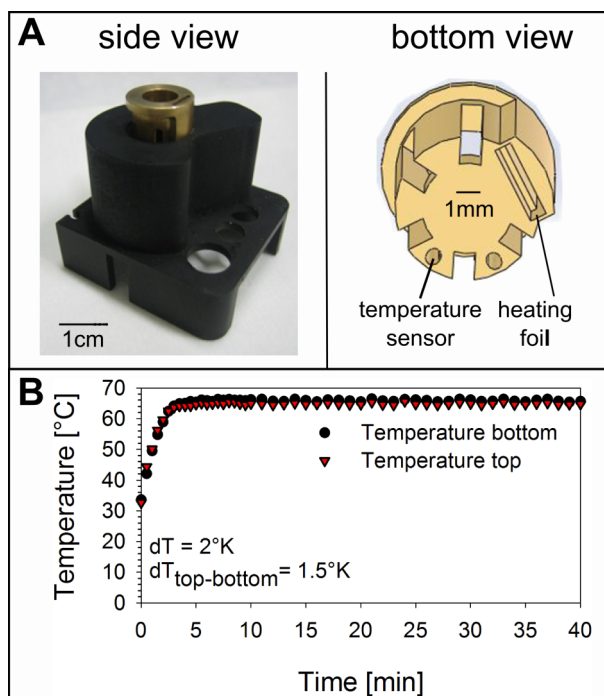
FIGURE 28: LabReader heater setup for LAMP. (A) Heated brass fitting for heating a PCR tube inside the LabReader. A Minco heating foil and a NTC are used as a temperature-sensor. (B) Temperature stability inside the heated LabReader.

4.3.2 CHEMICAL METHODS AND DATA ANALYSIS

For LAMP amplification of VTEC *E.coli*, an Isoplex VTEC screening kit (Mast Diagnostica) was used. For *A.acidoterrestris* amplification, a commercially available primer set (Eiken Chemicals) was used in combination with the DNA amplification kit from Mast Diagnostica. All LAMP reactions were visualized using the intercalating DNA dye SYTOX Orange (0.2µM). To start a reaction, 40µl of reaction mix were inserted into the LabReader and a control of 20µl was always run in parallel in the real-time cycler (7500, Applied Biosystems). The temperature was set to 65°C for 60 minutes. The amplification products were visualized using gel electrophoresis (Lonza Flash Gel). DNA extraction methods using the LabTube, as well as details of the control PCR reactions were described in Chapter 3.2.1.

In the LabReader LAMP amplification, fluorescence detector voltages were collected using a USB comport readout program H-term (www.heise.de). Data were averaged to one data point per minute. Each minute corresponded to one cycle in the analysis. The first minute was neglected in the analysis due to temperature dependencies of the dye during the initial heating process. The average values from minutes 2-4 were subtracted from each reading, in order to normalize the data to "relative fluorescence units (RFU)". The threshold value to determine the threshold cycle was picked at 800 RFU, which is inside the initial linear phase of the reaction near the maximum slope. This is the optimum range to determine the threshold cycle [172].

DETAILS OF INDIVIDUAL EXPERIMENTS:

In Table 24, the positive control provided with the Mast Diagnostica VTEC *E.coli* kit was run inside the real-time cycler at temperatures between 58-79°C.

The experiments in Figure 29 served as a proof-of-principle of the fluorescence LAMP reaction. Here, VTEC *E.coli* DNA sequences of uniform size from LAMP amplifications (provided by Mast Diagnostica) were used as templates of known copy numbers. 3 repeats were run at each concentration.

In the LabReader experiments of Figure 30, LabTube extractions and LAMP reactions were run with lysates of known concentrations for both VTEC *E.coli* in milk (3.6 wt%, fresh, Lidl) and water, as well as for *A.acidoterrestris* in apple juice. For all concentrations, at least three independent runs were measured in the LabReader and as a control five or more were measured inside the real-time cycler (for LAMP and qPCR amplifications).

Reagent	Volume (µl)
Master mix	32
BST polymerase	2
SYTOX Orange (4µM)	2
DNA sample	4

TABLE 25: VTEC *E.coli* LAMP protocol in the LabReader (Mast Isoplex VTEC screening kit, Mast Diagnostica).

Reagent	Volume (µl)
Reaction mix	23
BST Polymerase	2
Primer mix	5
SYTOX Orange (4µM)	2
Distilled water	4
DNA sample	4

TABLE 26: *Alicyclobacillus acidoterrestris* LAMP protocol in the LabReader (Mast Isoplex DNA kit and primer from Eiken Chemicals).

4.3.3 RESULTS

The results of the VTEC *E.coli* LAMP verification reaction are shown in Figure 29. The increase in relative fluorescence is plotted versus time for different copy numbers of VTEC *E.coli* DNA. A positive reaction was observed for ≥10 inserted copies. Even though high copy numbers reacted faster than lower ones, quantification was not reproducible for DNA target sequences and not possible at all when using purified DNA (with either silica columns or ethanol precipitation). In the literature, quantification of LAMP reactions using intercalating dyes (such as SYTO 85) has been described[173, 174]. However, the majority of publications and the manufacturer Mast Diagnostica, show qualitative results only. Some even specifically state that fluorescence quantification is not possible [175, 176]. The observed quantification inability could be explained by the inhomogeneous size of LAMP reaction products. It is expected that the signal from intercalating DNA dyes does not increase linearly with increasing DNA segment size, e.g. due to quenching effects, hence rendering quantification impossible.

The established fluorescence LAMP reactions were used for qualitative detection of VTEC *E.coli* in milk and water, as well as for *A.acidoterrestris* in apple juice. Prior to amplification, all

samples were extracted with the LabTube. The overall time-to-result for LabTube extraction and LAMP amplification is ≤1.5hrs.

Table 27 shows the results of fluorescence LAMP amplifications over at least 6 log-scales (with n=3 and 100µl inserted sample) in the LabReader. Inside the LabReader, the LoDs for both extraction and LAMP amplification are 10^2 and 10^3 copies of VTEC *E.coli* in water and milk and $4.5 \cdot 10^2$ copies for *A.acidoterrestris* in apple juice. The LoD was determined according to ICH standards (Chapter 2.2.1.6) and the data were not interpolated. Gel electrophoresis confirmed the presence of LAMP reaction products (Figure 30). Above the LoDs for VTEC *E.coli* and for *A.acidoterrestris* in all matrices, the average sensitivity (probability of a true-positive result) is 93.3±0.7%. The specificity (probability of a true-negative result) is 100±0%. The LoDs are identical to those achieved inside the real-time cycler and also to the qPCR control. Sensitivities are insignificantly higher in the LAMP real-time cycler control (96±3%), which is likely due to the larger number of repeats there. Overall, sensitivity and specificity values are comparable to those of qPCR, as shown in Table 28 [177], and are consistent with literature values.
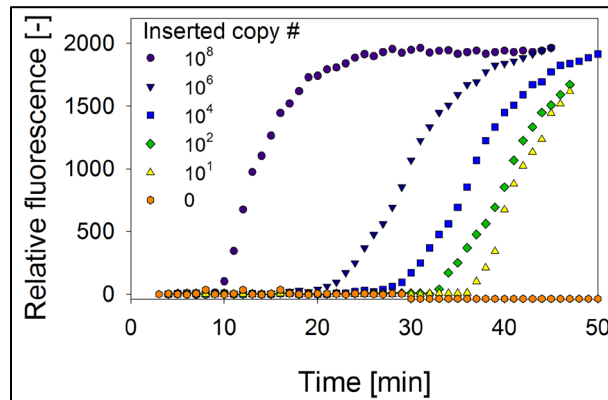
FIGURE 29: Normalized LAMP amplification curves in the LabReader using diluted target DNA sequences of VTEC *E.coli*. Here, high copy numbers reacted faster than lower ones.
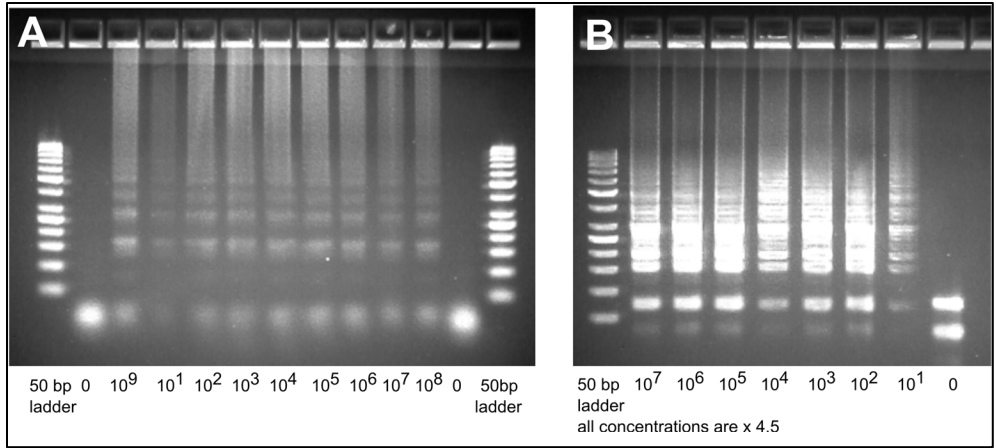
FIGURE 30: Gel electrophoresis results of (A) VTEC *E.coli* LAMP products extracted from water samples (B) *A.acidoterrestris* extracted from juice samples after LabTube extraction. The numbers correspond to inserted copies or the reference 50bp ladder.

Sample and inserted copy numbers into the LabTube		LAMP LabReader Positive reaction (%)	LAMP rt-cycler Positive reaction (%)	qPCR rt-cycler Positive reaction (%)
E.coli from water	10^9	100	100	100
	10^8	100	100	100
	10^7	100	100	100
	10^6	100	100	100
	10^5	100	100	100
	10^4	100	100	100
	10^3	100	88	88
	10^2	67	88	100
	10^1	33	17	0
	0	0	0	0
E.coli from milk	10^8	100	100	100
	10^7	100	100	100
	10^6	100	100	100
	10^5	100	100	100
	10^4	100	100	100
	10^3	67	88	94
	10^2	0	17	0
	10^1	0	0	0
	10^0	0	0	0
	0	0	0	0
Alicyclobacillus from apple juice	$4.5{\cdot}10^6$	100	100	100
	$4.5{\cdot}10^5$	100	100	100
	$4.5{\cdot}10^4$	100	100	100
	$4.5{\cdot}10^3$	100	100	100
	$4.5{\cdot}10^2$	67	80	100
	$4.5{\cdot}10^1$	33	34	0
	$4.5{\cdot}10^0$	0	0	0
	0	0	0	0

TABLE 27: LAMP DNA amplification of LabTube-extracted bacterial DNA. The percentage of positive reactions is depicted for LAMP reactions inside the LabReader, for the LAMP reaction control in the real-time cycler and for the qPCR control. The results are shown for different concentrations of DNA in the LabTube before the extraction of *E.coli* and *A.acidoterrestris* in water, milk and juice. The number of repeats at each concentration is n≥3 in the LabReader and n≥5 for LAMP in the real-time cycler and for qPCR.

Samples	LabReader		LAMP in rt-cycler		qPCR	
	Sn (%)	Sp(%)	Sn (%)	Sp(%)	Sn (%)	Sp(%)
E.coli water[1]	93	100	97	100	99	100
E.coli milk [2]	94	100	98	100	100	100
Alicycloba- cillus juice[3]	93	100	93	100	97	100

TABLE 28: Summarized sensitivity (Sn) and specificity (Sp) of the LAMP-LabSystem in different applications. The values were calculated from LabTube-extracted samples shown in Table 23 above their respective LoDs. ([1]$\geq 10^3$ copies, [2]$\geq 10^2$ copies, [3]$\geq 4.5 \cdot 10^2$ copies before the extraction).

4.4 SEMI-QUANTITATIVE DNA AMPLIFICATION

Qualitative DNA amplification was demonstrated in Chapter 4.3. With the introduced LabReader setup of 2 parallel detectors, quantification is not possible. However, using the same batch of reagents in combination with real-time PCR, semi-quantification is feasible. This is because the standard curve, controls and samples can be run consecutively rather than simultaneously when using the same batch of chemicals (Chapter 4.3). Furthermore, PCR is the most established DNA amplification method. It has multiplexing capability and many commercial systems are available. In this section, semi-quantitative PCR incorporated into the LabReader is described. As a first example, an *E.coli* PCR assay and readout method is presented.

4.4.1 TEMPERATURE REGULATION

In order to run a PCR reaction in the LabReader, it was necessary to incorporate temperature cycles into the system (see Chapter 1.2.2.4). The required temperature profile is described in Table 29. A metal (brass) piece was incorporated into the LabReader for temperature stabilization during LAMP amplification, as described in Chapter 4.3. The openings for heating elements in the metal are small, allowing only for built-in heaters with dimensions of less than 5x1mm. The power limits of heating foils used in the LAMP reaction are too low to heat a PCR reaction in a reasonable time. Instead, two SMD power resistors (Vitrohm 502-0, 270Ω) were incorporated as heaters, because they fulfill both the size and power requirements. In the setup, they were connected in parallel to increase the overall heating power without damaging the resistors through exceeded power limits (Figure 31). Due to high temperatures at the solder spots (>200°C), a high-melting- point solder, T_m=301°C, was chosen (DHMP, Reel).

Step	Temperature (°C)	Time (s)
Heating	95	180
Annealing (A)	95	3
Extension (E)	62	20
No. of cycles (A+E) = 40		

TABLE 29: Temperature profile for *E.coli* PCR reactions.
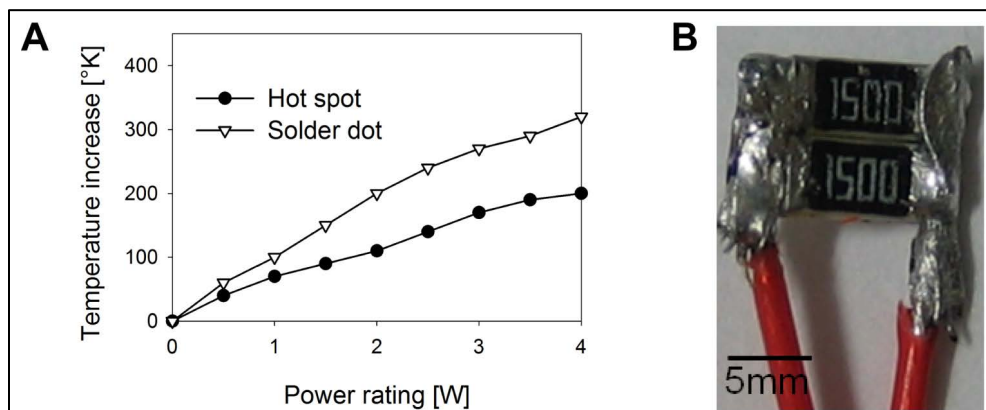
FIGURE 31: LabReader heater setup for PCR. (A) Heating profile of the power resistor (Vitrohm 502-0, from manufacturer data sheet). The temperature increase is indicated in °K from room temperature (20-25°C). (B) Parallel connected heating resistors.

The heat sink is all metal (brass), hence an electrical insulation was needed that could at the same time conduct heat. The insulation material further had to be small such as to still fit into the metal fitting and it had to endure high temperatures of at least 200°C, as the hot spot of the resistor had to be covered as well (Figure 31A). Out of several tested materials, only wrapping the resistors in thin "Kapton" foil fit the size requirements and it was shown to protect the heater from short circuits. Computer fans (NMB-MAT, 1606KL) added on top of each sensor (Figure 32A) were used for cooling. The temperature was controlled using a Lab VIEW program and executed by two modules from National Instruments: Type 9211 – an analog input for the temperature sensors (K-Type) – and Type 9478 – to digitally switch up to 16 ports. The latter was supplied with 24V DC voltage at a maximum current of 5A. The heaters were controlled by pulse width modulation (PWM) that control the heater power. The duty cycles for these PWMs were not fixed but limited to a maximum duty cycle to prevent destruction of the heaters. To reach good dynamic behavior without oscillation, the duty cycle was generated by PID control. When the measured temperature reached the set temperature, the heaters were turned off.
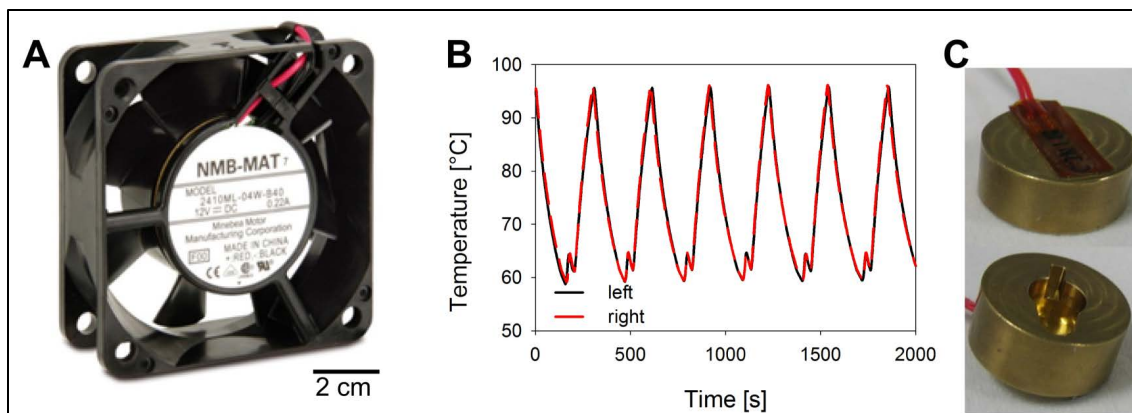
FIGURE 32: LabReader cooling setup and temperature profile for PCR (A) Heater fan (image reprinted with permission from Pollin Electronic[178]). (B) Achieved temperature profile for PCR in both the left and right LabReader chambers. (C) Caps with heat foil (Minco).

Once the specified temperature limits were exceeded, ventilation by the fans was started. Due to individual non-static deviations of heaters, fans and the face surface to the air current, each chamber needed to be controlled individually. The process was paused until the same temperature was reached in each chamber, such as to induce the same cycle time for both. The achieved temperature profile is shown in Figure 32B. Without further measures, the sample would evaporate, hence rendering the PCR reaction impossible. This is why PCR-compatible mineral oil (Sigma Aldrich) needed to be added to the top of the sample. It was shown that the process also works by applying heat from the top using heat foils (Minco, R = 10Ω, VDC = 5V) attached to brazen caps (Figure 32C). Here, the heaters on top are generally turned on except when the fans are active. For the experiments in this thesis, only mineral oil was used.

4.4.2 DATA ANALYSIS AND CHEMICAL METHODS

4.4.2.1   AMPLIFICATION OVER TIME

The detector voltage levels were readout using the com-port readout program H-term. The readout of the sensor generates a text file with nine columns for the different channels and a row for every measured second. In order to get the typical PCR curve, signal-processing is necessary. The raw data and the analyzed data of an exemplary run are depicted in Figure 33 A and B. The oscillation of the signal, as shown in Figure 33A, originates from a temperature
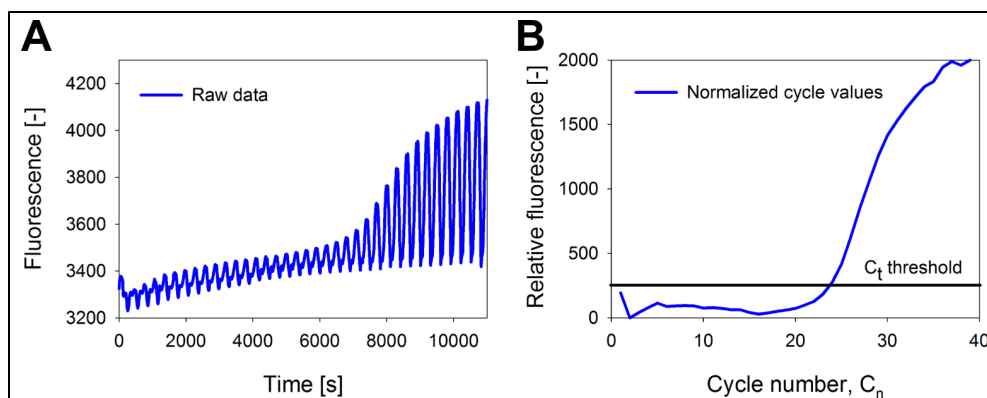
FIGURE 33: Raw and processed data. (A) Raw data. At high temperatures around 95°C the DNA denatures, causing a loss of fluorescence. (B) Processed data are normalized by subtracting the minimum from the maximum fluorescence value in each cycle.

dependency of the intercalating DNA dye, SYTOX Orange. This temperature dependency can be explained by the fact that the intercalating dye does not bind to denatured DNA at 95°C, hence causing signal loss (minima), whilst a maximum signal is achieved at 62°C (the readout temperature) when the maximum amount of dye is bound to the DNA. The difference between each cycle's minimum and maximum was calculated. This was achieved by determining the cycle time for each run, widening the time by some insecurity (310±40s) and determining the maxima and minima using dynamic references for each cycle. The greatest difference was set to a fixed value (2,000) and the lowest difference was set to zero. The procedure of subtracting minima also automatically normalized the signal - hence rendering the use of a passive reference dye unnecessary. For the identification of the threshold cycle, the average of the differences of the first ten cycles was taken and raised by 15%. The last cycle with a value below this threshold and the first above were connected by a straight line. The exact threshold cycle was determined by linear interpolation.

4.4.2.2   MELTING CURVE

When running PCR reactions with nonspecific intercalating DNA dyes, it is important to run a dissociation curve following the real-time PCR. This is due to the fact that intercalating dyes detect any double stranded DNA including primer dimers, contaminating DNA, and PCR product from misannealed primers [179]. Hence, nonspecific amplification may cause a false-positive amplification curve. In the melting curve, temperature of the DNA sample is increased during which the double strand begins to dissociate leading to a loss of bound dye and hence

fluorescence intensity [180]. The temperature at which 50% of DNA is denatured is known as the melting point and its temperature depends on the size and composition of the DNA piece. The graph of the negative first derivative of the melting-curve allows easier visualization of DNA dissociation, by virtue of the peaks thus formed [180]. In order to run a melting curve, a Lab VIEW program was used, which employs the same modules, voltages and heaters as previously described. In the melting curve, two cycles were executed: the first cycle was fast (20°C/min) and the second one in which data readout occurs was slow (4.7°K/min) (Figure 34A). The temperature was recorded using Lab VIEW. Simultaneously, LabReader data were acquired using H-term. This way, the fluorescence could be plotted as a function of temperature, shown in Figure 34B. Melting points of PCR products correspond to the inversion points of the curve. In order to visualize these inversion points, the negative derivative of the fluorescence was plotted (Figure 34C). In the figure, the PCR product and primer dimers are visualized as peaks at temperatures 87°C and 78°C. They can therefore be distinguished from each other.

Reagent	Volumes for each reaction (µl)
QuantiFast master mix	20
Forward primer	0.4
Reverse primer	0.4
SYTOX Orange (2µM)	2
RNAse free water	9.2
Template DNA	8

TABLE 30: SYTOX Orange PCR reaction composition.
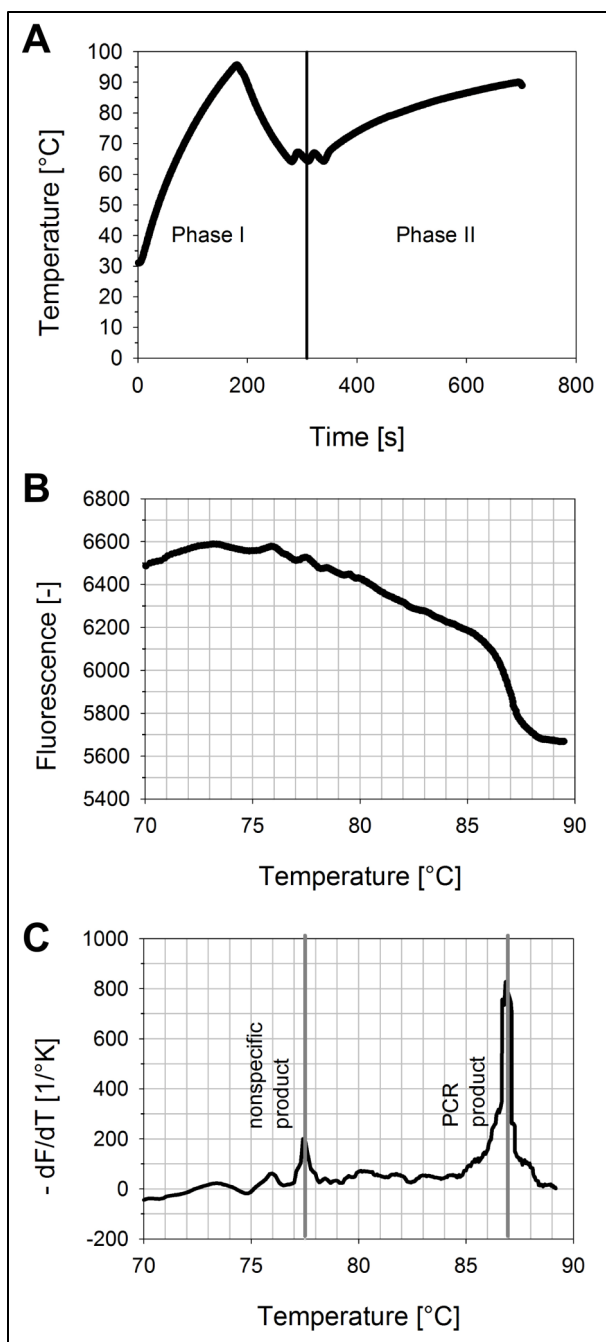
FIGURE 34: Data readout and analysis procedure for PCR. (A) Melting curve temperature profile. Data readout occurs after the quick cycle through 95°C and 62°C (20°K/min) during the slow heating cycle from 70°C to 90°C (4.7°K/min). (B) Fluorescence of the PCR product from VTEC *E.coli* as a function of temperature during heating phase II. (C) Negative first derivative of the fluorescence vs. temperature shows characteristic product peaks at ca. 88°C and primer dimers at 78°C. F stands for fluorescence and T for temperature.

4.4.2.3   DATA READOUT AT 85°C

To avoid running a melting curve, data was readout at temperatures above the melting point of nonspecific products and below that of specific products. This procedure eliminates signal from nonspecific products. In the *E.coli* PCR shown earlier, one could readout data above 78°C and below 87°C in order to eliminate signal from nonspecific products. Acquired signals from the amplification curve were therefore reanalyzed. The most reproducible results were achieved by dividing the difference in fluorescence signal between 85°C and 95°C by the difference in fluorescence signal between 62°C and 95°C in each temperature cycle – hence normalizing the data to differences between batches and cycles.

4.4.2.4   PCR PROTOCOLS AND CONTROLS

The used primers and probes were described in Chapter 3.2.1.5 and the data analysis in the LabReader was described in Chapter 4.4.2. For PCR experiments inside the LabReader, 40µl of reaction mix were used. The reaction mix had the ingredients shown in Table 30. For the standard curve, genomic DNA was diluted down from 10^6-10^0 inserted VTEC *E.coli* DNA copies, which according to Figure 22 would correspond to $1.1 \cdot 10^7$ DNA copies inserted into the LabTube. Three runs were performed per concentration. For all other experiments, juice, milk and water were spiked with lysates of VTEC *E.coli* at known concentrations and they were extracted with the LabTube prior to amplification. Each data point is the result of one experiment. The amplification products were visualized using gel electrophoresis (Lonza Flash Gel). A control was always run in parallel in a real-time cycler (Applied Biosystems, 7500). LoD and LoQ values were calculated according to ICH standards described in Chapter 2.2.1.6.

4.4.3   RESULTS

Figure 36 shows the PCR amplification of LabTube extracted VTEC *E.coli* lysates in water, milk and apple juice inside the LabReader. Figure 36A depicts a standard curve performed with genomic DNA. The standard curve consists of a log-dilution series of 10^6 inserted VTEC *E.coli* DNA copies, which according to Figure 22 corresponds to $1.1 \cdot 10^7$ DNA copies inserted into the LabTube (x-axis). Because the same batch of reagents was used, semi-quantification was possible. A fit revealed that the PCR has an efficiency of 110% in the real-time cycler and 95% in the LabReader, which is acceptable[172]. The lower efficiency in the LabReader is likely due to longer heating and cooling cycles (overall 3.2 instead of 1.3hrs), variations in cycle times (~310±20s), as well as the temperature inaccuracy of ±1.5°K in the LabReader. For the

standard curve, the average error in the LabReader is ±19.1% (corresponding to a threshold cycle variation, C_t ±0.26), whereas it is only ±8.7% (corresponding to C_t±0.13) in the real-time cycler. In addition to the mentioned causes, this difference is expected to develop due to the fact that in the LabReader samples are processed consecutively instead of in parallel.

After establishing the standard curve, VTEC *E.coli* from water, milk and apple juice were extracted with the LabTube and amplified in the LabReader at different concentrations. All data shown in Figure 36A falls onto a universal master curve. The LoD for both extraction and amplification in the PCR-based LabSystem is 10^2 and the LoQ $2 \cdot 10^3$ (interpolated) inserted copies of VTEC *E.coli* from water and apple juice. For VTEC *E.coli* from milk the LoD is 10^3 and the LoQ $2 \cdot 10^4$. Even though VTEC *E.coli* DNA was extracted from different matrices, the average error of the standard curve is only C_t±0.56, i.e. ±47%, in the LabReader. The average error of the real-time cycler control is C_t±0.42, i.e. ±33.7%. The error is larger than for genomic DNA in the standard curve. It is expected to be caused by the error of the LabTube extraction (26%, see 3.2.2.3) and pipetting errors. The error in the real-time cycler is expected to be lower than in the LabReader, because samples are run in parallel, rather than consecutively, and because the temperature profile may be better regulated, with cycle times being both faster and more constant than in the LabReader.

The standard curve is only linear above 10^3 inserted copies. Figure 36B shows the time curves of different genomic VTEC *E.coli* DNA concentrations in water, from which threshold cycle values were calculated. In this graph it is shown that even the negative control shows a false positive reaction, hence explaining the asymptotic calibration curve at low concentrations. The false positive result could be caused by nonspecific product formation, such as primer dimers. Figure 36C depicts the melting curve to differentiate specific from nonspecific products. The presence of nonspecific products and the lack of PCR products were observed at concentrations below 10^2 equivalent DNA copies in the LabTube (Figure 35). These results were confirmed by gel electrophoresis, which revealed the presence of primer dimers below 10^3 inserted copies. Running a melting curve after each PCR to confirm the presence of specific PCR product is therefore necessary.

The data shown in Figure 36 was effectively acquired at 62°C. Because the nonspecific product melts at 78°C the signal from both the nonspecific and specific PCR products are detected at 62°C. Unlike the real-time cycler, the LabReader reads out the signal continuously at all temperatures. Because the temperature is plotted along with the amplification data, it is possible to plot the normalized fluorescence signal at a temperature above the melting temperature of

the nonspecific product[181]. By taking the normalized slope at 85°C (Chapter 4.4.2.3), the signal from nonspecific product was eliminated as shown in Figure 37. The LoQ for the combined extraction, amplification and detection is 10^2 inserted copies for VTEC *E.coli* from water and apple juice and 10^3 inserted copies for VTEC *E.coli* from milk. The error of $C_t \pm 0.56$, i.e. 45.8%, is similar to the readout at 62°C shown in Figure 36. This method greatly simplifies data acquisition and analysis, as it eliminates the need to run a melting curve after each amplification reaction. The described readout option is not easily incorporated into a commercial real-time cycler without adding an additional readout step of several seconds to the temperature profile (e.g. 85°C for 20s/cycle). This additional step both elongates the run and results could be affected by altering the temperature profile in a commercial real-time cycler.
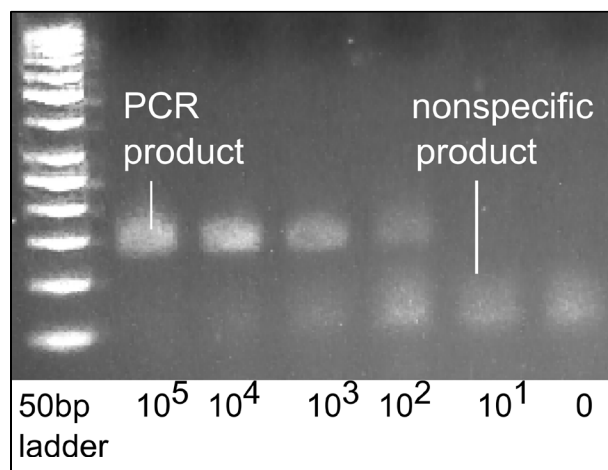
FIGURE 35: Gel electrophoresis of PCR product from *E.coli* in water. The PCR product is ~150bp in size and the nonspecific product ~50bp. The indicated concentrations correspond to equivalent copies inserted into the LabTube for extraction.
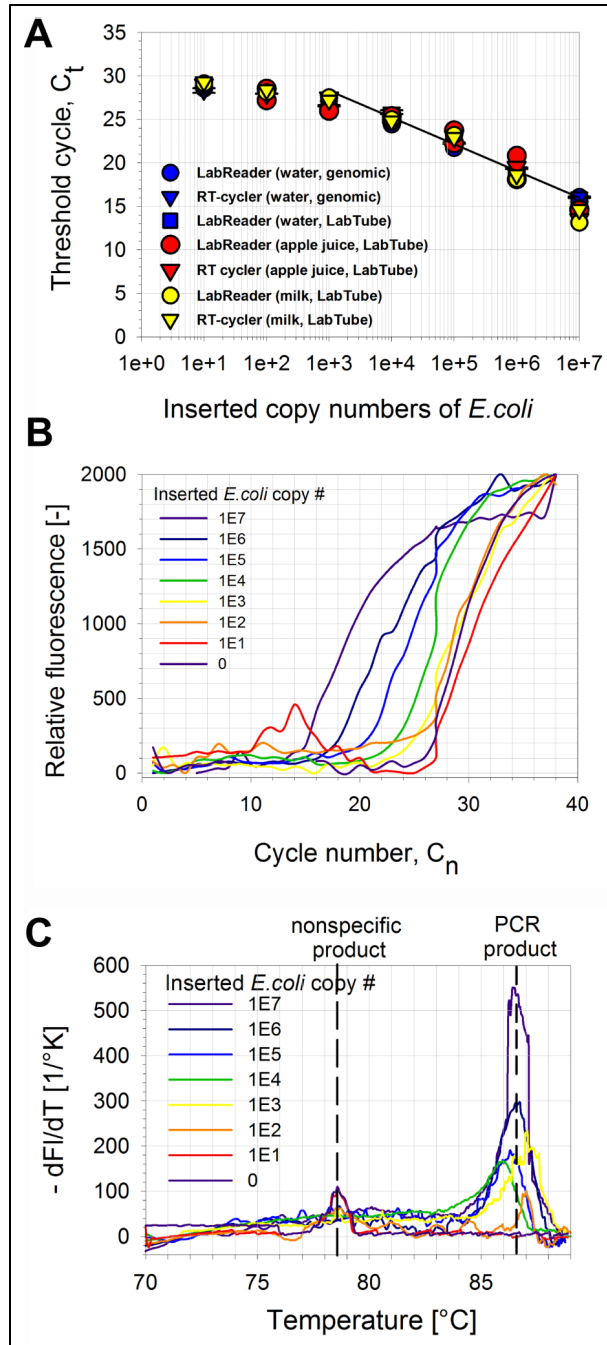
FIGURE 36: *E.coli* PCR in the LabReader. (A) Threshold cycles, C_t, for different copy numbers of *E.coli* extracted from real samples using the LabTube. The readout temperature was effectively 62°C (n=3 for the standard curve, n=1 for other samples). (B) Reaction curves for different copy numbers of genomic *E.coli* DNA in water. The negative control showed a false-positive reaction curve. (C) The melting curve distinguishes PCR products at T_{melt}=87°C from nonspecific products at T_{melt}=78°C. dF/dT is the change in SYTOX Orange fluorescence with temperature.
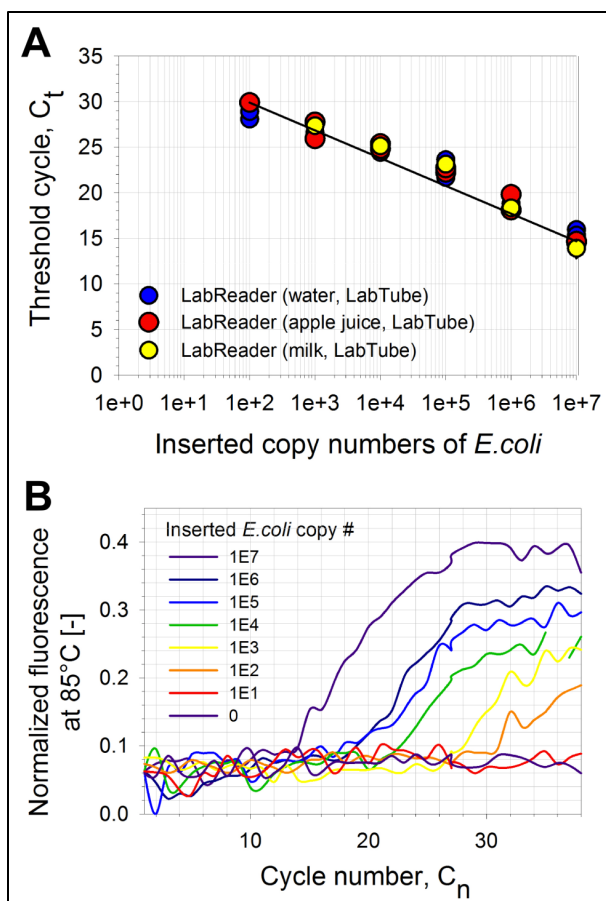
FIGURE 37: *E.coli* PCR in the LabReader using the intercalating dye SYTOX Orange with readout at 85°C above the melting point of nonspecific products. (A) The calibration curve no longer shows false positive signals below 14 inserted copies. (B) Reaction curves for different copy numbers of genomic *E.coli* DNA in water (effective fluorescence vs. cycle number).

4.5   DISCUSSION AND SUMMARY

In this chapter, the LabSystem, consisting of the LabTube and the LabReader, was used to extract, amplify and readout DNA. As first example organisms, pathogenic verotoxin-producing (VTEC) *E.coli* in water and milk, and the product-spoiler *Alicyclobacillus acidoterrestris* in apple juice were extracted and amplified. The extracted DNA was amplified using both the qualitative isothermal LAMP method (LAMP-LabSystem) and the semi-quantitative real-time PCR reaction (PCR-LabSystem). The product specificity was determined in the PCR-LabSystem by performing a melting curve or by reading out at temperatures above the melting point of

nonspecific products (here 85°C). The combined extraction and amplification LoD of the LAMP-LabSystem was 10^2 and 10^3 inserted copies of *E.coli* in water and milk and $4.5 \cdot 10^2$ copies of *Alicyclobacillus* in apple juice. The combined extraction and amplification LoQ of the PCR-LabSystem was 10^2 inserted copies for *E.coli* in water and juice and 10^3 inserted copies in milk using a readout temperature of 85°C.

Overall, the achieved detection limits for LAMP and real-time PCR (10^2-10^3 inserted copies) imply that no pre-incubation is needed for many food safety applications of *E.coli*, where the required LoD is often 10^2-10^4 CFU/g [182]. For *A.acidoterrestris* the required detection limit is usually 1 CFU/ml[85], hence pre-incubation or sample concentration is needed. In such cases, cells could be pre-concentrated, e.g. using a filter. Alternatively, a brief pre-incubation to increase cell concentrations could be performed inside cylinder I of the LabTube.

The achieved results can be improved in a variety of ways. 100μl sample were extracted in the LabTube, which can hold up to 4ml. For the LAMP-based LabSystem inserting 4ml of sample into the LabTube and inserting 2.5 times more extract into the LAMP solutions, will theoretically lead to a reduction of the LoDs to 10^1 and 10^2 inserted copies/ml for *E.coli* in water and milk and $4.5 \cdot 10^1$ inserted copies/ml for *A.acidoterrestris* in apple juice. Similarly, for the real-time PCR-based LabSystem the theoretical detection and quantification limits could be reduced to LoD=$2.5 \cdot 10^1$ and LoQ=$2.5 \cdot 10^2$ inserted copies/ml by employing 4ml of sample. In order to enable batch-independent quantification of real-time PCR, at least 4 different controls are needed[169]. Because detectors are low-cost, it would be possible to add four or more reaction chambers to the LabReader for quantification. In order to increase sensitivity and specificity a target-specific probe (for example TaqMan) could be used. Different PCR primers could be designed to eliminate nonspecific product formation. Temperature regulation could be optimized by using stronger heaters and stronger fans with a better geometry that cools from multiple sides. The time-to-result of the PCR reaction could be easily lowered by reducing the thermal mass of the metal inlet.

In a final product, robustness could be increased by incorporating the LabReader components into a completely closed and light-proof housing. Data analysis and display could be incorporated into the LabReader through a microcontroller or into a mobile device, such as a phone or a tablet computer, in order to make the heated LabReader truly portable.

Unlike many traditional and novel methods (e.g. biosensors; Chapter 1), the automated LabSystem can run with standard equipment. It is flexibly usable for a variety of applications

and assay types (e.g. isothermal or PCR amplification) at the production site, at food services, sales locations, etc.. Unlike many commercially available benchtop extraction and amplification devices, it is easily scalable, minimizes contamination through a standardized interface and is not limited to specialized kits. Its use is not limited to food safety, but it could in the future also be used for medical diagnostics, environmental contaminations and for quality control.

CHAPTER 5: DNA AMPLIFICATION INSIDE OF THE CENTRIFUGE (HEATED LABTUBE)

5.1   INTRODUCTION

This chapter outlines how to extract, amplify and readout DNA *inside* the centrifuge. For this approach, the round LabReader optical scheme can be integrated into the centrifuge-holders for readout. A heating method inside the centrifuge is needed for amplification.

In such a system, the heating method could not only be used for the amplification of DNA, but also for other applications outlined in Table 31 [183]. For example, it could be used for preheating lysis and elution buffers to increase DNA extraction yield and quality. The heating method could also be used to remove ethanol from the silica matrix. Ethanol removal is necessary to avoid inhibition of downstream processes (e.g. PCR gets inhibited at ethanol concentrations higher than 1-2.5wt% [184, 185]). Routinely, ethanol is removed from DNA extraction columns by centrifugation at high acceleration forces of 6,000-12,000g. However, these cannot be achieved by large centrifuges (with a capacity >10 LabTubes, which generally have a maximum acceleration forces of 3,600g). Here, heating to drive off ethanol from the column could be a viable alternative. Lastly, the heater can be used for other downstream applications like biochemical assays (e.g. immunoassays) or for other extractions, like those of proteins or RNA. For extractions in which heating yields higher extraction efficiencies and quality, amplification inside a custom-centrifuge may be preferable over the LabSystem outlined in Chapter 4.

This chapter consists of four sections. The first section is a theoretical temperature control evaluation of different heating methods. Following, DNA amplification inside an autonomously heated LabTube using a standard centrifuge is outlined.

Process	Cell lysis	Inhibition proteases	DNA elution	Removing ethanol	Isothermal DNA amplification
Temperature (°C)	56, 70	90	70	78	65
Time (min)	15	5	10	3-5	30-60
Volume (µl)	170	170	20 - 100	~20-100	100-150

TABLE 31: DNA extraction processes requiring heating [183].

The third section outlines theoretically how the LabReader optical scheme could be incorporated into the centrifuge. Finally, a critical evaluation of heating method applications inside the LabTube is presented.

5.2 THEORETICAL TEMPERATURE-CONTROL EVALUATION

A theoretical temperature-control evaluation was performed. The heating system inside the centrifuge or LabTube needs to meet several criteria:

- The heating component inside the disposable LabTube needs to be cheaper than $1 in mass production, since the LabTube is a disposable unit.
- The temperature ramping between 20 and 100°C needs to be faster than 3 minutes.
- The temperature stability needs to be ±6°K for heating buffers and ±2°K for DNA amplification for at least 40min.
- The heating system has to fit into the available space of the LabTube (1-2ml) and/or the centrifuge.
- The system has to be safe and easy-to-use.

Three different heating strategies were evaluated based on technical and economic feasibility, as well as based on energy profiles. These strategies include:

- Centrifugal heating based on frictional forces during centrifugation.
- Chemical heating based on the heat released during exothermic reactions.
- Electrical heating based on electric heating systems driven by external power sources or by induction.

The three heating strategies were expected to be associated with different risks, as can be seen in Table 32. The following chapter outlines the detailed theoretical evaluation of these methods. The goal was to select the most suitable heating method for the LabTube.

5.2.1 CENTRIFUGAL HEATING

Friction forces during the centrifugation process create heat. Friction occurs both between the rotor and the air, as well as inside of air turbulences caused by centrifugal rotation. A cooling system inside the centrifuge removes the developed heat. By reducing or turning off the cooling system, the centrifuge may hence be used as a heater. According to Hermle, a German centrifugal manufacturer, the maximum safe temperature inside the centrifuge is 50°C. Using

temperature loggers (Nexsens, micro-T DS 1922T), the temperature inside the LabTube cylinders (I-III) was measured during centrifugation. It was shown that the internal LabTube temperatures only deviate from that of the centrifuge by ±1°K. Hence, the maximum temperature inside the LabTube is also 50°C. This result implies that isothermal DNA amplification (e.g. LAMP, which operates at ~65°C) cannot be performed. Further, ethanol cannot be evaporated (T_{vap}=76°C) by centrifugal heating. Nevertheless, the system can be used for other isothermal amplification methods (such as RPA, which runs at 37°C) or for other applications, such as preheating DNA extraction buffers. This is the reason the centrifugal heating performance was evaluated as a next step. To do so, the cooling system of a centrifuge (Hermle, Type Z326K) was switched off. Using small temperature loggers (Nexsens, micro-T DS 1922T) in cylinders I-III of the LabTube and by varying centrifugal accelerations over time, the temperature increase was monitored. The measured temperature differences between LabTube cylinders I-III were negligible. The results at different temperature accelerations (n=3 in each of the three cylinders) are shown in Table 33. As depicted in Table 33, the time to heat a sample by 20°K ranges from 12min at 6,000g to 210min at 1,000g. These results demonstrate that the heating time is too long (>>3min) for LabTube heating. Additionally, the temperature profile is stable to on average ±4.8°K only, which is more than required for many biochemical reactions, such as DNA amplification. Controlling temperature using centrifugal heating is therefore not practical and was rejected.

Centrifugal	Chemical	Electrical
Heating may be time consuming (> 5 min) depending on rpm.	Required reagent volume may be too large (> 1-2ml).	Not cheap enough (> \$1).
Centrifuge might not heat up to the desired T.	Temperature may not be stable ($\Delta T > ±3°K$).	Size vs. weight.
	No precise temperature timing (no clear „on and off" switching possible).	

TABLE 32: Risks associated with different heating methods.

Acceleration (g)	Average heating rate (°K/min)	SD heating rate (°K/min)	Time to heat from 20-55°C (min)	Time to heat from 20-40°C (min)	Temperature stability (±°K)
1000	0.095	0.002	368	210	4.1
3000	0.204	0.000	171	98	5.0
5000	1.041	0.000	57	26	4.9
6000	1.710	0.006	20	12	5.3

TABLE 33: Heating rates and times at different centrifugal accelerations. Averages are taken from at least three independent measurements in each of the three LabTube cylinders. SD = standard deviation.

5.2.2 CHEMICAL HEATING

Exothermic reactions as means to heat the LabTube were evaluated.

Exothermic reactions create energy through e.g. heats of solution, phase changes (e.g. supersaturation or dissolution), as well as during redox reactions. In order to find suitable reactions, 25 exothermic chemical reactions were screened (see Table 34). From this list unsafe reactions were rejected, as determined by a "danger score" greater than 8 (see Table 34). The danger score is defined as the sum of HMIS scores of the most dangerous compound in the reaction. Reactions deemed unfeasible for use inside the centrifuge were also rejected. Those include supersaturated liquids, which were shown to occasionally crystallize spontaneously during centrifugation. Thermite reactions require large activation energies of ~150kJ/mol and were therefore also deemed unfeasible. Additionally, reactions with reaction enthalpies dH<50 kJ/mol were rejected as the LabTube can only hold additional ~1-2ml of reagents[4]. After the selection process, six chemical reaction candidates remained. They are summarized in Table 35.

As shown in Figure 38, exothermic reactions follow a peaking temperature reaction curve. In various publications, exothermic reaction temperatures were stabilized by putting a phase-

---

[4] With a reaction enthalpy, ΔH_{rctn}, of 50 kJ/mol, it is estimated that 2ml of reagent are needed to heat a sample from 25-65°C for 40min (assuming losses of a factor 34). This is calculated with the equations below, where M is the molar mass and ∂ the density of the reagents (assumed to be water), ΔH_{rctn} is the reaction enthalpy and Q_{sample} is the heat required to heat a sample with the heat capacity of water by a temperature, ΔT. $V_{reaction} = \frac{M}{\sigma} \cdot \frac{Q_{sample}}{\Delta H_{rctn}} = \frac{M_{H20}}{\sigma_{H20}} \cdot \frac{m_{sample} \cdot C_{H20} \cdot \Delta T}{\Delta H_{rctn}} \cdot losses \approx \frac{18}{1} \cdot \frac{1 \cdot 4.18 \cdot 40}{50000} \cdot 34 = 2ml.$

change material (PCM) in thermal contact with the exothermic reaction chamber [186, 187, 188]. A PCM has a high heat of fusion and it is often paraffin-based. It changes its phase at a certain temperature. Because it requires large amounts of energy in the process, it may be used to stabilize temperature [189]. Paraffin-based PCMs are available at melting temperatures between 0-100°C [190].
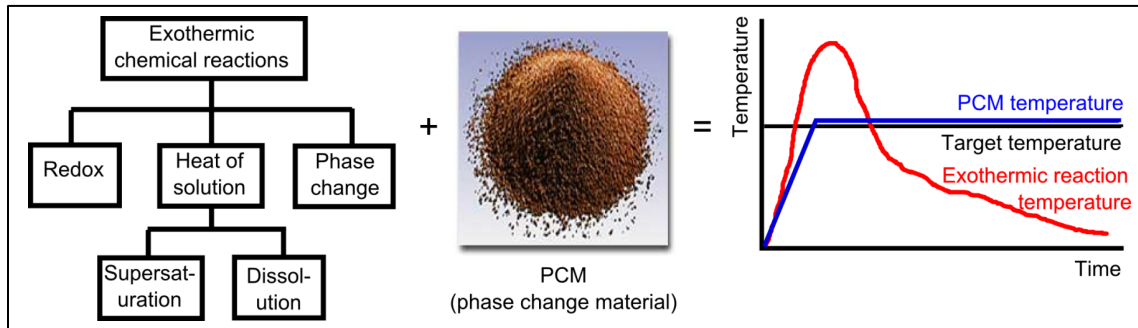

FIGURE 38: Exothermic chemical reaction and PCM temperature profile (image of the PCM is reprinted with permission from Rubitherm GmbH).

Reaction	Reaction Details	(-) dH° (kJ/mol) [191]	T_{max} from 20°C (°C)	Time to T_{max}	Time period at T_{max}	pH	Gas development	HMIS score of most dangerous ingredients[192]	Danger Score	Compatible with centrifuge	Application
Iron and Air [193]	$4\ Fe(s) + 3\ O_2(g) + 6H_2O\ (g) \rightarrow 4\ Fe(OH)_3(s)$	854	~ 70	min	hrs	-	yes	1,0,0,-	1	yes	activated carbon; hand warmers
Iron (pyrophor) [194]	$4FeS + 7O_2 \rightarrow 2Fe_2O_3 + 4\ SO_2$	5284	~ 200	sec	sec-min	-	yes	1, 4, 4, E (burns)	13	yes	
Raney-Nickel (pyrophor) [195]	$2AlNi_3 + 6\ O_2 \rightarrow 2Al_2O_3 + 6NiO$	4472	~ 300	sec	sec-min	-	yes	2, 3, 1, E (burns)	10	yes	catalyst
Magnesium and Water [196]	$Mg(s) + 2H_2O(g) \rightarrow Mg(OH)_2(aq) + H_2(g)$	352	> 100	min	min-hrs	base	yes	1,3,2,E	8	yes	ready to eat meals (REMs)
Calcium Oxide and Water [187]	$CaO(s) + H_2O \rightarrow Ca(OH)_2\ (aq)$	63	> 100	sec	sec-min	base	no	3,0,2,J	8	yes	ready to eat meals (REMs)
Calcium Oxide and Hydrochloric Acid [197]	$CaO + 2HCl \rightarrow CaCl_2 + H_2O$	14	> 100	sec	sec-min	acid	no	3,0,1,J	7	yes	ready to eat meals (REMs)
$CaCl_2$ and Water [187]	$CaCl_2(s) + H_2O \rightarrow CaCl_2\ (aq)$	81	< 80	sec	sec-min	acid	no	2,0,1,C	5	yes	
$CuSO_4$ and Zinc [191]	$Zn + CuSO_4 \rightarrow ZnSO_4 + Cu$	217	> 100	sec-min	min	acid	no	2, 0, 0, E	4	yes	
Potassium Permanganate and Glycerol [198]	$3\ C_3H_8O_3 + 14\ KMnO_4 \rightarrow 7\ K_2CO_3 + 14\ MnO_2 + 2\ CO_2 + 12\ H_2O$	7197	~ 200	sec	sec-min		yes	2, 0, 0, E (burns)	9	yes	activation of thermite reactions
Sulfuric Acid and Water [199]	heat of solution	87	~ 131	sec-min	min	acid	no	3, 0, 2, F	8	yes	
PEG and Water [200]	heat of solution	24	~ 40	sec	min	neutral	no	0,1,0,-	1	yes	self warming shampoo
Sodium Thiosulfate [201]	crystallization of supersaturated liquid	23	~ 45	sec	min	neutral	no	2, 0, 0, E	4	no	hand warmers
Ammonium Aluminum Sulfate [201]	crystallization of supersaturated liquid	25	~ 90	min	min	acid	no	2, 0, 0, E	4	no	hand warmers
Sodium Acetate Trihydrate [202]	crystallization of supersaturated liquid	24	< 56	sec	min	base	no	1, 1, 0, E	4	no	hand warmers
Sorbitol [201]	crystallization of supersaturated liquid	20	~ 40	min	min	acid	no	2, 1, 0, E	5	no	hand warmers
Magnesiumnitrate-Hexahydrate [201]	crystallization of supersaturated liquid	20	~ 70 - 80	min	min	acid	no	2, 1, 0, E	5	no	hand warmers
Iron-2-Oxide and Aluminum [203]	$Fe_2O_3 + 2Al \rightarrow 2Fe + Al_2O_3$	851		sec	sec		no	2,0,0,E (burns)	9	no	thermite reaction
Iron-3-Oxide and Aluminum [203]	$3Fe_3O_4 + 8Al \rightarrow 9Fe + 4Al_2O_3$	783		sec	sec		no	2,0,0,E (burns)	9	no	thermite reaction
Copper Oxide and Aluminum [203]	$3CuO + 2\ Al \rightarrow 3Cu + 2Al_2O_3$	979		sec	sec		no	2,0,0,E (burns)	9	no	thermite reaction
Copper-2-Oxide and Aluminum [203]	$3Cu_2O + 2Al \rightarrow 6Cu + 2Al_2O_3$	517		sec	sec		no	2,0,0,E (burns)	9	no	thermite reaction
Tin-Oxide and Aluminum [203]	$3SnO_2 + 4Al \rightarrow 3Sn + 2Al_2O_3$	613		sec	sec		no	2,0,0,E (burns)	9	no	thermite reaction
Titanium-Oxide and Aluminum [203]	$3TiO_2 + 4Al \rightarrow 3Ti + 2\ Al_2O_3$	319		sec	sec		no	1,0,0,E (burns)	8	no	thermite reaction
Magnesium-Oxide and Aluminum [203]	$3MnO_2 + 4Al \rightarrow 3Mn + 2Al_2O_3$	136		sec	sec		no	1,1,2,E (burns)	11	no	thermite reaction
Nickel-Oxide and Aluminum [203]	$3NiO + 2Al \rightarrow 3Ni + Al_2O_3$	735		sec	sec		no	2,0,0,E (burns)	9	no	thermite reaction
Silver-Oxide and Aluminum [203]	$3Ag_2O + 2Al \rightarrow 6Ag + Al_2O_3$	451		sec	sec		no	2,0,0,E (burns)	9	no	thermite reaction

TABLE 34: Chemical reaction candidates: Reactions marked in dark grey were excluded, whilst light grey ones are expected to be feasible. ([1]HMIS score: "Health", "Flammability", "Physical Hazard", and "Personal Protection"; [2]Danger Score: Sum of HMIS scores of the most dangerous compound in the reaction. For "Personal Protection" the following points were given: A,B=1; C,D,E,F=2; G,H,I,J=3. Fire/Burning =3 additional points).

Reaction	Reaction details	(-) dH° (kJ/mol)
Iron and Air	$4\ Fe(s) + 3\ O_2(g) + 6H_2O\ (g) \rightarrow 4\ Fe(OH)_3(s)$	854
Magnesium and Water	$Mg(s) + 2H_2O(g) \rightarrow Mg(OH)_2\ (aq) + H_2(g)$	352
Calcium Oxide and Water	$CaO(s) + H_2O \rightarrow Ca(OH)_2\ (aq)$	63
$CaCl_2$ and Water	$CaCl_2(s) + H_2O \rightarrow CaCl_2\ (aq)$	81
$CuSO_4$ and Zinc	$Zn + CuSO_4 \rightarrow ZnSO_4 + Cu$	217
Sulfuric Acid and Water	heat of solution	87

TABLE 35: Selected chemical reaction candidates.

5.2.2.1   ENERGY REQUIREMENTS

For the six preselected chemical reactions in Table 35, reaction volumes were estimated to identify the best candidate.

The volume estimation was based on the energy required to heat the samples and included heat losses. For heat losses, both a worst case (no insulation) and a best case scenario (10mm polystyrene insulation) were considered. The model for estimating the energy requirements is depicted in Figure 39. The exothermic reaction material was modeled as a cube. It was connected to the PCM on one side and to the insulation layer on the other five sides of the cube. It was expected that the PCM transfers heat from the exothermic reaction cube to the sample chamber. The following section outlines the approach used to estimate chemical reaction and PCM material volumes:

VOLUME OF PCM:

- The energy, Q, required to heat a sample of mass, m, with heat capacity, c, by a temperature difference, ΔT, can be determined as follows:

$$Q_{1a} = m \cdot C_{sample} \cdot \Delta T \approx m \cdot C_{H2O} \cdot \Delta T \qquad (1)$$

- Conductive heat losses of the sample are given by Fourier's law, using the thermal conduction coefficient, k and time, t. The sample is modeled with a surface, A, length, l, and mass m.

$$Q_{1b} = -k \cdot \frac{5 \cdot A}{l} \cdot m_{sample} \cdot t \qquad (2)$$
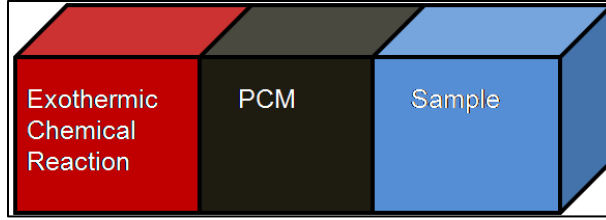
FIGURE 39: Heat transfer model consisting of three cubes (exothermic reaction, phase change material (PCM) and sample) in direct contact with each other and surrounded by insulation on the remaining sides.

- The required heat, Q, of the PCM is the sum of (1) and (2). The heat, Q, is used to calculate the required PCM mass, m, using its heat capacity, c.

$$Q_{1c} = Q_{1a} + Q_{1b} \qquad (3)$$

$$m_{PCM} = Q_{1c} \cdot C_{PCM} \qquad (4)$$

- Conductive heat losses, Q, from the PCM are given by using Fourier's law:

$$Q_{2a} = -k \cdot \frac{4 \cdot A}{l} \cdot m_{PCM} \cdot t \qquad (5)$$

- The adjusted PCM volume, V_{PCM}, is calculated by adding the PCM heats and heat losses from (3) and (5). From this, the PCM volume is determined using its density, σ.

$$Q_{2b} = Q_{1c} + Q_{2a} \qquad (6)$$

$$V_{PCM} = \sigma_{PCM} \cdot Q_{2b} \cdot C_{PCM} \qquad (7)$$

Assumptions made include:
- All energy transfer occurs via conduction. Conduction is modeled by Fourier's law. It is reasonable to neglect convection, because the reaction materials are modeled as stationary and because they are in direct contact without a gaseous interface [204]. Radiation is neglected as well, because the temperature differences between the sample and its surroundings (dT ≤40°K) are small [204].
- The PCM is made of paraffin [190].

- The sample has a cubic shape, losing heat on five of its six sides. Hence, heat transfer to the PCM only occurs on one side. The sample is in direct contact with the PCM without a gaseous interface.
- The heat capacity of the sample is that of water ($c_{sample} = c_{H2O}$).
- The samples are heated from room temperature T=25°C to the target temperature.

VOLUME OF EXOTHERMIC REACTION MIXTURE:

- The mass, m, of the exothermic reaction mixture with reaction enthalpy, ΔH_{rctn}, without heat losses is given by the following equations:

$$Q_{2b} = Q_{1c} + Q_{2a} \tag{8}$$

$$m_{2b} = M \cdot \frac{Q_{2b}}{\Delta H_{rctn}} \tag{9}$$

- Heat losses of the exothermic reaction mixture are given by Fourier's law:

$$Q_{2c} = -k \cdot \frac{4 \cdot A}{l} \cdot m_{2b} \cdot t \tag{10}$$

- The adjusted reaction mix volume, V, is determined from the sum of the required heat and heat losses, Q_{rctn}, the molar mass, M, the molar enthalpy change of the reaction, ΔH_{rctn}, and the density, σ, of each component in the reaction.

$$Q_{rctn} = Q_{2a} + Q_{2c} \tag{11}$$

$$V_{reaction} = \sum \sigma \cdot M \cdot \frac{Q_{rctn}}{\Delta H_{rctn}} \tag{12}$$

Assumptions made include:

- Heat losses from the reaction are based on the initially calculated volume of the reaction mixture and equal to ~$Q_{2c.}$
- As before, all losses are by conduction only. The PCM, exothermic reaction and sample volumes have the form of cubes.

Detailed calculations and inserted values and constants are attached in the appendix in tabular format.

5.2.2.2 RESULTS AND DISCUSSION

The energy estimations for different chemical reactions, Q_{rctn}, are shown in Table 36. The required volumes of reaction mix and PCM are summarized in Table 37. The results in Table 37 indicate that most of the chemical reactions require volumes >2ml, which is too large for use inside the LabTube. This is especially true for applications, where the sample has to be heated for a long time, such as isothermal DNA amplification. The reaction with the smallest volume is that of magnesium and water. With good insulation, this reaction could be used for short processes such as the heating of lysis or elution buffers or for removing ethanol. However, preliminary tests of this reaction suggest that the achieved temperature varies by ±4-7°K (IMTEK, University of Freiburg). It was therefore concluded that chemical reactions are not suitable for processes requiring precise temperature profiles (such as isothermal DNA amplification). In addition, it is generally difficult to precisely control the timing of the reaction and the temperature profile is inflexible. This means that, once a reaction is set up for a certain temperature profile, it is not easily changed without performing a complete redesign. Chemical heating was hence not further pursued in this thesis.

Process	Cell lysis	Inhibition proteases	DNA elution	Removing ethanol	Isothermal DNA amplification
Temperature (°C)	56	90	70	78	65
Time (min)	15	5	10	5	40
Volume (µl)	170	170	100	100	100
Energy (no insulation) (J)	977	692	88	464	2680
Energy (polystyrene 10mm) (J)	167	94	77	57	293

TABLE 36: Energy requirements for different processes in the LabTube.

Process	PCM (ml)	CaO + H_2O (ml)	CaCl + H_2O (ml)	Mg + H_2O (ml)	Fe + O_2 (ml)	H_2SO_4 + H_2O (ml)	CuSO4 + Zn (ml)
Cell lysis	0.38-2.2	0.96-1.5	0.16-0.25	0.16-0.25	28- 39	0.15-0.23	0.04-0.06
Inhibition proteases	0.11-0.78	0.33-0.79	0.58-1.4	0.05-0.13	9.3-19	0.54-1.3	0.01-0.03
DNA elution	0.14-1.3	0.53-0.99	0.94-1.7	0.09-0.16	9.3-19	0.88-1.6	0.01-0.03
Removing ethanol	0.08-0.64	0.24-0.60	0.4-1.1	0.04-0.10	6.6-13	0.39-1.0	0.01-0.02
Isothermal DNA amplification	0.54-4.9	0.36-3.9	6.3-6.9	0.60-0.66	106-112	5.9-6.5	0.14-0.15

TABLE 37: Reaction volumes for different processes.

5.2.3 ELECTRICAL HEATING

Electrical heating is another approach to control temperature within the centrifuge. It can be achieved in two ways: The first option is to incorporate electricity into a custom-built centrifuge. The second option is to use an autonomous energy source that is compatible with standard centrifuges.

5.2.3.1   CUSTOM CENTRIFUGE

ELECTROMAGNETIC INDUCTION

Heat can be created through electromagnetic induction inside a custom centrifuge. For example, the inner centrifuge bowl could be equipped with magnets or with a magnetic ring. By inserting a disposable coil into the LabTube as well as some form of energy storage, energy could be created. This energy could then be used for heating processes inside the LabTube. The advantages of such a system include that the disposable LabTube itself would not become significantly more expensive, because only a coil and a heat storage unit would need to be installed. The disadvantage is that this system requires a custom centrifuge. In standard centrifuges, metal rotors would heat up during rotation due to the presence of magnets and associated currents, so other materials may be required. In addition, the centrifuge bowl would need to be altered such that the presence of magnets and its associated geometry changes do not negatively affect the air flow within the system. According to the centrifuge manufacturer Hermle, this is especially true for operation at high g-forces.

MICROWAVES

Liquids inside the LabTube can be heated using microwaves inside a custom centrifuge. The advantages include that the disposable LabTube does not have to be changed and hence it does not become more expensive. Disadvantages include that a custom centrifuge containing a microwave unit needs to be built. Such custom centrifuge further needs to be leakage-proof such as to ensure stringent safety requirements. Lastly, microwaves non-selectively heat up all liquids inside the LabTube, unless certain parts are specially shielded - for example with metal. However, selective heating of individual LabTube cylinders is desirable for the applications outlined in section 5.1. Overall, the option of heating the LabTube using microwaves was rejected due to associated safety concerns.

ELECTRICITY THROUGH THE ROTOR

A heater can also be driven by an external power supply that is coupled with the rotor. Here, the LabTube could be contacted electrically, e.g. through sliding ring-contacts. An advantage of this system include that the disposable LabTube does not become significantly more expensive. The disadvantage is that this system requires a custom centrifuge design.

5.2.3.2   STANDARD CENTRIFUGE

ENERGY HARVESTING

Energy harvesting can be used to create electrical energy within the disposable LabTube inside a standard centrifuge. Generally, energy harvesting is a process by which energy is derived from external sources (e.g. pressure, kinetic energy, thermal energy, etc.) and is stored for small, wireless autonomous devices.

As shown in Figure 40, an energy harvesting unit can, for example, be put into the disposable LabTube. This unit can have a proof mass made of permanent magnets, two springs, a coil and an energy storage circuit. During operation, the proof mass vibrates along the transverse direction due to the variations of gravity [205]. As an example, the created power was estimated using the force, F, which is the product of the mass, m, and the change in acceleration, a, over the spring displacement, d.

$$W = \int_{-\frac{d}{2}}^{\frac{d}{2}} F \cdot dx = m \cdot \Delta a \cdot d = 1 \ [J] \qquad\qquad P = W \cdot f = 1 [W]$$
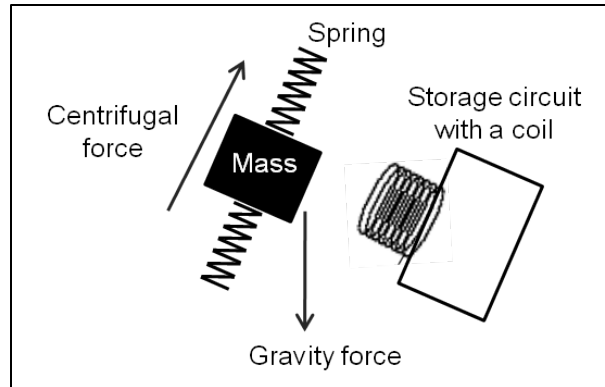
FIGURE 40: Disposable energy harvesting unit inside the LabTube, which is based on induction. It consists of two springs, a magnetic mass and an energy storage circuit that contains a coil for electromagnetic induction. Adapted from [205].

Because power is only created when the acceleration changes, which is on average once in 5min, the adjusted created power is:

$$P' = P \cdot \frac{1}{300} = 3 \cdot 10^{-3} \ [W]$$

Assumptions made include:

- The spring mass is m=10 g.
- The displacement is d=0.01m.
- The change in centrifugal force is Δa=2000g.
- The centrifuge acceleration frequency is f=1 Hz.
- Energy is conserved in the system.

Even though energy losses were neglected in the above calculation, this method does not yield sufficient power for the desired applications (which is roughly 0.5W for isothermal DNA amplification, as shown in Chapter 5.3). Generally, energy harvesting of any sort does not create enough energy for LabTube heating (usually not more than 0.1W with losses of more than one order of magnitude [206]). It was therefore rejected and not further pursued in this work.

BATTERY

Batteries can also be used to heat the LabTube. Batteries are cheap and can be purchased for as low as $0.2 in mass production [207]. Batteries are also disposable and in conjunction with a microcontroller they can be employed flexibly for a variety of different heating applications. In combination with a microcontroller, the system can be autonomous, disposable and heating applications could be easily parallelized. Another advantage is that a battery-driven system can be compatible with standard, commercially available centrifuges. Therefore, a centrifuge redesign is not necessary. Disadvantages of the battery include waste disposal issues. To minimize the environmental impact, a rechargeable battery can be used.

5.2.4 HYBRID METHODS

Hybrid methods of centrifugal, chemical and/or electrical heating methods were also evaluated. Generally, there are two types of hybrids:

CHEMICAL AND ELECTRICAL HYBRIDS: The first hybrid type is the combination of chemical and electrical heating methods, which include the following combinations:

- The sample is heated chemically and heat losses are compensated electrically.
- The sample is heated electrically and losses are compensated chemically (e.g. with a phase change material as a temperature stabilizer).
- An exothermic chemical reaction is initiated electrically.

The first two options were expected to be feasible, whilst controlling chemical reactions electrically seemed unnecessarily complicated.

CENTRIFUGAL AND CHEMICAL/ELECTRICAL HYBRIDS: The second hybrid method type is a combination of centrifugal and chemical or electrical methods:

- The sample is heated centrifugally and losses could be compensated electrically.
- The sample is heated electrically/chemically and losses are compensated centrifugally.

Heating the sample centrifugally was not desirable, as the time required to heat the sample is too long (>12min, see 5.2.1). Compensating losses centrifugally is also expected to be imprecise (±5°K) and slow. It was therefore rejected.

Overall, only the combination of chemical and electrical heating was deemed feasible. However, due to their added complexity, hybrid methods were less desirable than electrical heating alone and they hence served as a backup only.

<hr/>

5.2.5   SUMMARY

<hr/>

In this section, centrifugal, chemical, electrical and hybrid methods for heating were evaluated.

Centrifugal heating was rejected, because it is slow (>>12min), imprecise (temperature deviation ~±5°K) and has a maximum temperature of 50°C, which is too low for its use with isothermal LAMP DNA amplification or with ethanol evaporation.

In chemical heating through exothermic reactions, temperatures in the desired range (40-90°C) can be created. However, estimations for energy requirements revealed that the required volumes are often too large (>2ml) to fit into the LabTube. Only the reaction between magnesium and water could be used for short processes, such as the heating of lysis or elution buffers or for removing ethanol. Overall, chemical heating was thought to be an inflexible method that is difficult to control (low T precision >5°K) and to parallelize. It was therefore rejected.

Two types of electrical heating methods were outlined: those that can be used with a standard laboratory centrifuge and those that require a custom centrifuge. Out of the autonomous heating methods that can be used with a standard centrifuge, energy harvesting does not yield sufficient power to heat the LabTube. However, batteries, both disposable and rechargeable, are a viable alternative. Out of the methods that require a custom centrifuge, microwaves were deemed unsafe, whilst coupling energy through a rotor or electromagnetic induction was considered feasible. Generally, electrical heating methods were deemed more flexible and more robust than chemical or centrifugal methods.

For hybrid methods, it would be feasible to combine chemical and electrical heating methods. These were, however, expected to be more complicated than electrical methods alone and hence served as a backup only.

In this thesis, the priority was to develop a heating system for the LabTube that is compatible with a standard laboratory centrifuge (see Chapter 3.3). It was therefore decided to build a heating system based on a disposable battery. The system design is outlined in the next section.

5.3   HEATED LABTUBE (DISPOSABLE)

In this section, an autonomous, disposable battery-driven heating system for isothermal LAMP DNA amplification is described. It can be integrated as a building block into the LabTube in conjunction with a standard laboratory centrifuge. As a first application, LAMP amplification of VTEC *E.coli* was incorporated into the LabTube with an overall time-to-result <1.5hrs. The detection of VTEC *E.coli* in water and foods is often time-critical (see Chapter 2.2.1.4). The introduced detection method is a rapid, automated and easy-to-use DNA-extraction and amplification method that is widely deployable.

5.3.1   MATERIALS AND METHODS

5.3.1.1   BATTERY TESTING

An endurance test was performed for pre-selected batteries. The endurance test was performed at an initial power of 2.5W with a resistor combination consisting of SMD thick film resistors (3.6, 14.4 and 57Ω respectively), as well as a potentiometer connected in parallel (Bourns, 3400S). For the endurance test both current, I, over time, t, and voltage, U, over current, I, were recorded.

5.3.1.2   HEATER UNIT SELECTION

The heater selection test consisted of heating 150µl of fluid up to 65°C using a constant power of about 2.5W. The time to reach a final temperature was measured using a stopwatch and a temperature logger (Ebro, 40 TC02). As heating units a PTC resistor (EPCOS, 8.2Ω at 25°C) was tested using a constant voltage of 5V. Also, heaters that can be used in conjunction with a NTC as a temperature sensor were tested. Here, a controller module (Carel IR33), a 12V DC power supply and a motherboard with a temperature control circuit voltage regulator were set up in order to test different heating elements (see ESI 1.1). The NTC (EPCOS, NTC B57540G1103F) was connected to a serial resistor of 1.2kΩ. The voltage was picked off from the temperature regulation module (Carel, IR33DIN) in order to regulate the prevalent temperature. As heaters, Nickel wire (d=0.03mm, 140Ω/m, Bedra), as well as a heat foil (140Ω, Minco) and a thick film resistor (10Ω, Yageo) were tested.

5.3.1.3   DNA EXTRACTION

DNA was extracted using the QIAamp Micro DNA kit both in the LabTube and for manual references. The procedure was described in Chapter 3.2.1.2.

5.3.1.4   ISOTHERMAL DNA AMPLIFICATION

LAMP amplification of verotoxin-producing *E.coli* was performed using a commercial kit (Mast Diagnostica, Cat. No. 67vtsck3). 130μl of master mix were placed into the reaction chamber in cylinder III at the beginning of the extraction. The DNA was eluted in 20μl of liquid - hence the overall reaction volume for the LAMP amplification was 150μl. The master mix contained 117μl reaction mix, 7μL visual detection dye and 7μL BST polymerase, which are all provided in the kit. The amplification occurred at 65°C for 40min. The heating was initiated by a microcontroller timer after DNA extraction was completed. Afterwards, the color change of the visual detection dye (Mast Diagnostica) was inspected, with blue being a positive and purple being a negative result. Positive and negative (water only) controls were always run in parallel in a thermomixer (Eppendorf, 5438).

5.3.1.5   PCR AND QUANTITATIVE ELECTROPHORESIS

As a control, the extracted VTEC *E.coli* DNA was quantified using qPCR, which was described in Chapter 3.2.1.5. The amplification products were quantified and characterized with electrophoresis on an Agilent 2100 bioanalyzer using the DNA 1000 kit.

5.3.2 ELECTRICAL DESIGN

5.3.2.1   HEATER REQUIREMENTS

The goal was to develop a disposable LabTube heater to drive a VTEC *E.coli* DNA amplification reaction. The LAMP reaction was chosen over other amplification methods, such as PCR. This is because the desired test results do not have to be quantitative (a simple yes or no answer suffices), yet it has to be sensitive, temperature robust (ideally without ramping) and specific for the target organism. LAMP was chosen, because unlike PCR, it does not require thermal cycling and it is more temperature robust than other isothermal amplification methods (67±5°C) [126]. For LAMP amplification, the heater needs to heat 50-150μl liquid for >40min at 65°C in cylinder III of the LabTube, where the extracted DNA is collected. Additionally, the entire heating system needs to be temperature stable (±2°K), have a ramping time <10min, be disposable, cost-efficient (<$1) and bioassay-compatible. It also needs to be small enough to fit into the

LabTube, which has the format of a 50ml Falcon-tube and a cap with a maximum height of 18.5mm (to still fit into the centrifuge) and an outer diameter of 70mm. The heater should be designed to have the potential for flexible use for other heating applications. These applications were described in Table 31. They include pre-heating of lysis or wash buffers, removing ethanol from the silica-matrix and providing heat for downstream reactions, such as immunoassays or other amplification reactions.

5.3.2.2 POWER SUPPLY

In order to get the best compromise between economic and performance features, a battery-driven heating system was chosen (see Chapter 5.2). Initially, suitable batteries for isothermal LAMP DNA amplification were selected based on the above requirements for temperature stability, ramping times, price and physical size: It was experimentally determined that heating up a 150µl sample of water to 65°C within 2 minutes using standard resistors as heating elements, required a constant power input of ~2.5W and ~1.5W to keep the temperature stable for 40 min (no insulation). Keeping this in mind, the current drawn from a battery with a nominal voltage between 1.5V-12V during the initial heating period is between 670-80mA. Required electric charges are between 80mAhr for 12V batteries and 580 mAhr for 3V batteries. 53 batteries were screened based on the requirements from Chapter 5.3.2.1[208]. It was determined theoretically and experimentally that most lithium button cell batteries, as well as silver-oxide and zinc-air batteries can provide the required power in the heating up period for a few seconds only. Based on the evaluation, two batteries were able to fulfill the requirements: CR-2 (3V) and 4LR44 (6V). The A23 (12V) battery contains a charge of 55mAhr, which is only slightly lower than the calculated requirements and it was also chosen, as good thermal insulation could reduce the required charge. The three selected batteries are summarized in Table 38. An endurance test for the three selected batteries was conducted at an initial power of ~2.5W. The test was performed for 40 minutes to ensure that the battery can provide sufficient power to drive the LAMP reaction. As the primary interest was to evaluate the battery performance over time, the current drawn from the battery, as well as the supplied voltage were plotted over time (Figure 41A). The power released by the battery is shown in Figure 41B. As shown in Figure 41, only the CR-2 battery sustained the test, whilst the current for the other two decreased dramatically after less than 20 minutes, literally causing the battery power to break down. It was also shown that the CR-2 battery could not sustain the initial power of 2.5W, but instead yielded a constant power of ~1.5W. This implies that good thermal insulation is required to ensure proper heating.

Battery	L (mm)	D (mm)	M (g)	V (V)	Q (mAhr)
CR-2	15.6	27.0	10	3	300
4LR44	12.8	25.1	9	6	160
A 23	10.3	27.5	9	12	55

TABLE 38: Selected batteries. L is the length, D the diameter, M the mass, V the volume and Q stored electric charge inside the batteries.
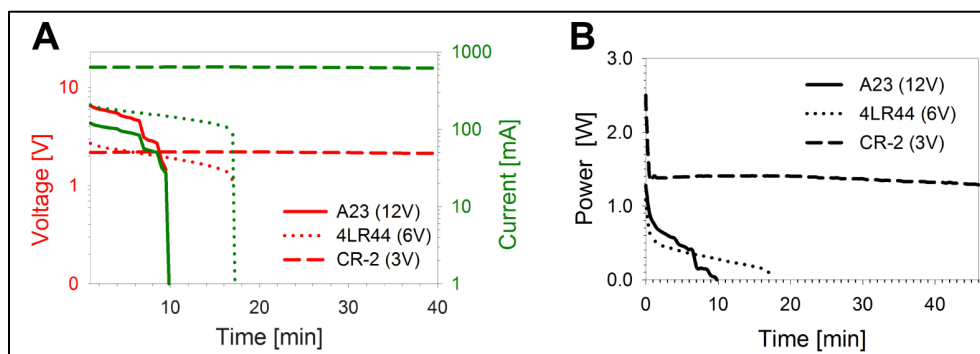
FIGURE 41: Battery endurance test with an initial power of 2.5W. (A) Current and voltage over time. (B) Power over time.

5.3.2.3   HEATER AND SENSOR

Different heaters and sensors were tested and evaluated. The test consisted of heating 150µl of fluid up to 65°C using a power of ~2.5W. Initially, a PTC resistor (EPCOS, 8.2Ω at 25°C) was tested as a heater using a constant voltage of 5V. It was hypothesized that the PTC can be used to self-regulate the current drawn from the voltage source and therefore the temperature produced by the resistor due to its temperature-dependent resistance. Even though the PTC was able to heat the sample to the required temperature, it could not precisely and reproducibly control its temperature (±2°K) due to its exponential temperature dependency and due to production tolerances. Heaters that can be used in conjunction with a NTC as a temperature sensor were tested using a regulation module (Carel). Nickel wire (d=0.03mm, 140Ω/m) was evaluated, but it was shown to not be feasible: Due to its thin diameter and associated difficulties with winding a nickel coil of exactly 10Ω without any overlaps, the wire burned through after <2min. However, a SMD thick film resistor (10Ω, Yageo) as well as a heating foil (Minco, 10Ω) was shown to be feasible. Both units could heat the liquid up to 65°C within 1.5min

114

at a tolerance of ±0.5°K. In summary, both the SMD resistor and heating foil can be used as heating elements. Due to size and cost considerations, the SMD thick film resistor was selected.

Using the SMD resistor, a heating system was set up in cylinder III of the LabTube, where isothermal DNA amplification should take place. Here, thermal insulation was important to reduce power requirements to ~0.5W. It was shown that placing heater and sensor into the reaction chamber inhibited DNA amplification reagents, likely due to the release of interfering substances, such as copper. In order to make the system bioassay-compatible, the electronic parts were placed outside a PCR tube, which serves as the reaction chamber in cylinder III. As shown in Figure 42, the heater consists of two SMD thick film resistors (5.6Ω, Yageo), which are connected in parallel and hence represent an overall electrical load of 2.8Ω. In the center between the two resistors, the NTC resistor is located to modify the voltage over the 1.2kΩ serial resistor, depending on its temperature values. In order to ensure homogeneous temperatures, the PCR tube is wrapped in aluminum foil and embedded in heat-conducting cement (Figure 42). The temperature stability of this system was tested by heating 150µl of water in the PCR tube of cylinder III. As depicted in Figure 42, a stable temperature profile of 65±2°C is reached after ~3 minutes. The time needed for the heating process is doubled from the initial heater selection tests, mainly due to the presence of thermally conductive cement and the aluminum cover, which themselves need to be heated up first. The heat can be held at the target temperature for at least 40 minutes. To test the biocompatibility of the system, 150µl of VTEC *E.coli* LAMP master mix, target DNA and visual dye were heated up to 65°C and kept at this temperature for 40 minutes. For the positive control, a color change of the visual dye was detected and the desired product showed up on electrophoresis; whilst nothing was detected in the negative control. It was therefore concluded that the heating system is bioassay-compatible. Additionally, isothermal DNA amplification was successfully repeated with different volumes (50µl and 100µl) of reagent, demonstrating that the heating system can also be run at lower volumes with shorter heating times (~1.5 and 2min, respectively) yielding temperatures stable at 65±2°C.
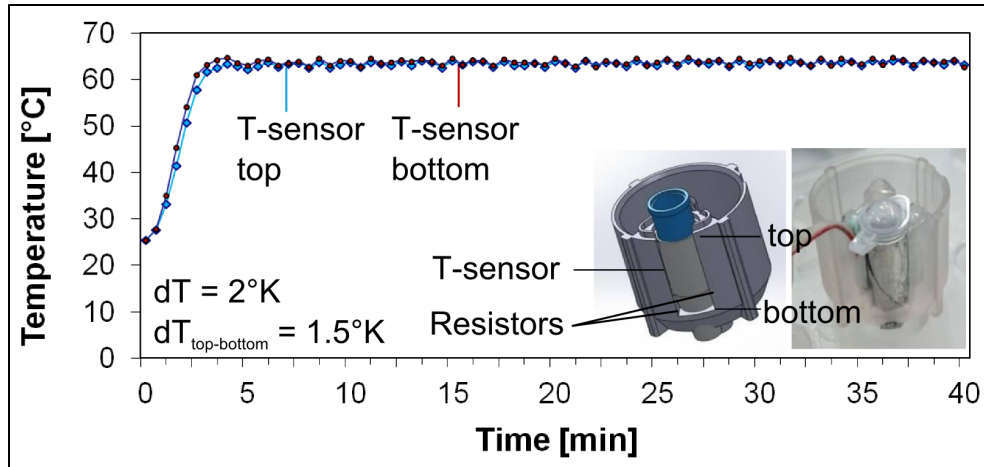
FIGURE 42: Heater setup for LAMP amplification inside the LabTube. The heater consists of two SMD thick film resistors and an NTC resistor as a temperature sensor. The PCR tube, which contains the sample, is surrounded by aluminum foil. To characterize the temperature profile, temperature is measured at the top and bottom of the PCR tube filled with 150μl of water. It is stable to ±2°K.
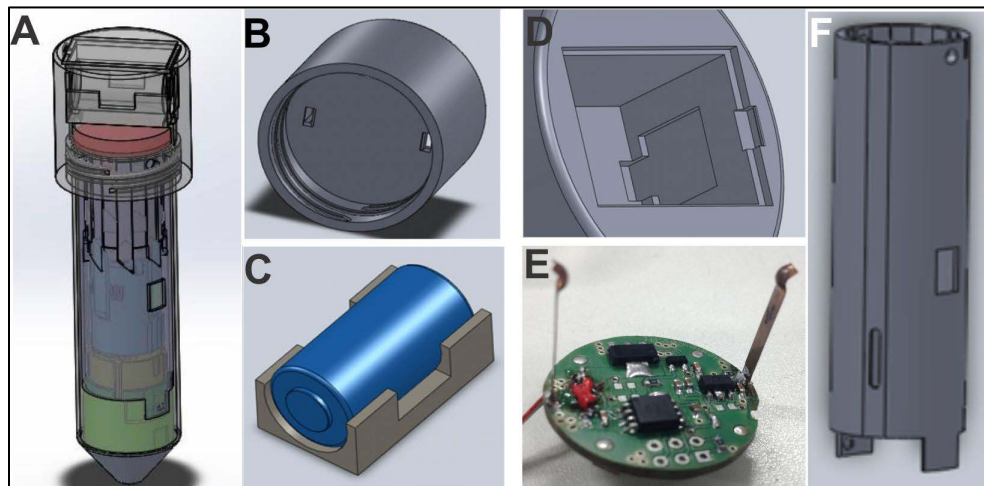
FIGURE 43: Mechanical design of the heated LabTube. (A) Complete LabTube with battery encasing. (B) Cap with holes for electrical contacts of the microcontroller to contact the battery sitting above it. (C) The battery is embedded in a soft constricted piece. (D) It is sitting in a cavity. (E) Below it sits the round circuit board with the microcontroller. (F) The LabTube encasing is depicted, which has a hole for cables. The cable runs on the outside of the LabTube from the microcontroller and via the hole to the heater in cylinder III.

5.3.2.4 HEATER CONTROL

In order to keep the system flexible the heating system is controlled with a microcontroller rather than an analog circuit. This allows the user to change control parameters and/or applications more flexibly and to perform several heating applications independently and in parallel. Because a CR-2 battery with 3V supply voltage is used, a microcontroller with an operating range beginning at 1.6V was chosen. To keep the costs low a microcontroller with the minimal pin number is used (ATXmega, ATMEL), costing less than $0.5. A round circuit board with the dimensions of the screw cap of a 50ml BD tube was designed using the program Eagle (Figure 43E). The microcontroller was programmed using C++ and can be set to different temperature profiles, as well as ramping times and start/stop times.

5.3.3 MECHANICAL DESIGN

Encasings for the CR-2 battery, as well as for the circuit board were designed using Solid Works (Figure 43). The encasing has a geometry of a 50ml falcon tube with a screw cap that holds the battery. It has a height of 18.5mm, which is the maximum height that still fits into the centrifuge. The encasing was rapid-prototyped using stereolithography and it consists of walls <3mm, allowing it to sustain high centrifugal acceleration of up to 6,000g, as experimentally determined. The battery sitting in the cap cavity (Figure 43A and B) is embedded in a soft constricted piece to protect it from centrifugal forces (Figure 43C). The circuit board is located in the bottom of the cap (Figure 43D and E) with the electrical contacts fitting through two holes into the battery cavity above (Figure 43B and D). The heating system in cylinder III is connected with the microcontroller and battery through a cable. Because the cylinders move up and down in parallel to the centrifugal force the cable is arranged such as not to obstruct the pen-mechanism of the remaining cylinders. Hence, the cable is guided on the outside of the LabTube and it is connected with the heater through a hole at the bottom (Figure 43F).

5.3.4 RESULTS

5.3.4.1 MECHANICAL AND FLUIDIC TEST

Mechanical and fluidic functionalities were verified by running the system inside the centrifuge (Hermle, Z326K). In the standard protocol, pen mechanics, actuated by centrifugal forces, rotate cylinder II by changing the centrifugal acceleration over time [8]. This mechanism allows for opening and closing of fluidic paths through the stack and thus liquid routing (see Chapter 3.1).

FIGURE 44: Mechanical and fluidic verification of the modified, heated LabTube. Cylinder I was filled with water colors instead of chemicals, in order to track their fluid flow. After running the system, the PCR tube had collected the desired amount of eluate (blue), whilst all the remaining liquids were transferred to the waste chamber (orange). The window (middle, white rectangle) indicates different processing steps.

The mechanics of the system was successfully verified as cylinder II moved from the start (S) to end (E) position during the centrifugation protocol, whilst all components remained intact (Figure 44). The fluidics of the system was also verified. Cylinder I was filled with water colors instead of chemicals in order to track the fluid flow. After running the system, the PCR tube had collected the desired amount of eluate (blue), whilst all the remaining liquids were transferred to the waste chamber (orange) (Figure 44). During this run, the heating system was also tested and successfully verified: at the end of the run the blue eluate sample (150µl) had a temperature of 64±2°C in the top and bottom of the reaction chamber.

5.3.4.2 DNA EXTRACTION

DNA extraction was performed with the heated LabTube by extracting *E.coli* lysate in water, milk and apple juice with the Qiagen DNA Micro Kit at known concentrations between 0-10^8 inserted copies. A manual reference was always run in parallel as a control. The eluates were subsequently quantified using qPCR. As shown in Figure 45A, the extraction limit is 10^2 inserted copies for water and 10^3 inserted copies for apple juice and milk. The tested efficiency of *E.coli* DNA extraction is 147±37% compared with the manual reference. The achieved detection limit implies that if 4ml of sample are inserted into the LabTube, the extraction limit can theoretically be reduced to ≥25 inserted copies/ml.

5.3.4.3   DNA AMPLIFICATION

Complete DNA extraction protocols were run in the LabTube by inserting 10^3 copies of verotoxin-producing *E.coli* lysate (VTEC, EDL 933), extracting its DNA and amplifying the extracted DNA by using loop-mediated isothermal DNA amplification (n=3). Positive and negative controls were run in parallel in a thermomixer at 65°C for 40min. The amplified DNA was detected with a visual dye. The results was verified using quantitative electrophoresis. As can be seen in Figure 45B the negative control stayed purple, whilst the positive control changed its color to dark blue for all three runs. Moreover, quantitative electrophoresis identified the desired amplification product in the positive sample, whilst the negative contained no product. The overall time-to-result for DNA extraction and amplification is <1.5hrs.

5.3.5   CONCLUSION

A disposable, microcontroller-based, battery-driven heating system for loop-mediated isothermal DNA amplification (LAMP) was introduced. It can be integrated as a building block into a centrifugally-driven DNA-extraction platform (LabTube). Fully automated DNA extraction was demonstrated in a standard laboratory centrifuge for $\geq 10^2$ verotoxin-producing (VTEC) *E.coli,* followed by subsequent automatic LAMP amplification with an overall time-to-result <1.5hrs*.* The heating system consists of two parallel SMD thick film resistors and a NTC resistor as heating and temperature sensing elements. They are driven by a 3V battery and controlled by a microcontroller. The LAMP reagents are stored in the elution chamber and the amplification starts immediately after the eluate is purged into the chamber. Furthermore, the heating system can be parallelized and enables the control of multiple independent heating zones within one LabTube. To reduce waste, it could also be run with rechargeable batteries. The heated LabTube can also be used for multiple other applications, such as for the removal of ethanol from the eluate or the column, the pre-heating of extraction buffers or the temperature control of other (bio-)chemical reactions, such immunoassays or other amplifications. It could also be used for measurements (e.g. pH) and for quality control.
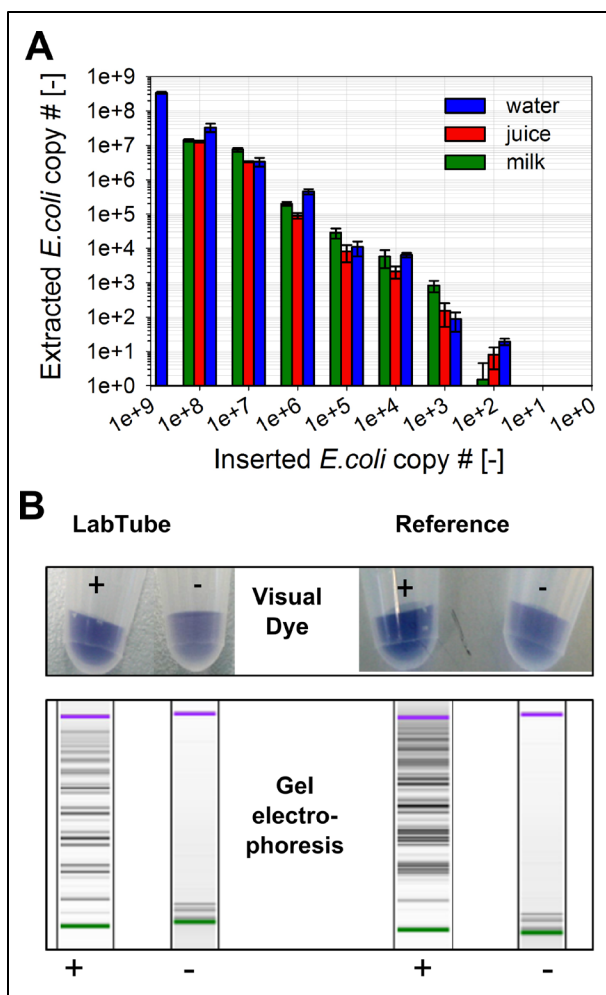
FIGURE 45: DNA extraction and amplification inside the LabTube. (A) DNA extraction in the LabTube using VTEC *E.coli* (EDL 933) lysate in water, milk and apple juice (n=3). (B) Results of a complete extraction and amplification reaction of 10^3 inserted DNA copies of VTEC *E.coli* lysate in the LabTube. Both the LabTube and reference positive control show a color change and amplification product both visually and in quantitative electrophoresis, whilst the negative control shows no change or product.

5.4   CUSTOM CENTRIFUGE

In some instances, especially in the developed world where cost-pressures are not so severe, it may be desirable to build a custom centrifuge that can both heat and automatically readout the LabTube. This approach would lower indirect LabTube costs (whilst raising centrifuge costs) and would allow for quantitative, real-time data readout and analysis. The disposable LabTube

heater introduced in Chapter 5.3 serves as a proof-of-principle demonstrating that controlled heating inside the LabTube is feasible. When building a custom centrifuge for heating, the energy can either be coupled through the rotor or be exploited using electromagnetic induction through a magnet in the centrifuge (and coils in the LabTube). These options were described in Chapter 5.2.3.

For quantitative and/or real-time readout, an optical setup can be incorporated into the LabTube. Here, the round LabReader geometry can be integrated into the sample holders of the centrifuge as depicted in Figure 46. For data readout, the LEDs can shine through the bottom cylinder III of a modified LabTube. The advantages of such a system include that assays can be readout in real-time and at high sensitivity using multiple wavelengths, and that all processing steps occur simultaneously inside one system without requiring additional handling steps, hence lowering contamination risks (see Chapter 3.3).
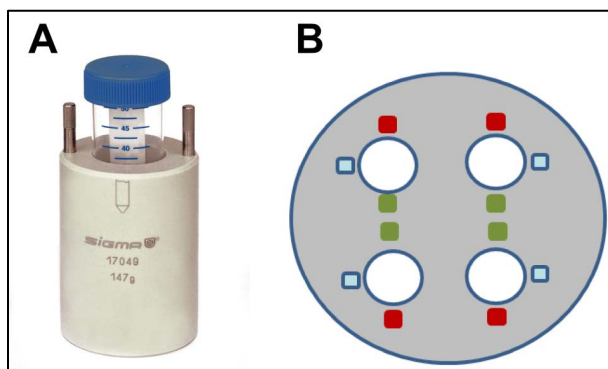
FIGURE 46: Optics integration inside the centrifuge. (A) A typical centrifuge holder for 50ml falcon tubes (image courtesy www.sartorius.com). (B) The schematic shows a top view of a centrifuge holding 4 round LabTubes (white circles) in centrifuge holders. Here, the green, blue and red dots indicate LEDs of the LabReader round geometry, which are incorporated into the centrifuge holders. They are used to readout the LabTube in real-time. The components are not shown to scale.

5.5   CRITICAL EVALUATION OF HEATING METHODS

As described in Chapter 5.1, the heated LabTube cannot only be used for DNA amplification, but also for different processing steps involved in DNA extraction. According to the manufacturers, heating lysis and elution buffers may be necessary to increase the extraction efficiency and quality [183]. In addition, heat may be used to remove ethanol, an inhibitor of many downstream processes including PCR (see Chapter 5.1). In this section it is evaluated whether these heating applications are relevant for the most common LabTube applications.

5.5.1   PRE-HEATING OF LYSIS AND ELUTION BUFFERS

To test the effect of pre-heating lysis and elution buffers, human blood was extracted. Blood was used as a first example, because it could be an important application for the LabTube and it is a sample matrix, for which the manufacturer protocols require elevated lysis and elution temperatures to improve extraction yield and efficiency. *E.coli* and *Alicyclobacillus* extractions with the QIAamp Micro DNA kit were not tested at elevated temperatures, as the manufacturer protocol recommends running all steps at room temperature[183]. Hence quality and efficiency increases were not expected to occur at elevated temperatures.

METHODS:

Two kits, the Macherey Nagel NucleoSpin Blood kit and the QIAamp DNA Blood kit, were tested both at room temperature and using the temperatures recommended by the manufacturer's protocol. According to the user manual of the Macherey Nagel NucleoSpin Blood kit the lysis and elution buffers both needed to be pre-heated to 70°C. The QIAamp DNA Blood kit was also tested. Here, the lysis step needed to occur at 56°C. The DNA contents and quality were tested using the Nanodrop spectrophotometer.

RESULTS:

The results of the experiments are shown in Table 39 and in Table 40. As indicated, there is no significant difference in extraction yield or product purity in either of the two kits. There is no significant protein contamination (recommended value 260/280nm ≥1.8) or other contaminations (recommended value 260/230nm ≥2.0). All curves of absorbance versus wavelength further showed the desired S-shape. Hence, heating lysis and elution buffers does not improve DNA yield or quality for blood using the Qiagen and MN kits and heating is therefore not required in these cases. However, according to the manufacturers, heating may be necessary for difficult to

Experiment	Number of repeats	DNA conc. (ng/µl)	260/280	260/230
Room temperature	3	63±7	1.8±0.0	2.2±0.1
56°C lysis	3	49±5	1.8±0.0	2.3±0.1

TABLE 39: Blood extraction from the NucleoSpin Blood kit.

Experiment	Number of repeats	Relative DNA conc. (%)	260/280	260/230
Room temperature	3	102±12	2.0	2.3
70°C lysis and elution	3	100±7	1.8	2.2

TABLE 40: Blood extraction from the QIAamp Blood kit (experiments by HSG-IMIT).

extract matrices (such as plants, tissues or gram-positive bacteria [183]) and for other extraction methods (such as protein extraction).

5.5.2 REMOVAL OF ETHANOL

Ethanol is commonly removed during DNA extraction, because it inhibits downstream processes. In PCR, for example, ethanol concentrations higher than 1-2.5wt% in the reaction mix can cause inhibition [184, 185]. This corresponds to a limit of 5wt% ethanol in the DNA eluate. In a standard protocol, ethanol is removed from a silica-column by dry-spinning at high centrifugation forces (≥10,000g) for at least 1min. However, in order to be able to process more than 4 LabTubes simultaneously the use of big centrifuges with a maximum centrifugal acceleration of 3,900g is necessary. As shown in Table 41, it was therefore tested whether or not ethanol can be removed at 3,900g rather than at ≥10,000g (samples B-D). It was hypothesized that other methods, such as heating could be used to remove ethanol, if it was not possible to sufficiently remove ethanol at 3,900g. Evaporating ethanol from the silica column through heating was evaluated (samples E, F), as well as the possibility of evaporating ethanol from the eluate after successful DNA extraction (sample G). In the latter case, it would be possible to drive off ethanol in the external optical reader rather than inside a heated LabTube. This option would again render LabTube heating superfluous.

METHODS:

For the tests shown in Table 41 the Macherey Nagel Tissue XS kit was used to manually extract *E.coli* DNA from an overnight culture. The cell concentration before extraction was 10^8 copies/µl

and for each condition at least two repeats were run. The extracted DNA was analyzed using qPCR with three repeats each (see Chapter 3.2.1.5) to determine both the yield and ethanol inhibition effects. The ethanol content was checked using gas chromatography by the chemical analytics department (CR/ARA) at Bosch.

RESULTS:

Table 42 shows the results of the ethanol content analysis by gas-chromatography. It demonstrates that dry spinning the column at 3,900g between 1-5min (B, C, D) yields inacceptable ethanol contents between 7.4-8wt%. It shows further that heating the column or eluate both yield acceptable ethanol contents (<5wt%). Either of the two options is hence suitable to remove ethanol. The results also indicate that the recovery of DNA is lower in experiments employing low g-forces (3,900g) than using the standard protocol at 11,000g. No significant differences in DNA yield between the adjusted extraction protocols (experiments B-G) are shown, confirming that the lower extraction yield is indeed due to the reduced g-forces and not caused by other factors, like ethanol residues. Overall, driving off ethanol inside the LabTube is not necessary, as ethanol can also be removed from the eluate outside the LabTube.

Experi-ment name	Description	Processing steps force (g)	Processing steps time (min)	Dry spin force (g)	Dry spin time (min)	Column heating	Eluate heating
A	Standard	11000	1	11000	1	-	-
B	Low g	3900	1	3900	1	-	-
C	Low g, long spin all steps	3900	5	3900	5	-	-
D	Low g long spin dry	3900	1	3900	5	-	-
E	Heat column 1	3900	1	3900	1	95°C;10min	-
F	Heat column 2	3900	1	3900	1	85°C;5min	-
G	Heat eluate	3900	1	3900	1	-	85°C;5min
X	Negative standard	11000	1	11000	1	-	-

TABLE 41: Ethanol removal experiments, n≥2 for each experiment.

Experiment name	Description	Recovered DNA (10^4 copies/µl in PCR)	Recovered DNA wrt experiment A (in %)	EtOH in eluate (wt%)
A	Standard	7.6±1.1	100±14	5.0
B	Low g	4.6±2.7	61±35	8.0
C	Low g, long spin all	1.3±9.5	18±12	7.4
D	Low g long spin dry	3.4±2.9	44±38	7.5
E	Heat column 1	3.1±1.9	41±25	0.0
F	Heat column 2	3.0±1.6	39±21	0.0
G	Heat eluate	3.6±1.7	47±22	3.4
X	Negative standard	$(1.2±5.0)·10^{-4}$	0±0	4.1

TABLE 42: Recovered DNA and ethanol content as determined by qPCR and by gas chromatography, n=3 for each sample from Table 41. The cell concentration before extraction was 10^8 copies/µl. (Gas chromatography measurements for EtOH contents were performed by the Chemical Analytics Department at Robert Bosch GmbH).

5.6   SUMMARY

In this chapter, it was outlined how to heat and readout assays *inside* the centrifuge. This approach was expected to be preferable, when contamination risks are high or when heating is needed inside the LabTube anyways. For heating, a theoretical temperature control evaluation was performed. Here, centrifugal, chemical and electrical heating methods were theoretically compared. It was shown that only electrical methods are feasible, whilst chemical methods are feasible only for short heating applications that can tolerate high temperature deviations (>±4°K). For electrical heating, one could build a custom centrifuge with integrated optics and heating based on e.g. induction or external power sources. Alternatively, an autonomous battery-driven system could be used which can be used with standard laboratory centrifuges. Here, readout could occur qualitatively through visual detection. As a proof-of-principle, an autonomous heating system consisting of a microcontroller, SMD resistor heaters and a battery was built. The system is versatile, disposable, mechanically stable and achieves robust temperature control (±2°C), which can be easily parallelized. The system was used to successfully extract and isothermally amplify VTEC *E.coli* DNA by a LAMP reaction inside the LabTube. In the system, the results are readout with a visual dye. For quantitative readout, the round LabReader optics could be integrated into the centrifuge-holders. The heating system can also be used for other heating applications, such as the preheating of lysis and elution buffers to increase extraction yield, the removal of ethanol and/or for other downstream assays (such as

immunoassays or other DNA amplification methods). It is expected that for applications with high contamination risk performing heating steps within a closed system inside the centrifuge is beneficial. It could further be required for difficult to extract matrices (e.g. gram-positive bacteria or plants) and for other extraction types (e.g. proteins or RNA). For applications in which heating extraction buffers does not improve the yield or quality and where contamination-risks are low, amplification/readout *outside* of the centrifuge remain the prioritized solution.

CHAPTER 6: OVERALL SUMMARY AND DISCUSSION

6.1 OVERALL SUMMARY

Mass outbreaks worldwide are repeatedly caused by contamination of medicine, food, water and ingestible consumer goods [9, 10] (Chapter 1). Traditional laboratory methods are used to detect these contaminants in an accurate, sensitive and specific fashion. However, they are usually expensive [7], require a specialized laboratory and training to perform numerous manual steps [1, 2, 3, 4, 5, 6] (Chapter 1). Biosensors and portable devices have been developed to overcome the limitations of traditional methods, to make them field-deployable and to reduce the overall time-to-result. Overall, these methods could be used for food safety, medical diagnostics, academic and environmental testing. Even though first products are available, biosensors generally lack commercial maturity, require expensive hardware and are often inflexible, suitable for a single application only. These disadvantages motivate the development of broadly deployable detection methods that are flexible, robust and economical.

The LabReader was introduced, which employs an optical detection scheme with fluorescence and/or UV absorption measurements (Chapter 2). The round geometry allows for a simultaneous viewing of 4 channels. It consists of low-cost LEDs and light-to-voltage converters in conjunction with injection-molded housings. The LabReader has green-to-red fluorescent sensitivities comparable to commercial plate readers (e.g. LoD 7µM for glucose). Compared with commercially available, portable readers, it is expected to be more versatile (4 channels) and lower in cost. Contaminants were detected directly in various substances, without separation, purification, concentration or incubation. Enzyme methods based on alcohol- and aldehyde dehydrogenase coupled with fluorescent dyes were developed to detect (di-)ethylene glycol in consumables above 0.1wt% and alcohols (in groundwater and blood) above 1ppb. For fluorescence-based detection of bacteria, a nonspecific DNA intercalator dye was chosen due to its low cost and high stability. As a proof-of-principle, pathogens (*salmonella, cholera, E.coli* and a model for malaria) in water, foods and blood were detected at LoDs as low as 10^4 CFU/ml. The chemistry is stable for weeks without refrigeration and the rapid detection time of the assays allows testing of perishable foods and ingestible products. In addition, the measured contaminant concentrations do not change with background substrate, which demonstrates that these detection methods are broadly effective in a wide variety of substances. Enzyme-based detection for contaminants and toxins is specific and sensitive enough to comply with safety limits. The introduced bacterial detection assays are robust, but insensitive to the actual

genome being detected and the sensitivity is limited. In situations where cost-pressure is not so severe, safety requirements demand specific and sensitive detection of bacteria below 10^4 CFU/ml. To gain both sensitivity and specificity, methods like DNA amplification needed to be incorporated into the LabReader. In addition, the sample preparation of the LabReader had to be automated to be broadly deployable, even outside a specialized laboratory.

To incorporate automated sample preparation, the LabReader was combined with the LabTube, a disposable platform for automated DNA extraction. The LabTube is based on modules integrated in a 50ml falcon tube, in which the DNA extraction workflow is automated by applying process specific centrifugation protocols to a standard laboratory centrifuge (Chapter 3)[8]. Due to market and feasibility reasons, food safety was chosen as a first application with *E.coli* and *Alicyclobacilli* as example organisms. DNA from *E.coli* lysate in milk and buffer, as well as from *Alicyclobacillus* lysate in apple juice were extracted to as low as 10^2 copies using the standard protocol of the QIAamp Micro DNA kit inside the LabTube, yielding the best performance of all screened kits. By optimizing the extraction protocol using 4 re-elutions, as little as $4.5 \cdot 10^1$ copies were extracted, whilst multiple binding steps did not increase the yield (Chapter 3).

In the combined system of the LabTube for DNA extraction and the LabReader for amplification and readout, it is possible to amplify and readout the extracted DNA *inside* or *outside* the centrifuge, in which the LabTube is processed. As the aim of this thesis was to develop a method that can be used broadly with standard laboratory equipment, it was decided to amplify and readout DNA *outside* of the standard centrifuge/LabTube - rather than using a custom centrifuge/LabTube for amplification/readout, which would increase costs and reduce flexibility.

In Chapter 4, the LabSystem was introduced, which consists of the LabTube for automated DNA extraction and the LabReader, for portable specific DNA amplification and readout *outside* of the centrifuge. A removable PCR tube serves as an interface between the LabTube and the LabReader to minimize contamination risks. The extracted DNA can be amplified using both the qualitative isothermal LAMP method (LAMP-LabSystem) and the semi-quantitative real-time PCR reaction (PCR-LabSystem). The product specificity is determined in the PCR-LabSystem by performing a melting curve or by reading out at specific temperatures above the melting point of nonspecific products. The combined extraction and amplification LoD of the LAMP-LabSystem is 10^2 and 10^3 copies of *E.coli* in water and milk and $4.5 \cdot 10^2$ copies of *Alicyclobacillus* in apple juice. The combined extraction and amplification LoQ of the PCR-LabSystem is 10^2 copies for *E.coli* in water and juice and 10^3 inserted copies for *E.coli* in milk. This result implies that for many applications pre-enrichment steps are no longer necessary,

hence saving time and money (such as for detecting *E.coli* in production processes). However, in some instances, where lower LoDs are required, the use of larger sample volumes or short pre-enrichment steps inside the LabTube will be necessary (e.g. for *Alicyclobacillus* detection in juice).

In chapter 5, performing extraction, amplification and readout *inside* the centrifuge was outlined. Even though this approach was not the focus of this thesis, it is expected to be preferable when contamination risks are high or when extraction buffers need to be heated in the LabTube to increase the extraction yield. For DNA amplification inside the centrifuge, a heating method needed to be added to the LabTube. A theoretical temperature control evaluation was performed, in which centrifugal, chemical and electrical heating methods were compared. Based on the results, it was decided to build an autonomous battery-driven heated LabTube that can be processed in a standard centrifuge. The heated LabTube is controlled by a microcontroller, it employs SMD resistors and a NTC as heaters and sensor and it is driven by a 3V, CR-2 battery. The system was successfully used to extract and to isothermally amplify VTEC *E.coli* DNA in a heated LabTube using the LAMP reaction. The result was readout qualitatively with a visual dye. The heating system is versatile deployable and could be used for other heating applications, such as the preheating of lysis and elution buffers to increase extraction yield, the removal of ethanol and/or for downstream assays, like immunoassays or other DNA amplification methods. A critical evaluation of heating methods was performed. It was shown that ethanol can also be removed from the eluate in a separate readout unit and hence it does not necessarily have to be removed during LabTube processing. Heating extraction buffers was further shown to not increase DNA extraction yields from blood. However, the heated, closed-system LabTube is expected to be preferable when contamination risks are high. Further, it could be beneficial for improving extraction yields in difficult to extract matrices (such as gram-positive bacteria and plants) or the extraction of other molecules (e.g. RNA and proteins).

Overall, the combined LabSystem and the heated LabTube are versatile deployable for different applications, assay types, kits and amplification methods and because they are automated and frugal they can be used at flexible locations. The LabSystem component, the LabReader, is expected to be more flexible than other portable readers (Chapter 1), as it can readout four wavelengths simultaneously and it can perform isothermal and PCR amplification of DNA without being restricted to specialized kits. Its ability to readout data continuously during temperature cycling enables advanced data analysis procedures. Due to the use of LEDs and theater light filters, it is expected to be lower in cost. The LabTube has the advantage over other

129

automated DNA extraction devices that it can run on a standard laboratory centrifuge (rather than an expensive, specialized device). It is easily scalable and it minimizes contamination risks by using prepackaged reagents for each extraction and by having an interface with the LabReader.

6.2   OUTLOOK

In the future, the introduced methods could be improved in a variety of ways. In a final product, the LabReader could be controlled with a microcontroller or a mobile device rather than with a computer and it could run on batteries for mobility. For stability, the LabReader could be incorporated into a completely closed and light-proof housing. For mass production, the housing should be injection molded and for reproducible positioning, SMD LEDs should be used. The sensitivity of the detectors could be improved by adding a third LED or by optimizing LEDs, excitation times, filters and optical paths. Additionally, the use of more than two detection chambers would allow for higher throughput, as well as the ability to quantify the PCR reaction independently of the used batch, which requires at least four controls per run[169]. Automated calibration between the reaction chambers should be added. For the PCR reactions, the time-to-result could be increased by reducing the thermal mass of the metal inlet, which has not yet been optimized. Using specific probes (such as TaqMan) rather than nonspecific intercalating dyes, multiplexing could be performed inside the LabReader.

For DNA extraction, the LabTube errors during extraction (~26%, which is comparable to manual extractions) could be improved by achieving better fluidic and mechanic reproducibility of the system. Higher reproducibility could be achieved e.g. by injection molding the pieces, rather than using stereolithography as for the experimental units. Extraction yields could be increased by incorporating multiple elution steps into the LabTube. It was observed in this thesis that extraction efficiency is largely dependent on the extraction kit used. As a next step, reasons for different kit performances should be verified and the LabTube should be made broadly compatible with a variety of extraction kits, in order to gain even more flexibility. In this thesis, only cell lysates were used for extractions. In the future, whole cells should be used. For applications, where required detection limits demand pre-enrichment, a cell-incubation chamber could be incorporated into the LabTube cap. The incorporation of other DNA extraction methods (such as bead or organic solvent based methods, see Chapter 1.2.2.4) and other target molecule extractions (e.g. DNA, RNA and proteins) will increase the application range.

For external amplification (Chapter 4), the entire LabTube (rather than a PCR tube) could be placed into the LabReader to further reduce contamination risks. The heated LabTube described in Chapter 5 could be run on rechargeable batteries, rather than disposable ones in order to minimize waste. The end user could be equipped with a testing device indicating the battery status before each run. To add quantitative realtime readout, the LabReader optics could be incorporated into a custom centrifuge.

The focus of this thesis was food safety. The introduced systems are generally applicable for a variety of applications in food, environmental, consumer product and medical diagnostics, quality control and research applications, which should be covered in the future.

Overall, the introduced methods can be combined and extended flexibly depending on the application. Some of the mentioned improvements would make the LabTube and the LabReader more expensive and they should be incorporated depending on the performance requirements for the desired application. These include applications in developed countries (e.g. production sites) and in third-world countries. For example, in developed countries a more sensitive and higher throughput LabReader may be desirable, whilst in the field or in developing countries the LabReader may be used without the LabTube. Here, the (heated) LabReader may serve as a sample enrichment and heat-lysis chamber, prior to amplification and readout. Alternatively, a low-budget centrifuge or a pressure-driven device could be developed to process the LabTube in low resource scenarios.

6.3   CONCLUSION

The fundamental contributions of this thesis include the combination, optimization and system-integration of components for versatile, automated and frugal sample preparation and detection at low-to-medium throughput: Compared with commercially available readers, the portable LabReader is expected to be more versatile (4 channels, continuous data readout) and more frugal (due to the low cost of its components). The LabSystem, consisting of the LabReader, for DNA amplification and readout, and the LabTube, for automated DNA extraction, is expected to be more flexible and more broadly deployable than commercial systems. This is because it is not restricted to specialized kits, it is easily scalable, it can be combined flexibly with other components and because it runs with standard laboratory equipment. The LabSystem further has an interface between its components to reduce contamination risks, which many commercial systems do not have. Unlike the LabSystem and unlike most existing devices, the

131

heated LabTube is a sample preparation and detection system that is disposable and fully closed (hence even further minimizing contamination risks).

The second major contribution of this thesis includes the development and integration of example assays into the components and systems. The developed applications focus on food safety, but also cover medical, product and environmental contaminations and quality control: For the LabReader, enzyme and dye-based assays were developed to detect chemical contaminants (EG, DEG and alcohols), as well as bacteria in foods, water, consumer products and blood. The achieved detection limits are at or below the required safety limits and they are comparable with existing devices. In the LabSystem and heated LabTube, DNA extraction and amplification methods were integrated with a focus on detecting bacteria for food quality and safety. The achieved detection limits as low as 10^2 CFU/ml are comparable with existing reference methods.

The sample preparation and detection systems are fully integrated and automated. Unlike many analytic strategies, they offer great application flexibility, yet are low-cost and due to the employment of standard laboratory equipment they are versatile deployable. Together or in part with other systems, these contributions could help hasten more testing and analysis in the field, which could increase safety, reduce contamination outbreaks, as well as the waste of precious resources. The systems can be used to increase safety and product quality in food applications, but also in other areas, such as environmental and consumer products and in medical diagnostics.

APPENDIX

A1: CHEMICAL REACTION VOLUME CALCULATIONS

Goal:
0.2ml for 5 Minutes to 65 °C
starting T=25°C
V=0.2ml
M=0.2g
T=5min
dT=40°K
T=65°C
Q_{rctn}=33.5J

Step 1: How much PCM?

$Q_{rctn} = c_{sample} * m *$
$dT = c_{H20} * m * dT$
Q_{rctn} 3.35E+01 J
assumption: heat capacity of sample = heat capacity of water

1.a) m(PCM) without heat losses

$Q_{water} = Q_{PCM}$

m_{PCM} 5.23E-02 g
assumption: PCM is a paraffin

1.b) Heat losses from sample

assumption: heat losses by conduction only

Worst case (air isolation):

Fourier's law
q=-k*A*dT/dx

V   2.00E-01 ml
d   5.85E-03 m
A   3.42E-05 m
d/2   2.92E-03 m
assumption: cubic shape; sample is made of water

XII

q	2.80E-01	W
$q_{total}=5q$	1.40E+00	W
Q_{5min}	4.20E+02	J

Best case (0.1cm polystyrene isolation):

R =	L/kA		
q =	dT/SUM(R)		

R_{sample}	1.43E+02	k/W
$R_{transition}$	8.04E+00	k/W
$R_{polystyrene}$	9.75E+02	k/W

q=-k*A*dT/dx	3.55E-02	W

$q_{total}=5q$	1.78E-01	W
Q_{5min}	5.33E+01	J

1.c) PCM with heat losses from sample

$Q_{total(max)}$	4.53E+02	J			
$Q_{total(min)}$	8.68E+01	J			
$Q_{total} = Q_{losses} + Q_{rctn}$					
m_{max}	7.08E-01	g	V_{min}	8.33E-01	ml
m_{min}	1.36E-01	g	V_{max}	1.59E-01	ml

1.d) Heat losses of PCM

Worst case (air isolation):

Fourier's law
q=-k*A*dT/dx

V_{PCM}	8.33E-01	ml
d	9.41E-03	m
d/2	4.70E-03	m
q	1.96E-01	W
q_{total}	9.79E-01	W
Q_{5min}	2.94E+02	J
$Q_{tot,5min}$	**7.47E+02**	**J**

Best case (0.1cm polystyrene isolation):

R   L/kA

q   dT/SUM(R)

R_{sample} 2.04E+02   k/W

                                             assume: interface layer thickness is

R_{layer} 3.11E+00   k/W   0.27 mm

$R_{polystyrene}$ 3.77E+02   k/W

q   6.85E-02   W

Q_{5min} 3.08E+02   J

$Q_{tot, 5min}$ **3.95E+02**   **J**

$Q_{total(max)}$ 1.20E+03   J

$Q_{total(min)}$ 4.82E+02   J

$Q_{total} = Q_{losses} + Q_{rctn}$

$m_{PCM, max}$ 1.87E+00   g $V_{PCM, max}$ 2.21E+00   ml

$m_{PCM, min}$ 7.53E-01   g $V_{PCM, min}$ 8.86E-01   ml

CONTRIBUTIONS

This section summarizes individual contributions to thesis parts, wherever they were performed not by the author alone but in collaboration with others. Further contributions are marked specifically in the text, where applicable. The listed contributions are also specifically documented in the publications listed in the next section.

CHAPTER 2: The author individually started the LabReader work as an undergraduate student in Prof Slocum's laboratory at MIT in 2007 under the supervision of Prof. Hong Ma for two summers. The author was involved in the overall system design, developed chemical assays and performed full-system integration. For the design, the author collaborated with Jim MacArthur (electrical design), Alexander Slocum (mechanical design) and Peter Lu (optical layout and data readout) starting in 2008/09, with whom the publications in references [96] and [154] were published.

CHAPTER 3: The basic LabTube mechanics and DNA extraction functionalities were developed by the HSG IMIT and IMTEK, University of Freiburg.

CHAPTER 5: For DNA extraction and LAMP amplifications, the author worked together with the Master student, Nobu Karippai. For the PCR-LAMP system, the author worked together with intern student Eva Schulte Bocholt. The author supervised both students.

CHAPTER 6: For the mechanical design, the author worked together with student Michael Weissert, which she supervised. The author collaborated with Nesch Engineering for electronics design.

PUBLICATIONS AND PATENTS

JOURNAL ARTICLES

<u>M. Hoehl</u>, P. Lu, P. Sims and A. Slocum, "Rapid and robust detection methods for poison and microbial contamination", *J. Agric. Food Chem.,* vol. 60, no. 25, p. 6349-6358, 2012.

P. Lu, <u>M. Hoehl</u>, J. Macarthur, P. Sims, H. Ma and A.H. Slocum, "Robust and economical multi-sample, multi-wavelength UV/vis absorption and fluorescence detector for biological and chemical contamination", *AIP Adv.,* vol. 2, no. 3, p. 032110, 2012.

<u>M. Hoehl</u>, E. Schulte Bocholt, N. Karippai, R. Zengerle, A.H. Slocum, J. Steigert, "Low-cost bacterial detection system for food safety based on automated DNA extraction, amplification and readout", *Lab Chip* (in preparation).

<u>M. Hoehl</u>, M. Weissert, R. Zengerle, A.H. Slocum, J. Steigert, "Centrifugal LabTube platform for fully automated DNA extraction & LAMP assay based on an integrated low-cost heating system", *Lab Chip* (in preparation).

CONFERENCE PROCEEDINGS AND PRESENTATIONS

<u>M. Hoehl,</u> S. Dougan, H. Ploegh, J. Voldman, "Massively parallel microfluidic cell-pairing platform for the statistical study of immunological cell-cell interactions", *MTL Conference*, MIT, USA, 2010.

<u>M. Hoehl.,</u> S. Dougan, H. Ploegh, J. Voldman, "Massively parallel microfluidic cell-pairing platform for the statistical study of immunological cell-cell interactions", 15th International *Conference on Miniaturized Systems for Chemistry and Life Sciences (µTAS)*, Seattle, WA USA, p.1508-10, 2010.

<u>M. Hoehl,</u> "Rapid and robust detection methods for poison and microbial contamination", presentation at the PhD colloquium of the *German National Academic Foundation*, Frankfurt, 2010.

<u>M. Hoehl,</u> P. Lu, P. Sims and A. Slocum, "Rapid and Robust Detection Methods for Poison and Microbial Contamination", *Gordon Research Conference for Biosensors*, RI, USA, 2011.

M. Hoehl, M. Weissert, A.H. Slocum, R. Zengerle, F. von Stetten, N. Paust and J. Steigert, "Battery-driven, low-cost heating system for performing a fully automated DNA extraction & LAMP assay in the centrifugal LabTube platform", *European Lab-on-a-Chip Congress*, Barcelona, 2013.

M. Hoehl, E. Schulte Bocholt, N. Karippai, R. Zengerle, A.H. Slocum, J. Steigert, "Low-cost bacterial detection system for food safety based on automated DNA extraction, amplification and readout", *Micro TOTAL Analysis Systems*, Freiburg, 2013 (submitted).

M. Hoehl, M. Weissert, R. Zengerle, N. Paust, A.H. Slocum, J. Steigert, "Centrifugal LabTube platform for fully automated DNA extraction & LAMP assay based on an integrated low-cost heating system", *Micro TOTAL Analysis Systems*, Freiburg, 2013. (submitted).

SUPERVISED MASTER THESES AND INTERNS

M. Weissert, "Temperaturkontrolle in gestapelter, auf Zentrifugalkräften basierender mikrofluidischer Anordnung", Diplomarbeit, Universität Stuttgart, 09.2012.

N. Karippai, "Rapid and automated bacterial DNA extraction, amplification and detection using a centrifugal force based microfluidic device and an LED-based optical sensor", Master Thesis, University of Applied Sciences Aachen, 03.2013.

E. Schulte Bocholt, 5 months internship, Department of Electrical Engineering, RWTH Aachen University, 11.12-04.13

PATENT APPLICATIONS AND INVENTION REPORTS

23 Invention Reports at Robert Bosch GmbH: 11 filed patent applications (or currently in preparation with the lawyer) with Robert Bosch GmbH, 5 are under internal review.

M. Hoehl et al, "Apparatus and method for detecting glycols", Pub. No. WO/2010/057005, USA, China and India Patent, 2008. Filed at MIT and sold to Robert Bosch GmbH in 2012.

BIBLIOGRAPHY

[1] FDA, "Guidance for industry: Testing of glycerin for diethylene glycol," FDA, Silver Spring, MD, 2010.

[2] P. Leonard, S. Hearty, J. Brennan, L. Dunne, J. Quinn, T. Chakraborty and R. O'Kennedy, "Advances in biosensors for detection of pathogens in food and water," *Enzyme Microb. Technol.,* vol. 32, no. 1, pp. 3-13, 2003.

[3] S. Nugen and A. Baeumner, "Trends and opportunities in food pathogen detection," *Anal. Bioanal. Chem.,* vol. 391, no. 2, pp. 451-454, 2008.

[4] V. Velusamy, K. Arshak, O. Korostynska, K. Oliwa and C. Adley, "An overview of foodborne pathogen detection: In the perspective of biosensors," *Biotech. Adv.,* vol. 28, p. 232–254, 2010.

[5] A. Kenyon, S. Xiaoye, Y. Wang, N. Har, R. Prestridge and K. Sharp, "Simple, at-site detection of diethylene glycol/ethylene glycol contamination of glycerin and glycerin-based raw materials by thin-layer chromatography," *J. AOAC Int.,* vol. 81, no. 1, pp. 44-50, 1998.

[6] P. Yager, G. Domingo and J. Gerdes, "Point-of-care diagnostics for global health," *Annu. Rev. Biomed. Eng.,* vol. 10, pp. 107-144, 2008.

[7] G. Kost, "Newdemics, public health, small-world networks, and point-of-care testing," *Point of Care,* vol. 5, no. 4, p. 138, 2006.

[8] R. Zengerle, J. Hoffmann, G. Roth, O. Strohmeier, A. Fiebach, S. Zhang, A. Kloke, A. Paust, D. Mark and F. von Stetten, "Microfluidic apps on standard lab equipment," *MicroTAS,* 2012.

[9] FDA, "FDA science and mission at risk; report of the subcommittee on science and technology," FDA, Silver Spring, MD, 2007.

[10] K. Sack and T. Williams, "Deaths of 9 Alabama patients tied to intravenous supplement," *NY Times Mag.,* 30 March 2011.

[11] J. Tagliabue, "Scandal over poisoned wine embitters village in Austria," *NY Times Mag.,* 2 August 1985.

[12] W. Bogdanich and J. Hooker, "Toxic toothpaste made in china is found in the U.S.," *N. Y. Times Mag.,* 6 May 2007.

[13] E. Scallan, R. Hoekstra, F. Angulo, R. Tauxe, M. Widdowson, S. Roy, J. Jones and P. Griffin, "Foodborne illness acquired in the United States - major pathogens," *Emerg. Infect. Dis.,* vol. 17, 2011.

[14] D. Sack, R. Sack and C. Chaignat, "Getting serious about cholera," *N. Engl. J. Med.,* vol. 355, no. 7, pp. 649-651, 2006.

[15] CDC, "Outbreaks of Escherichia coli O157:H7 infection and cryptosporidiosis associated with drinking unpasteurized apple cider -- Connecticut and New York, October 1996," *MMWR,* vol. 96, pp. 4-8, 1997.

[16] CDC, Center of Disease Control, "Outbreaks involving E.coli," CDC, 2011. [Online]. Available: http://www.cdc.gov/ecoli/outbreaks.html. [Accessed 10 4 2013].

[17] P. Mead, L. Slutsker, V. Dietz, L. McCaig, J. Bresee, C. Shapiro, P. Griffin and R. Tauxe, "Food-related illness and death in the United States," *Emerg. Infect. Dis.,* vol. 5, no. 5, p. 607, 1999.

[18] D. Griffith, L. Kelly-Hope and M. Miller, "Review of reported cholera outbreaks worldwide, 1995-2005," *Am. J. Trop. Med. Hyg. ,* vol. 75, no. 5, pp. 973-977, 2006.

[19] J. Theron, J. Cilliers, M. Du Preez, V. Brozel and S. Venter, "Detection of toxigenic Vibrio cholerae from environmental water samples by an enrichment broth cultivation--pit-stop semi-nested PCR procedure," *J. Appl. Microbiol.,* vol. 89, no. 3, pp. 539-546, 2000.

[20] J. Waters, J. Sharp and V. Dev, "Infection caused by Escherichia coli O157: H7 in Alberta, Canada, and in Scotland: a five-year review, 1987-1991," *Clin. Inf. Dis.,* vol. 19, no. 5, pp. 834-843, 1994.

[21] S.-S. Chang and D.-H. Kang, "Alicyclobacillus spp. in the fruit juice industry: history, characteristics, and current isolation/detection procedures," *Crit. Rev. Microbiol.,* vol. 30,

no. 2, pp. 55-74, 2004.

[22] "Alicyclobacillus, the beverage industry and the biosys," Rapid Microbiology, 1 2004. [Online]. Available: www.rapidmicrobiology.com.

[23] P. Wax, "Elixirs, diluents, and the passage of the 1938 Federal Food, Drug and Cosmetic Act," *Ann. Intern. Med.,* vol. 122, no. 6, pp. 456-461, 1995.

[24] R. Gomes, R. Liteplo and M. Meek, "Ethylene glycol: human health aspects," World Health Organization, Genf, CH, 2002.

[25] J. Schier, L. Conklin, R. Sabogal, D. Della Aglio, C. Sanchez and J. Sejvar, "Medical toxicology and public health, update on research and activities at the centers for disease control and prevention and the agency for toxic substances and disease registry," *J. Med. Toxicol.,* vol. 4, no. 1, pp. 40-42, 2008.

[26] SCCP (European Commission Scientific Committeeon Consumer Products), "Opinion on diethylene glycol," SCCP, Brussels, 2008.

[27] J. Leikin, T. Toerne, A. Burda, K. McAllister and T. Erickson, "Summertime cluster of intentional ethylene glycol ingestions," *JAMA,* vol. 278, no. 17, pp. 1406-1406, 1997.

[28] S. Schultz, M. Kinde and D. Johnson, "Ethylene glycol intoxication due to contamination of water systems," *MMWR ,* vol. 36, pp. 611-614, 1987.

[29] U.S. Environmental Protection Agency, "Potential contamination due to cross-connections and backflow and the associated health risks," US EPA, Washington, D.C., 2001.

[30] A. Abubukar, E. Awosanya, O. Badaru, S. Haladu, P. Nguku, P. Edwards, R. Noe, M. Teran-Maciver, A. Wolkin and L. Lewis, "Fatal poisoning among young children from diethylene glycol-contaminated acetaminophen-Nigeria, 2008-2009," *MMWR,* vol. 58, no. 48, pp. 1345-1347, 2009.

[31] K. O'Brien, J. Selanikio, C. Hecdivert, M. Placide, M. Louis, D. Barr, J. Barr, C. Hospedales, M. Lewis and B. Schwartz, "Epidemic of pediatric deaths from acute renal failure caused by diethylene glycol poisoning," *JAMA,* vol. 279, no. 15, pp. 1175-1180, 1998.

[32]   M. Hanif, M. Mobarak, A. Ronan, D. Rahman, J. Donovan and M. Bennish, "Fatal renal failure caused by diethylene glycol in paracetamol elixir: the Bangladesh epidemic," *BMJ,* vol. 311, no. 6997, pp. 88-91, 1995.

[33]   H. Okuonghae, I. Ighogboja, J. Lawson and E. Nwana, "Diethylene glycol poisoning in Nigerian children," *Ann. Trop. Paediatr.,* vol. 12, no. 3, p. 235, 1992.

[34]   S. Pandya, "Letter from Bombay. An unmitigated tragedy," *Br. Med. J.,* vol. 297, no. 6641, pp. 117-119, 1988.

[35]   P. Wax, "It's happening again-another diethylene glycol mass poisoning," *Clin. Toxicol.,* vol. 34, no. 5, pp. 517-520, 1996.

[36]   R. Osterberg and N. See, "Toxicity of excipients: A Food and Drug Administration perspective," *Int. J. Toxicol.,* vol. 22, no. 5, pp. 377-380, 2003.

[37]   J. Singh, A. Dutta, S. Khare, N. Dubey, A. Harit and N. Jain, "Diethylene glycol poisoning in Gurgaon," *Bull. World Health Organ.,* vol. 79, pp. 88-95, 2001.

[38]   P. Leth and M. Gregersen, "Ethylene glycol poisoning," *Forensic Sci. Int.,* vol. 155, no. 2, pp. 179-184, 2005.

[39]   O. Obasanjo, "An open letter to the president of the Federal Republic of Nigeria," The Pharmaceutical Society of Nigeria, Abuja, 2007.

[40]   R. Drut, G. Quijano, M. Jones and P. Scanferla, "Pathologic findings in diethylene glycol poisoning," *Medicina (Mex.),* vol. 54, no. 1, p. 1, 1994.

[41]   L. Ferrari and L. Giannuzzi, "Clinical parameters, postmortem analysis and estimation of lethal dose in victims of a massive intoxication with diethylene glycol," *Forensic Sci. Int.,* vol. 153, no. 1, pp. 45-51, 2005.

[42]   M. Cantarell, J. Fort, J. Camps, M. Sans, L. Piera and M. Rodamilans, "Acute intoxication due to topical application of diethylene glycol," *Ann. Intern. Med.,* vol. 106, no. 3, pp. 478-479, 1987.

[43]   Anonymous, "The global history of di-ethylene glycol contamination," Panama Guide, 21

October 2006. [Online]. Available: http://www.panama-guide.com/article.php/20061021172845483. [Accessed 13 03 2013].

[44] Wikipedia, "Blood alcohol content," Wikipedia, [Online]. Available: http://en.wikipedia.org/wiki/Blood_alcohol_content. [Accessed 14 04 2013].

[45] The Groundwater Foundation, "Sources of groundwater contamination," [Online]. Available: http://www.groundwater.org/gi/sourcesofgwcontam.html. [Accessed 13 04 2013].

[46] I. Jubany, "Groundwater contamination," 26-30 09 2011. [Online]. Available: http://www.stream-project.eu/sites/default/files/1_Groundwater_contamination.pdf. [Accessed 14 04 2013].

[47] T. Shih, Y. Rong, T. Harmon and M. Suffet, "Evaluation of the impact of fuel hydrocarbons and oxygenates on groundwater resources," *Environ. Sci. Technol.,* vol. 38, no. 1, pp. 42-48, 2004.

[48] Interstate Technology and Research Council, "Overview of groundwater remediation," ITRC, Concord, NH, 2005.

[49] TNN, "Punjab: Now, alcohol in groundwater," *The Times of India,* 20 06 2010.

[50] University of Flordia, "Innovations in groundwater remediation," University of Florida, Gainesville, Fl.

[51] New Jersey Dept. of Environmental Protection, "Ground water quality standards - class IIA by constituent," New Jersey Dept. of Environmental Protection, NJ, 2011.

[52] A. Bhunia and A. Lathrop, "Foodborne pathogen detection," in *McGraw-Hill Yearbook of Science & Technology*, New York, NY, McGraw-Hill, 2003, 1-3, pp. 320-323.

[53] J. Wells, B. Davis, I. Wachsmuth, L. Riley, R. Remis, R. Sokolow and G. Morris, "Laboratory investigation of hemorrhagic colitis outbreaks associated with a rare Escherichia coli serotype," *J. Clin. Microbiol.,* vol. 18, no. 3, pp. 512-520, 1983.

[54] L. Riley, R. Remis, S. Helgerson, H. McGee, J. Wells, B. Davis, R. Hebert, E. Olcott, L.

Johnson and N. Hargrett, "Hemorrhagic colitis associated with a rare Escherichia coli serotype," *N. Engl. J. Med.,* vol. 308, no. 12, pp. 681-685, 1983.

[55] G. Armstrong, J. Hollingsworth and J. Morris Jr, "Emerging foodborne pathogens: Escherichia coli O157: H7 as a model of entry of a new pathogen into the food supply of the developed world," *Epidemiol. Rev.,* vol. 18, no. 1, p. 29, 1996.

[56] D. Swerdlow, B. Woodruff, R. Brady, P. Griffin, S. Tippen, H. Donnell Jr, E. Geldreich, B. Payne, A. Meyer Jr and J. Wells, "A waterborne outbreak in Missouri of Escherichia coli O157: H7 associated with bloody diarrhea and death," *Ann. Intern. Med.,* vol. 117, no. 10, pp. 812-819, 1992.

[57] A. Carter, A. Borczyk, J. Carlson, B. Harvey, J. Hockin, M. Karmali, C. Krishnan, D. Korn and H. Lior, "A severe outbreak of Escherichia coli O157: H7 associated hemorrhagic colitis in a nursing home," *N. Engl. J. Med.,* vol. 317, no. 24, pp. 1496-1500, 1987.

[58] S. Olsen, G. Miller, T. Breuer, M. Kennedy, C. Higgins, J. Walford, G. McKee, K. Fox, W. Bibb and P. Mead, "A waterborne outbreak of Escherichia coli O157: H7 infections and hemolytic uremic syndrome: implications for rural water systems," *Emerg. Infect. Dis.,* vol. 8, no. 4, p. 370, 2002.

[59] D. Ackman, S. Marks, P. Mack, M. Caldwell, T. Root and G. Birkhead, "Swimming-associated haemorrhagic colitis due to Escherichia coli O157: H7 infection: evidence of prolonged contamination of a fresh water lake," *Epidemiol. Infect.,* vol. 119, no. 1, pp. 1-8, 1997.

[60] G. Lopez-Campos, J. Martinez-Suarez, M. Aguado-Urda and V. Lopez-Alonso, Microarray detection and characterization of bacterial foodborne pathogens, Springer, 2012.

[61] Marketsandmarkets, "Food safety testing market by contaminants, technology, food types, geography: trends & global forecast (2010 – 2015)," Marketsandmarkets, 2011.

[62] Gulf Standards, "Microbiological criteria for foodstuffs, part 1.," Saudia Arabia, 2000.

[63] A. Ziermann, "Mikrobiologische Kriterien für Milch, Milchprodukte und andere Lebensmittel in Europa," Technische Universität München, München, 2005.

[64] CDC, Centers for Disease Control and Prevention, "Salmonella outbreaks," CDC, 2011. [Online]. Available: http://www.cdc.gov/salmonella/outbreaks.html. [Accessed 10 4 2013].

[65] B. Mishu, J. Koehler, L. Lee, D. Rodrigue, F. Brenner, P. Blake and R. Tauxe, "Outbreaks of salmonella enteritidis infections in the United States, 1985-1991," *J. Infect. Dis.,* vol. 169, no. 3, p. 547, 1994.

[66] M. St Louis, D. Morse, M. Potter, T. DeMelfi, J. Guzewich, R. Tauxe and P. Blake, "The emergence of grade A eggs as a major source of Salmonella enteritidis infections. New implications for the control of salmonellosis," *JAMA,* vol. 259, no. 14, p. 2103, 1988.

[67] D. Sack, R. Sack, G. Nair and A. Siddique, "Cholera," *The Lancet,* vol. 363, no. 9404, pp. 223-233, 2004.

[68] J. Reidl and K. Klose, "Vibrio cholerae and cholera: out of the water and into the host," *FEMS Microbiol. Rev.,* vol. 26, no. 2, pp. 125-139, 2002.

[69] WHO, "Cholera surveillance and number of cases," WHO, 2005. [Online]. Available: http://www.who.int/topics/cholera/surveillance/en/. [Accessed 10 04 2013].

[70] The Associated Press, *Cholera death toll in Haiti has passed 1,000,* The Associated Press, 2010.

[71] B. Adigun, "Nigeria: Cholera epidemic death toll rises to 352," 2010.

[72] WHO, "Cholera in Siera Leone," World Health Organization, 08 09 2012. [Online]. Available: http://www.who.int/csr/don/2012_09_08/en/index.html. [Accessed 10 04 2013].

[73] P. Blake, "Epidemiology of cholera in the Americas," *Gastroenterol. Clin. North Am.,* vol. 22, no. 3, p. 639, 1993.

[74] N. Cohen, D. Slaten, N. Marano, J. Tappero, M. Wellman, R. Albert, V. Hill and D. Espey, "Preventing maritime transfer of toxigenic vibrio cholerae.," vol. 18, no. 10, 2012.

[75] WHO, "World malaria report 2012," WHO, Geneva, 2012.

[76] D. Gollin and C. Zimmermann, "Malaria: Disease impacts and long-run income differences," Center for International Development at Harvard University, Cambridge, MA,

2007.

[77] R. Snow, C. Guerra, A. Noor, H. Myint and S. Hay, "The global distribution of clinical episodes of Plasmodium falciparum malaria," *Nature,* vol. 434, no. 7030, pp. 214-217, 2005.

[78] S. Huan, Interviewee, *Interview on malaria infection and cell concentrations.* [Interview]. 01 2011.

[79] N. Tangpukdee, C. Duangdee, P. Wilairatana and S. Krudsood, "Malaria diagnosis: a brief review," *Korean J. Paras.,* vol. 47, no. 2, pp. 93-102, 2009.

[80] E. Chmal-Fudali and A. Papiewska, "The possibility of thermal inactivation of Alicyclobacillus in fruit and vegetable juices," *Biotechnol. Food Sci.,* vol. 1, no. 87-96, p. 75, 2011.

[81] M. Walker and C. Phillips, "Alicyclobacillus acidoterrestris: an increasing threat to the fruit juice industry?," *Int. J. Food. Sci. Techn.,* vol. 43, no. 2, pp. 250-260, 2008.

[82] European Fruit Juice Association, AIJN, "ACB best practice guideline," AIJN, Brussels, 2008.

[83] C. Steyn, M. Cameron, G. Brittin and R. Witthuhn, "Contamination of pear concentrate by Alicyclobacillus from recirculating flume water during fruit concentrate production," *World J. Microbiol. Biotechn.,* vol. 27, no. 10, pp. 2449-2454, 2011.

[84] A. Ellenberger, "Validierung des mikrobiologischen Nachweises von Alicyclobacillus spp. IFU-Methode Nr. 12 versus Real time PCR," University of Applied Sciences Hamburg, Hamburg, 2009.

[85] S. Volkmar, Interviewee, *Personal communication with Biotecon GmbH.* [Interview]. January 2013.

[86] Reference Online, "just-drinks.com. (19. Mai 2010). Accessed i2013.2012 on," 19 May 2010. [Online]. Available: http://www.just-drinks.com. [Accessed 3 March 2013].

[87] Wikipedia, "Alicyclobacillus," Wikipedia, [Online]. Available:

http://en.wikipedia.org/wiki/Alicyclobacillus. [Accessed 23 04 2013].

[88] Sheffield Hallam University, "Gas chromatography notes," [Online]. Available: http://teaching.shu.ac.uk/hwb/chemistry/tutorials/chrom/gaschrm.htm. [Accessed 13 March 2013].

[89] J. Sun and Z. Peng, "GC determination of diethylene glycol in toothpaste," *Phys. Test. Chem. Anal. B,* vol. 4, p. 023, 2009.

[90] Michigan State University, "Mass spectrometry notes," [Online]. Available: http://www2.chemistry.msu.edu/faculty/reusch/VirtTxtJml/Spectrpy/MassSpec/masspec1. htm. [Accessed 13 March 2013].

[91] J. Ding, H. Gu, S. Yang, M. Li, J. Li and H. Chen, "Selective detection of diethylene glycol in toothpaste products using neutral desorption reactive extractive electrospray ionization tandem mass spectrometry," *Anal. Chem.,* vol. 81, no. 20, pp. 8632-8638, 2009.

[92] A. Deisingh and M. Thompson, "Detection of infectious and toxigenic bacteria," *Analyst,* vol. 127, p. 567–581, 2002.

[93] The Chemistry Hypermedia Project, "Atomic absorption spectroscopy," [Online]. Available: http://www.files.chem.vt.edu/chem-ed/spec/atomic/aa.html. [Accessed 13 03 2013].

[94] University of Berkeley, "Fluorescence," [Online]. Available: http://icecube.berkeley.edu/~bramall/work/astrobiology/fluorescence.htm. [Accessed 13 March 2013].

[95] R. Batchelor and M. Zhou, "A resorufin-based fluorescent assay for quantifying NADH," *Anal. Biochem.,* vol. 305, no. 1, pp. 118-119, 2002.

[96] M. Hoehl, P. Lu, P. Sims and A. Slocum, "Rapid and robust detection methods for poison and microbial contamination," *J. Agric. Food Chem.,* vol. 60, no. 25, pp. 6349--6358, 2012.

[97] P. Elmer, Spectramax and Tecan, Interviewees, *Price Enquiry Plate readers.* [Interview]. 03 05 2012.

[98] O. Lazcka, F. Campo and F. X. Munoz, "Pathogen detection: A perspective of traditional methods and biosensors," *Biosens. Bioelectron.,* vol. 22, p. 1205–1217, 2006.

[99] WISC online, "Urine colony counts," [Online]. Available: http://www.wisc-online.com/objects/ViewObject.aspx?ID=MBY4607. [Accessed 13 March 2013].

[100] Ultra-Violet-Products, "Colony Doc-It," [Online]. Available: http://www.uvp.com/colony.html. [Accessed 13 March 2013].

[101] Oregon State University, "Flow cytometry - How does it work?," [Online]. Available: http://www.unsolvedmysteries.oregonstate.edu/flow_06. [Accessed 13 March 2013].

[102] Danish Society for Flow Cytometry, "FCM introduction," [Online]. Available: http://www.flowcytometri.dk/IntroFCMeng.htm. [Accessed 13 March 2013].

[103] R. Noble and S. Weisberg, "A review of technologies for rapid detection of bacteria in recreational waters," *J. Water Health,* vol. 3, no. 4, pp. 381-392, 2005.

[104] Wikipedia, "Immunoassays," Wikipedia, [Online]. Available: http://en.wikipedia.org/wiki/Immunoassay. [Accessed 09 04 2013].

[105] S. Landers, "ELISA test marks 35 years of answering medical questions," American Medical News, 2012.

[106] www.america.gov, "Rosalyn Sussman Yalow," www.america.gov, 27 04 2008. [Online]. Available: www.america.gov. [Accessed 10 04 2013].

[107] E.-M. Rajkovic, "Immunoquantitative real-time PCR for detection and quantification of Staphylococcus aureus enterotoxin B in foods," *Appl. Environ. Microbiol. ,* vol. 72, no. 10, p. 6593–9, 2012.

[108] E. Gofflot, "Immuno-quantitative polymerase chain reaction for detection and quantitation of prion protein," *J. Immunoassay Immunochem.,* vol. 25, no. 3, p. 241–58, 2012.

[109] Millipore Corporation, "Luminex xMAP Technology," Millipore, [Online]. Available: www.millipore.com. [Accessed 10 04 2013].

[110] Roche, "PCR: eine ausgezeichnete Methode," [Online]. Available: http://www.roche.com/pages/facetten/pcr_d.pdf. [Accessed 09 04 2013].

[111] S. Qiagin, "DNA isolation methods," [Online]. Available: http://science.marshall.edu/murraye/links%20for%20students/samantha_20qiagin_20method.pdf. [Accessed 13 04 2013].

[112] Enotes, "DNA purification methods," [Online]. Available: http://www.enotes.com/dna-isolation-methods-reference/dna-isolation-methods. [Accessed 14 03 2013].

[113] Qiagen, "DNA protocols and applications," [Online]. Available: http://www.qiagen.com/Knowledge-and-Support/Spotlight/Protocols-and-Applications-Guide/DNA/#DNA%20extraction%20technologies. [Accessed 14 04 2013].

[114] Roche Molecular Diagnostics, " COBAS® AmpliPrep/COBAS® TaqMan® System," [Online]. Available: http://molecular.roche.com/instruments/Pages/COBASAmpliPrepCOBASTaqManSystem.aspx. [Accessed 05 06 2013].

[115] Abbott Molecular, "Instrumentation and Automation," Abbott , [Online]. Available: www.abbottmolecular.com. [Accessed 6 6 2013].

[116] WHO, "Sources and prices of selected medicines and diagnostics for people living with HIV/AIDS," World Health Organisation, [Online]. Available: http://apps.who.int/medicinedocs/en/d/Js8112e/8.2.html. [Accessed 06 06 2013].

[117] N. Langendorf, Interviewee, *Promega customer support; Product enquiry Maxwell 16.* [Interview]. 06 06 2013.

[118] Autogen, Interviewee, *Autogen customer support; Product enquiry about Nordiag Arrow.* [Interview]. 05 06 2013.

[119] *Qiagen customer support; product enquiry.* [Interview]. 05 06 2013.

[120] Roche Diagnostics, "Magna Pure products," Roche Diagnostics, [Online]. Available: http://www.roche-diagnostics.de/diagnostics/systeme/forschung/magna_pure_produkte/. [Accessed 05 06 2013].

[121] Biomérieux, "Nuclisens EasyMAG," Biomérieux, [Online]. Available: http://www.biomerieux-usa.com/. [Accessed 05 06 2013].

[122] Qiagen, "QIACube," [Online]. Available: www.qiagen.com. [Accessed 04 06 2013].

[123] Qiagen, "EZ1 Advance," Qiagen, [Online]. Available: http://www.qiagen.com/Products/Catalog/Automated-Solutions/Sample-Prep/EZ1-Advanced-Instruments#orderinginformation. [Accessed 06 06 2013].

[124] W. Check, " For nucleic acid extraction, choices galore (Cap Today)," 2008. [Online]. Available: http://www.cap.org. [Accessed 03 02 2013].

[125] M. Murtagh, "Viral Load: Current Technologies and the Pipeline, including Point-of-Care Assays," 18-20 04 2013. [Online]. Available: http://216.172.160.206/~afslm/images/Resource%20centre/Viral%20Load%20presentations/Murtagh_ASLM%20Viral%20Load%20Mtg_04%2019%202013.pdf. [Accessed 06 06 103].

[126] P. Gill and A. Ghaemi, "Nucleic acid isothermal amplification technologies - a review," *Nulceos. Nucleot. Nucl.,* vol. 27, p. 224–243, 2008.

[127] Spartan Biosciences Inc., "Hunter," [Online]. Available: http://www.spartanbio.com/products/spartan-dx-12/pricing/#Pricing. [Accessed 06 06 2013].

[128] Qiagen, "ESEQuant," [Online]. Available: http://www.qiagen.com/About-Us/Contact/Corporate-Contacts/OEM-Services/ESE-Instruments/ESEQuant-Tube-Scanner/. [Accessed 06 06 2013].

[129] Instantlabs, "Hunter Product Information," [Online]. Available: www.instantlabs.com. [Accessed 05 06 2013].

[130] US EPA, "Technology Information Summary BioSeeq Plus," 07 2009. [Online]. Available: U.S. EPA ORD NHSRC. [Accessed 05 06 2013].

[131] Molecular Devices, "Microplate Readers," Molecular Devices, [Online]. Available: http://www.moleculardevices.com/Products/Instruments/Microplate-Readers/. [Accessed

04 01 2013].

[132] Roche, A. Biosystems, A. Jena and Qiagen, Interviewees, *Price enquiry realtime PCR machines.* [Interview]. 03 06 2011.

[133] *Spartan Biosciences Inc.; product enquiry.* [Interview]. 05 06 2013.

[134] Applied Biosystems, "Applied Biosystems Real-Time PCR System," Life Technologies, [Online]. Available: http://de-de.invitrogen.com/site/de/de/home/Products-and-Services/Applications/PCR/real-time-pcr/real-time-pcr-instruments.html. [Accessed 06 06 2013].

[135] Smiths Detection, "Bioseeq Plus," [Online]. Available: http://www.smithsdetection.com/deu/1348.php. [Accessed 05 06 2013].

[136] J. Heo and S. Hua, "An overview of recent strategies in pathogen sensing," *Sensors,* vol. 9, no. 6, pp. 4483-4502, 2009.

[137] M. Marazuela and M. Moreno-Bondi, "Fiber-optic biosensors – an overview," *Anal. Bional. Chem.,* vol. 372, pp. 664-682, 2002.

[138] J.-Y. Jyounga, S. Hongc, W. Leea and J. Choi, "Immunosensor for the detection of Vibrio cholerae O1 using surface plasmon resonance," *Biosens. Bioelectron.,* vol. 21, p. 2315–2319, 2006.

[139] Freedonia Group, "Food safety products to 2016 - Demand and sales forecasts, market share, market size, market leaders," *Study #: 2887,* 2012.

[140] BCC Research, "Global markets and technologies for food safety testing," 2012.

[141] B. Ge and J. Meng, "Advanced technologies for pathogen and toxin detection in foods: current applications and future directions," *Journal of the Association for Laboratory Automation,* vol. 14, no. 4, pp. 235-241, 2009.

[142] Strategic Consulting Inc., "Food microbiology - 2008 to 2013," Strategic Consulting Inc., WA, USA, 2008.

[143] R. Lawley, "A revolution in the food safety laboratory," Food Safety Watch, [Online]. Available: http://www.foodsafetywatch.com/public/1050.cfm. [Accessed 25 03 2013].

[144] P. Mandal, A. Biswas, K. Choi and U. Pal, "Methods for rapid detection of foodborne pathogens: an overview," *Am. J. Food Technol.,* vol. 6, pp. 87--102, 2011.

[145] PRweb, "Global food safety products market forecast to reach $18 Billion in 2016," 01 December 2012. [Online]. Available: http://www.prweb.com/releases/food-safety-products/global-market-forecast/prweb10189645.htm. [Accessed 25 03 2013].

[146] Markets and Markets, "In-Vitro Diagnostic (IVD) market (applications, end-users & types) trends & global forecasts (major & emerging markets – G7, Japan & BRIC) (2011 - 2016)," Report Code: PH 1751, 2012.

[147] A. Angelis, "Food safety diagnostics market to hit $1.6 billion over the coming years," Companies and Markets, 2012. [Online]. Available: http://www.companiesandmarkets.com/News/Food-and-Drink/Food-safety-diagnostics-market-to-hit-1-6-billion-over-the-coming-years/NI6583. [Accessed 25 03 2013].

[148] European Policy Evaluation Consortium (EPEC), "Detailed assessment of the market potential, and demand for, an EU ETV scheme," EU, Brussels, 2011.

[149] National Academy of Engineering, "Characterization of the environmental testing industry," in *Risk & Innovation:Small Companies in Six Industries: Background Papers Prepared for the NAE Risk and Innovation Study*, Washington, National Academy Press, 1996, pp. 86-87.

[150] Edstrom Industries, "Drinking water quality standards," Edstrom Industries, Waterford, 2003.

[151] EPA, "2012 recreational water quality criteria," EPA, Washington, 2012.

[152] Qiagen, "Qiagen annual report 2008," Qiagen, 2008.

[153] LSI, "Worldwide markets and emerging technologies for point-of-care testing," LSI, Huntington Beach, Inc., 2009.

[154] P. Lu, M. Hoehl, J. Macarthur, P. Sims, H. Ma and A. H. Slocum, "Robust and economical multi-sample, multi-wavelength UV/vis absorption and fluorescence detector for biological and chemical contamination," *AIP Adv.,* vol. 2, no. 3, p. 032110, 2012.

[155] A. Shrivastava and V. Gupta, "Methods for the determination of limit of detection and limit of quantitation of the analytical methods.," *Chr. Young Sci.,* vol. 2, no. 1, pp. 21-25, 2011.

[156] Wikipedia, "Detection Limit," [Online]. Available: http://en.wikipedia.org/wiki/Detection_limit. [Accessed 09 05 2013].

[157] Department of Human Health and Services, "Toxicological profile for ethylene glycol," AfTSaDR, Washington, D.C., 2010.

[158] A. Danley and M. Watts, "Installation of bio-sand filters in petite paradise, Haiti," *Proc. Water Environ. Fed.,* vol. 12, pp. 3892-3897, 2009.

[159] A. Gadgil, "Drinking water in developing countries," *Annu. Rev. Energy Environ.,* vol. 23, p. 253–86, 1998.

[160] L. Yang and R. Bashir, "Electrical/electrochemical impedance for rapid detection of foodborne pathogenic bacteria," *Biotech. Adv.,* vol. 26, no. 2, pp. 135-150, 2008.

[161] D. Ivnitski, I. P. Abdel-Hamid and E. Wilkins, "Biosensors for detection of pathogenic bacteria," *Biosens. Bioelectron.,* vol. 14, no. 7, pp. 599-624, 1999.

[162] D. Ivnitski, I. Abdel-Hamid, P. Atanasov, E. Wilkins and S. Stricker, "Application of electrochemical biosensors for detection of food pathogenic bacteria," *Electroanal.,* vol. 12, no. 5, pp. 317-325, 2000.

[163] A. Rand, "Optical biosensors for food pathogen detection," *Food Technol.,* vol. 56, no. 3, pp. 32-39, 2002.

[164] X. Su and L. Y., " A self-assembled monolayer-based piezoelectric immunosensor for rapid detection of Escherichia coli O157: H7," *Biosens. Bioelectron.,* vol. 19, no. 6, pp. 563-574, 2004.

[165] Manufacturers, Interviewee, *Price and product enquiry.* [Interview]. 08 2012.

[166] K. Sriprawat, S. Kaewpongsri, R. Suwanarusk, M. Leimanis, A. Phyo, B. Snounou, B. Russell, L. Renia and F. Nosten, "Effective and cheap removal of leukocytes and platelets from Plasmodium vivax infected blood," *Malar. J.,* vol. 8, p. 115, 2009.

[167] Eppendorf, "Eppendorf product website," [Online]. Available: www.eppendorf.com. [Accessed 06 06 2013].

[168] Clinical and Laboratory Standards Institute, "Guideline on nucleic acid amplification assays for molecular hematopathology - second edition," in *MM05-A2*, Wayne, PA, CLSI, 2012, p. 32(6).

[169] Drosten, C. et al, "Qualitätsstandards in der mikrobiologischen Diagnostik," in *MiQ 01: Nukleinsäure-Amplifikationstechniken, 3. Auflage*, Urban & Fischer, 2011, pp. 39-42.

[170] P. Francois, M. Tangomo, J. Hibbs, E. Bonetti and C. Boehme, "Robustness of a loop-mediated isothermal amplification reaction for diagnostic applications," *FEMS Immunol.Med. Microbiol.,* vol. 62, no. 1, pp. 41-48, 2011.

[171] M. Parida, S. Sannarangaiah, P. Dash, P. Rao and K. Morita, "Loop mediated isothermal amplification (LAMP): a new generation of innovative gene amplification technique; perspectives in clinical diagnosis of infectious diseases.," *Rev. Med. Virol.,* vol. 18, no. 6, pp. 407-21, 2008.

[172] Applied Biosystems, "Real-Time PCR: Understanding CT," Applied Biosystems Application Note, Forster City, CA, 2008.

[173] D. M. Tourlousse, F. Ahmad, R. D. Stedtfeld, G. Seyrig, J. M. Tiedje and S. A. Hashsham, "A polymer microfluidic chip for quantitative detection of multiple water- and foodborne pathogens using real-time fluorogenic loop-mediated isothermal amplification," *Biomed. Microd.,* vol. 14, no. 4, pp. 769-778, 2012.

[174] T. Cai, G. Lou, J. Yang, D. Xu and Z. Meng, "Development and evaluation of real-time loop-mediated isothermal," *Clin. Virol.,* vol. 41, no. 4, pp. 270-276, 2008.

[175] H. Manneck, Interviewee, *Mast Diagnostica GmbH, Quantification of LAMP reactions using intercalating dyes.* [Interview]. 02 2013.

[176] Y. Mori and T. Notomi, "Real-time fluorescence loop mediated isothermal amplification for the diagnosis of malaria," *PLoS One,* vol. 5, no. 10, p. e13733, 2010.

[177] N. Lucchi, A. Demas, J. Narayanan, D. Sumari, A. Kabanywanyi, S. Kachur, J. Barnwell and V. Udhayakumar, "Real-time fluorescence loop mediated isothermal amplification for the diagnosis of malaria," *PLoS One,* vol. 5, no. 10, p. e13733, 2010.

[178] Pollin Electronic, "Axiallüfter NMB-MAT 2410ML-04W-B40," [Online]. Available: www.pollin.de. [Accessed 05 06 2013].

[179] University of Chicago, "Realtime PCR handbook," RRC Core Genomics Facility, 2003. [Online]. Available: http://www.uic.edu/depts/rrc/cgf/realtime/melt.html. [Accessed 29 03 2013].

[180] Wikipedia, "Melting curve analysis," Wikipedia, [Online]. Available: http://en.wikipedia.org/wiki/Melting_curve_analysis. [Accessed 29 03 29].

[181] M. Brisson, L. Tan, R. Park and K. Hamby, "Identification of nonspecific products using melt-curve analysis on the iCycler iQ detection system," BioRad Laboratories Inc., 2010.

[182] European Union, "Verordnung der europäischen Kommission über mikro-biologische Kriterien für Lebensmittel," in *Milchverordnung*, Brussels, 2004, p. Anl. 6 Nr.3.3.

[183] Qiagen and Macherey-Nagel, Interviewees, *Telephone-interview with manufacturer.* [Interview]. 03 2012.

[184] M. Karle, Interviewee, *Inhibition of qPCR reactions by ethanol.* [Interview]. 19 07 2012.

[185] L. Rossen, P. Norskov, K. Hoimstrom and O. Rasmussen, "Inhibition of PCR by components of food samples, microbial diagnostic assays and DNA extraction solutions," *Int. J. Food. Microbiol.,* pp. 37-45, 17 1992.

[186] B. Hatano, T. Maki, T. Obara, H. Fukumoto, K. Hagisawa, Y. Matsushita, ... and H. Katano, "LAMP using a disposable pocket warmer for anthrax detection, a highly mobile and reliable method for anti-bioterrorism.," *Jpn. J. Infect. Dis.,* vol. 63, no. 1, pp. 36-40, 2013.

[187] P. LaBarre, J. Gerlach, J. Wilmoth, A. Beddoe, J. Singleton and B. Weigl, "Non-instrumented nucleic acid amplification (NINA): Instrument-free molecular malaria diagnostics for low-resource settings," in *Ann. Int. Conf. IEEE*, 2010.

[188] P. LaBarre, K. R. Hawkins, J. Gerlach, J. Wilmoth, A. Beddoe, J. Singleton, ... and B. Weigl, "A simple, inexpensive device for nucleic acid amplification without electricity—toward instrument-free molecular diagnostics in low-resource settings," *PLoS One,* vol. 6, no. 5, p. e19738, 2011.

[189] Wikipedia, "Phase change materials," Wikipedia, [Online]. Available: http://en.wikipedia.org/wiki/Phase-change_material. [Accessed 23 01 2013].

[190] Rubitherm, "Rubitherm," [Online]. Available: http://www.rubitherm.de/. [Accessed 02 04 2013].

[191] National Institute of Standards, NIST, "NIST Chemistry WebBook," [Online]. Available: http://webbook.nist.gov/chemistry/. [Accessed 21 11 2012].

[192] Science Lab, "MSDS," [Online]. Available: http://www.sciencelab.com/msds. [Accessed 23 05 2013].

[193] Wikipedia, "Hand warmers," [Online]. Available: http://en.wikipedia.org/wiki/Hand_warmer. [Accessed 23 05 2013].

[194] Chemical and Process Engineering Ressources, "Pyrophoric iron fires," [Online]. Available: http://cheresources.com/content/articles/safety/pyrophoric-iron-fires?pg=1. [Accessed 05 01 2013].

[195] T. Solomons and C. B. Fryhle, Organic Chemistry, Hoboken, NJ: Wiley International Edition, 2004.

[196] S. Summer, "The fire safety hazard of the use of flameless ration heaters onboard commercial aircraft," U.S. Department of Transportation, Springfield, VA, 2006.

[197] R. Bie, L. Li and L. Yang, "Reaction mechanism of CaO with HCl in incineration of wastewater in fluidized bed," *Chem. Eng. Sc.,* vol. 60, no. 3, pp. 609-616, 2005.

[198] I. Kuhn, "Praktikumsprotokoll Organisch Chemisches Grundpraktikum Lehramt WS 2006/07," [Online]. Available: http://www.chids.de/dachs/praktikumsprotokolle/PP0050kaliumpermanganat_und_glycerin.pdf. [Accessed 05 01 2013].

[199] Prevor, "Sulfuric Acid - management of eye and skin chemical splashes.," [Online]. Available: http://www.prevor.com/EN/sante/RisqueChimique/diphoterine/publications/media/Acide_sulfur_Ang_BD.pdf. [Accessed 31 05 2013].

[200] A. Schefer and S. Schefer, "Self-warming or self-heating cosmetic and dermatological compositions and method of use". USA Patent 10/454,915, 2003.

[201] Wikipedia, "Handwarmers," [Online]. Available: http://en.wikipedia.org/wiki/Hand_warmer. [Accessed 05 01 2013].

[202] N/A, "Salze_1_Arbeitsauftrag_exoendoPackungen," [Online]. Available: http://www.chungo.de/Unterricht/Chemie/Klasse12GK/salze/Salze_1_Arbeitsauftrag_exoendoPackungen.pdf. [Accessed 13 05 2013].

[203] Amazing Rust, "Thermite Reactions," [Online]. Available: http://www.amazingrust.com/Experiments/how_to/Thermite.html. [Accessed 23 05 2013].

[204] R. Winterton, Heat transfer, Oxford: Oxford University Press, 1997.

[205] C. Chen, Y. Wang and C. Sung, "A novel energy harvesting device embedded in a rotating wheel," *Proceedings of Power MEMS and MicroMEMS2008,* pp. 185-188, 2008.

[206] Bosch, Interviewee, *Robert Bosch GmbH Dept. of Microsystems Technology; Energy harvesting methods inside a centrifuge.* [Interview]. 01 11 2011.

[207] F. Lärmer, Interviewee, *Discussion about batteries.* [Interview]. 12 2011.

[208] Ralf Hottmeyer GmbH, "Vergleichslisten und Informationen für Knopfzellen und Batterien," Ralf Hottmeyer, Würselen, 2012.

[209] NSF, "Expanding global research pool," [Online]. Available:

http://www.nsf.gov/statistics/seind10/c0/c0s5.htm. [Accessed 04 04 2013].

[210] NSF, "Science and engineering indicators 2010," NSF, 2007. [Online]. Available: http://www.nsf.gov/statistics/seind10/append/c2/at02-01.pdf. [Accessed 05 04 2013].